EVALUATION OF LONGITUDINAL DISPERSIVITY FROM TRACER TEST DATA

by
CLAIRE WELTY
and
LYNN W. GELHAR

RALPH M. PARSONS LABORATORY
FOR WATER RESOURCES AND HYDRODYNAMICS
Massachusetts Institute of Technology
Cambridge, Massachusetts 02139

Report Number 320

Prepared with the support of
U.S. Environmental Protection Agency and
National Science Foundation

March, 1989

MIT

DEPARTMENT
OF
CIVIL
ENGINEERING

SCHOOL OF ENGINEERING
MASSACHUSETTS INSTITUTE OF TECHNOLOGY
Cambridge, Massachusetts 02139

ACKNOWLEDGEMENTS

This work was funded in part by U.S. Environmental Protection Agency Cooperative Agreement CR-811135-01-2 and the National Science Foundation under Grant No. CES-8814615. The authors gratefully acknowledge reviews by Paul Hsieh and Kenneth Rehfeldt. Their comments have improved this report.

This report has not undergone formal technical and administrative review by the sponsoring agencies. Any opinions, findings, and conclusions or recommendations expressed in this report are those of the authors and do not necessarily reflect the views of the sponsors.

CONTENTS

LIST OF FIGURES

LIST OF TABLES

SECTION 1

INTRODUCTION

Mathematical modeling of solute transport has become a standard tool for evaluating the movement and spreading of chemical contaminants in the subsurface aquatic environment. Most frequently, numerical techniques such as finite element or finite difference methods are used to solve the governing partial differential equations of flow and solute transport over a large aquifer region, in order to predict the concentration of a chemical contaminant at some future time and at points distant in space from a source. One problem that continues to plague users of these techniques is estimation of mixing or dilution parameters, or more specifically the dispersivity (if the dispersion coefficient is assumed to be the product of dispersivity and mean pore velocity), in the governing equations. Summaries of field observations (e.g., Lallemand-Barres and Peaudecerf, 1978; Anderson, 1979; and Gelhar, et al., 1985) and theoretical studies (e.g., Gelhar and Axness, 1983) both have indicated that dispersivity is a function of the heterogeneity of the geologic formation and that there is a dependence of the value of dispersivity on the solute displacement distance in the aquifer. Typically, then, there is a need to determine a value for dispersivity for the aquifer material and scale of problem at hand. Tracer tests are often attempted as a means of estimating the required dispersivity.

Figure 1-1 from Gelhar, et al. (1985), summarizes the information available on longitudinal dispersivity values determined from tracer tests conducted at various length scales and on many type of aquifer materials around the world. Figure 1-2 illustrates the ranking of the relative reliability for these same data, based on judgements about the type of experiment and method of data interpretation. This graphical summary reinforces the fact that modelers indeed face difficulties in determining the proper value of dispersivity for a given problem. It is with this motivation in mind that we explore improved methods for analysis of tracer tests to yield accurate information on dispersivity values. This will contribute to more realistic modeling of the solute transport process in evaluation of groundwater contamination cases.

The two overall goals of this study are:

1) to develop and demonstrate improved methods of analyzing existing tracer test data; and
2) to use this information and experience to better define the reliability of existing data and to provide an improved basis for selecting, designing, and analyzing tracer tests.

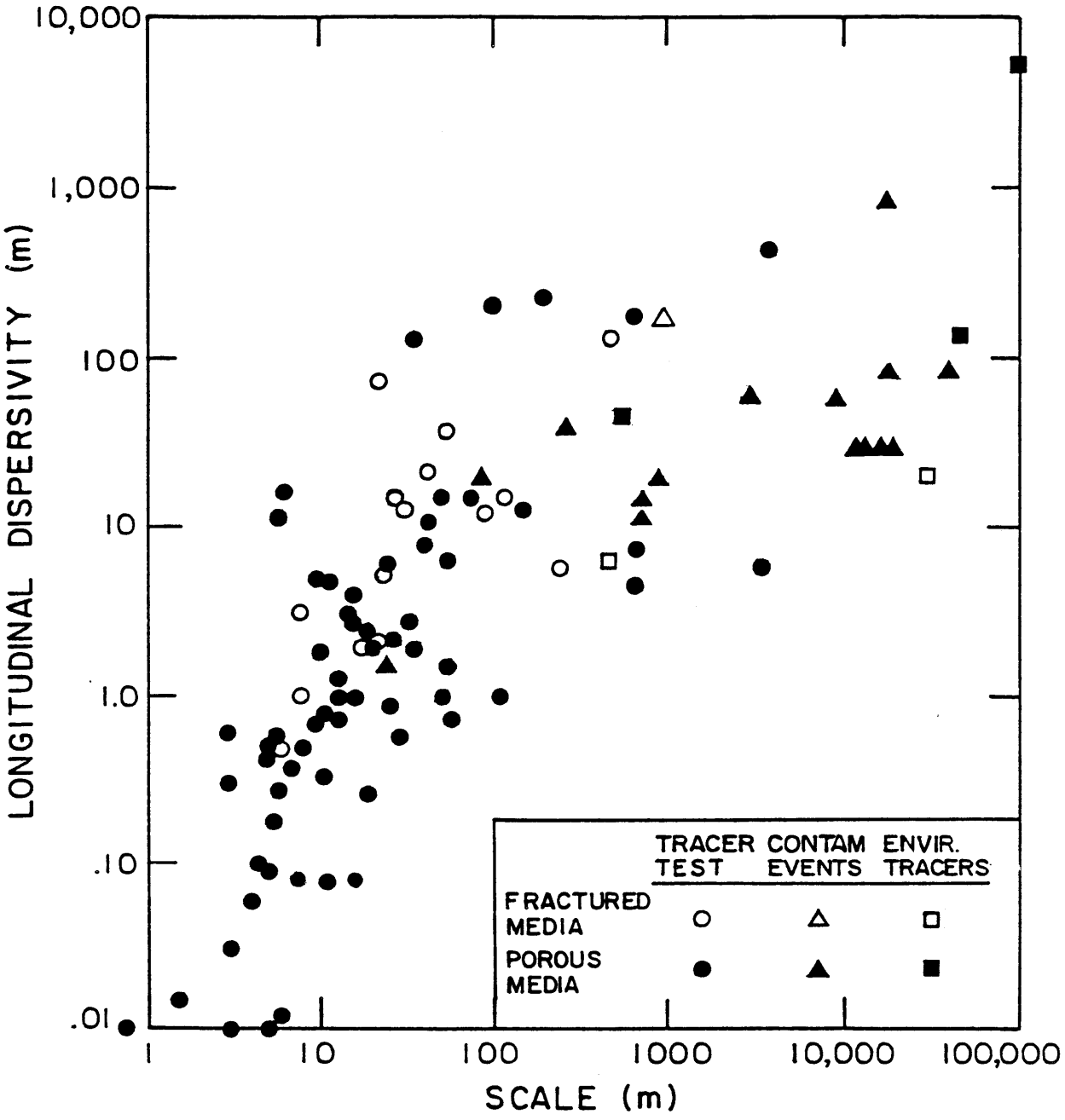

Figure 1-1. Scale of observation versus longitudinal dispersivity for the saturated zone (from Gelhar et al., 1985).

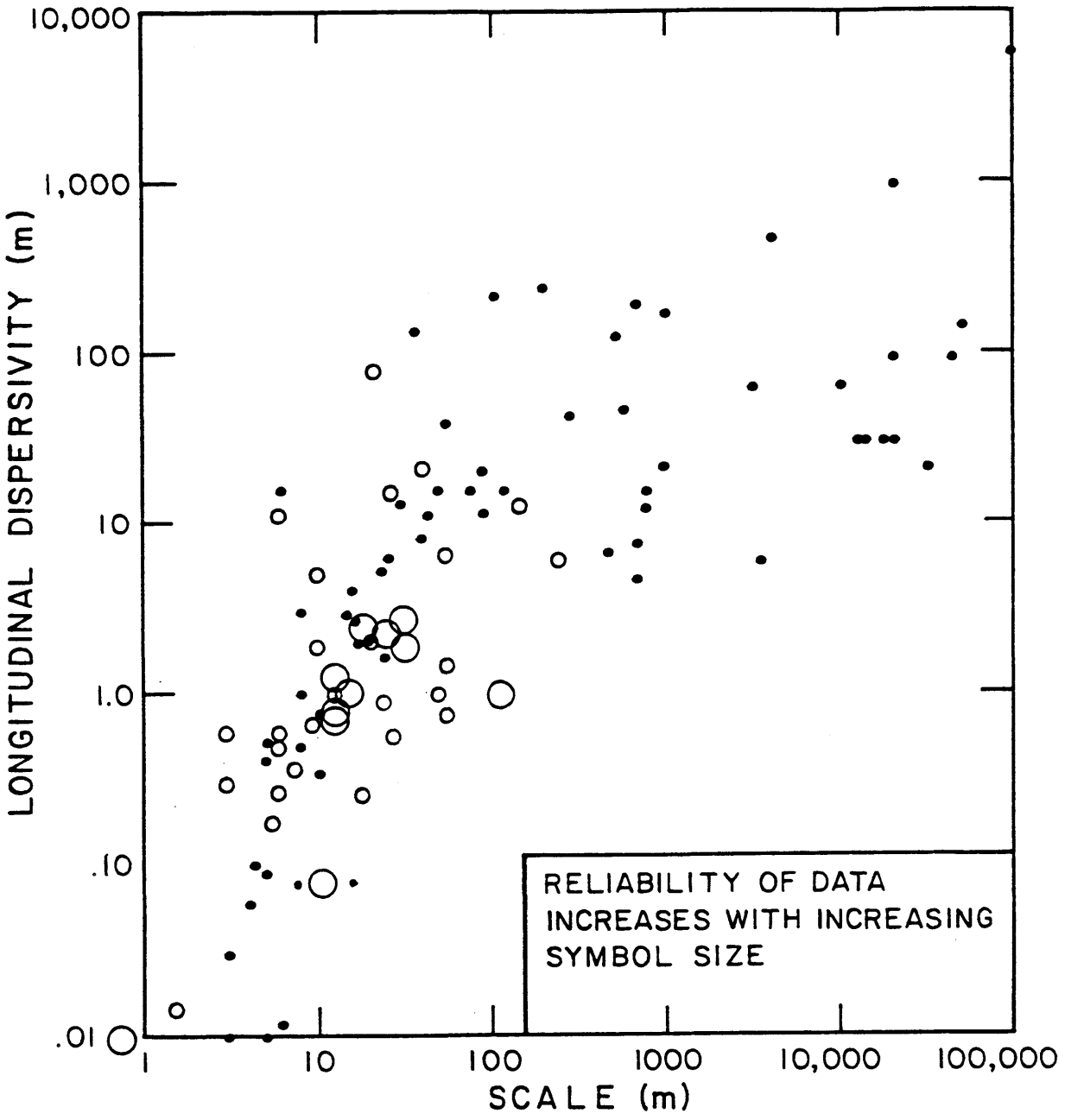

Figure 1-2. Scale of observation versus longitudinal dispersivity for the saturated zone: reliability classification (from Gelhar et al., 1985).

SECTION 2

CONCLUSIONS AND RECOMMENDATIONS

Of interest in modeling solute transport to evaluate groundwater contamination problems is the determination of the dispersion coefficient or, more specifically, the dispersivity parameter that characterizes the mixing in the aquifer under study. This report discusses the types of small-scale, short-term tracer tests that can be used to determine dispersivity. A variety of methods are available for analyzing tracer test data to determine dispersivity; these are reviewed in this report.

Unfortunately, many of the methods which have been used to analyze tracer tests make simplifying assumptions which may lead to errors in estimating the value of dispersivity for the aquifer material of interest. We demonstrate how the general solution of Gelhar and Collins (1971) for dispersion in non-uniform flow can be used to evaluate the results of radial flow and two-well tracer tests to include effects not accounted for in most other analyses. Type curves are developed for radially divergent flow with step and pulse inputs, radially convergent flow with a pulse input, and two-well tests with a pulse or step input. The effects of borehole flushing and dispersivity increasing linearly with distance are examined to determine their effects on type curve shapes. Several case studies demonstrate the applicability of the theoretical results to field data.

The findings in this report suggest that many previous interpretations of longitudinal dispersivity from breakthrough curve data are faulty due to the simplifying assumptions associated with the methods of analysis used. Our re-analyses have shown that such misinterpretations tend to overestimate the longitudinal dispersivity, in some cases by as much as an order of magnitude. If improved theoretical solutions corresponding more closely to the physical situation at hand are instead employed, in many cases the simplifying assumptions do not have to be made (for example, assumption of geologic layers when no evidence for such layers is available to explain the tailing in breakthrough curves). Although there are inherent problems with running small-scale, short-term tracer tests, if proper precautions are taken, these tests coupled with appropriate analysis can provide a useful means for determining dispersivity on a short-term basis.

This report provides an improved series of type curves which can be used to design and analyze tracer tests. Our experience indicates that the two-well (doublet) configuration with a pulse input and the radial divergent tests produce the most reliable results. The radial convergent test with a pulse input is attractive because of its simplicity of operation, but the results are frequently difficult to interpret precisely. The two-well (doublet) configuration with a step input is not recommended as a method for finding the longitudinal dispersivity.

SECTION 3

NON-UNIFORM FLOW TRACER TESTS FOR DISPERSIVITY

Design considerations for tracer tests to determine longitudinal dispersivity include flow configuration (uniform, radial or two-well); mass injection form (pulse or step input); and choice of chemical tracer species. Tracer tests carried out in large-scale, uniform natural gradient flow configurations (e.g., Sudicky, et al., 1983) can be accurately interpreted using, for example, the method of moments (e.g., see example analysis in Gelhar, et al., 1985). However, these tests are not simple to run in a field setting, due to the large travel times and distances required for plume development, and because of the very extensive multi-dimensional monitoring (e.g., hundreds of multilevel sampling wells) required to delineate the plume. In view of these complications which make the natural gradient test essentially a research tool, the focus of this report is on short-term tracer tests -- radial flow and two-well tests -- that can be carried out in a matter of hours or several days, and where the flow regime is controlled by pumping or injection through wells.

Figure 3-1 depicts the six configurations of radial flow and two-well tracer tests that will be described in this report. It should be noted that the data obtained from all of these tests -- i.e., the breakthrough curves -- may be analyzed in a similar manner, but that the practical operational aspects vary considerably among tests. Also, the reliability of the information obtained from analyses of data from different types of tests will vary as a result of complications in the aquifer flow system and/or improper application of solutions of the advection-dispersion equation. Several of these problems will be discussed in this section; the details of the mathematical analysis will be presented later. However, it should be recognized that there are strong theoretical reasons (e.g., Gelhar, et al., 1979; Gelhar and Axness, 1983) to expect significant deviations from the classical Fickian advection-dispersion equation at the small scale typical of these tracer tests. In all cases our discussion will pertain to conservative tracers (e.g., Cl^-, Br^-) so that radioactive decay or chemical retardation are not factors in the analyses. For a complete description of the various types of tracer materials commonly used for tracer tests, see Davis, et al., 1980; Davis, et al., 1985; and Betson, et al., 1985.

Divergent Radial Flow Test

In the divergent radial flow test (Figs. 3-1a and 3-1b), water is injected at the recharge well from an outside source, generally at a constant rate. After a steady flow field is established, the tracer is introduced as either a pulse or step input at the recharge well, and the concentration of the radially dispersed tracer is measured at a distant observation well. The advantage this test offers over other radial flow tests is that the tracer is quickly forced from the injection well, thus producing a well-defined initial condition and a breakthrough curve which can be interpreted simply. It will

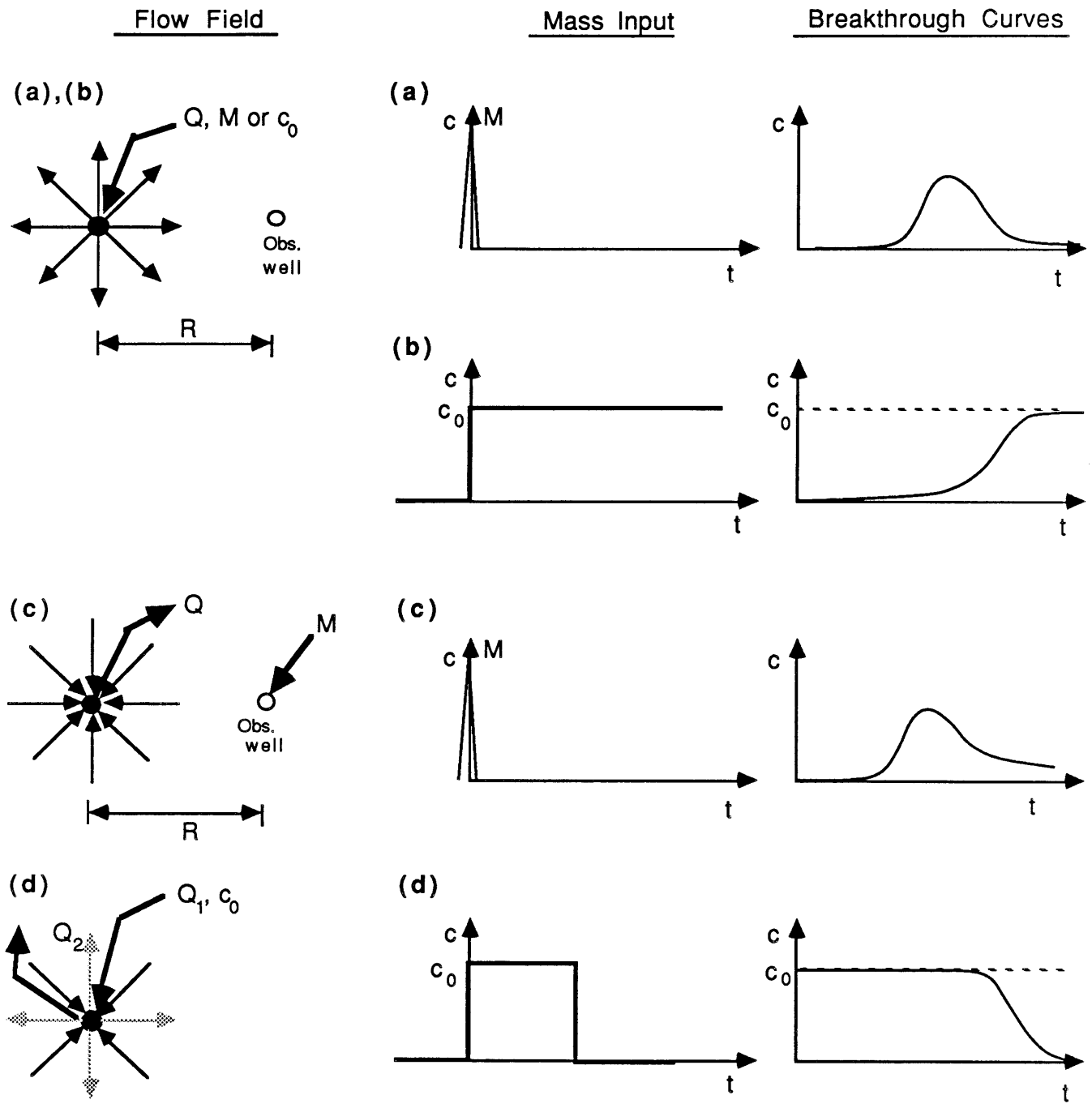

Figure 3-1. Tracer Test Configurations. Radial flow tests: (a) divergent radial flow with pulse input; (b) divergent radial flow with step input; (c) convergent radial flow with pulse input; and (d) the single well test. Q = pumping or injection rate (vol/time); R = radial distance; c_0 = input concentration; ⟶ = flow direction.

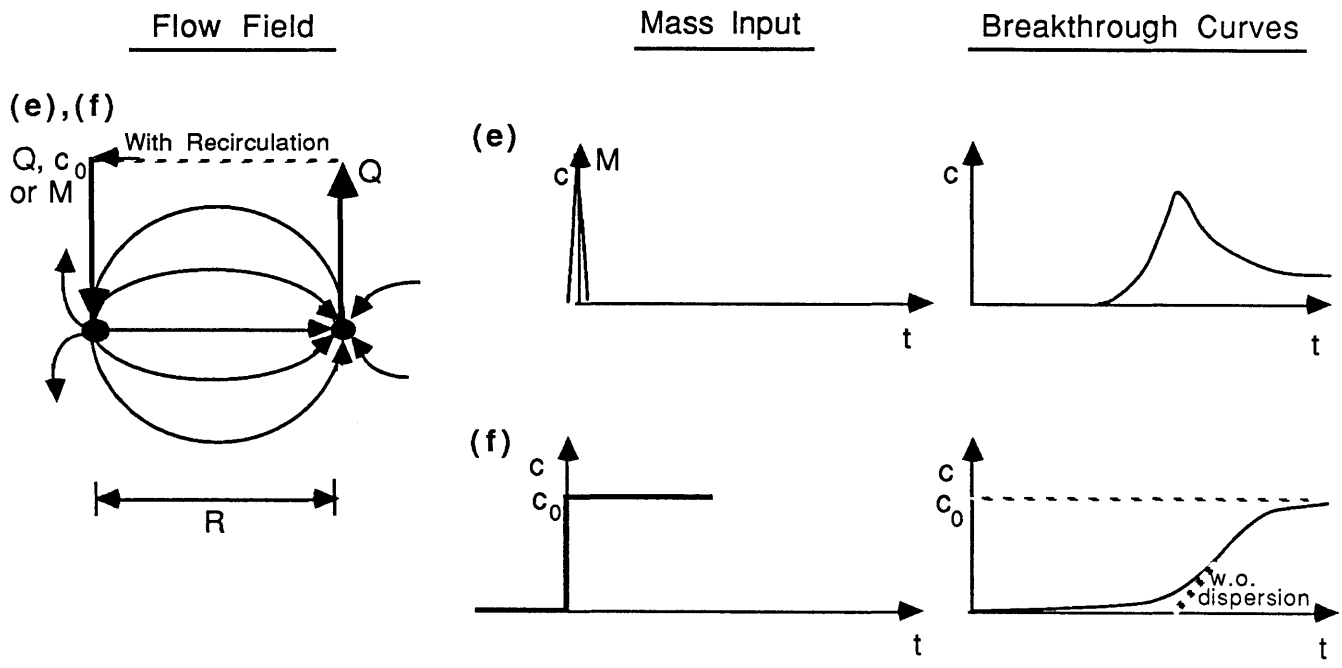

Figure 3-1. Tracer Test Configurations, continued. Two-well tests: (e) pulse input and (f) step input, without recirculation.

be shown later that for the type-curve-matching method of analysis, the divergent radial flow test utilizing a pulse input provides breakthrough curves from which determination of the appropriate value of dispersivity is somewhat simpler than from those generated by a step input. The divergent radial flow test has the disadvantage that clogging of the recharge well may be a concern with some water sources. Tracer source control is simpler for the pulse than for the step input.

Convergent Radial Flow Test

Some of the disadvantages of the divergent radial flow test can be avoided by using instead the convergent radial flow test (Fig. 3-1c), where after a steady flow field is established, the tracer is introduced as a slug into a borehole and the dispersed tracer concentration is measured at a pumping well. In this case, the plumbing requirements are much simpler -- a pump test facility (a pumping well and an observation well) can be used which is already in place, and the pumped water is discharged to waste. The disadvantage of this test is that in some geologic settings the tracer may not flush out of the borehole quickly, so that the slug input may not leave the borehole as a true "pulse", but rather as a gradually decreasing concentration input. This input generates a breakthrough curve with a long tail, which is more difficult to interpret (e.g., to fit to a type curve) than the breakthrough curve generated by the divergent radial flow test. As will be discussed later, this "borehole flushing effect" is most important in settings with one or more of the following characteristics: (1) very low porosity; (2) large borehole diameter; and (3) short distance between borehole and pumping well.

Single-Well Test

In the single-well test (Fig. 3-1d), the tracer is pumped into, then out of, one well, with observations taken at the same well. From the point of view of equipment requirements, this test is advantageous over other radial flow tests in that only one well is required; however, the disadvantages are more numerous, in that: (1) the plumbing system for a recharge-discharge system is more complex; (2) there may be problems with clogging of the well during recharge; and (3) as with the divergent test, an outside water source is needed for the recharge cycle. It should be noted that a more fundamental problem with this test is that what is being measured here is not the large-scale dispersivity of the porous medium, but rather the small-scale dispersivity caused by local (pore-scale) heterogeneities. Large-scale dispersion is produced by the velocity differences along and among streamlines as they move around and through large-scale heterogeneities. However, this test does not capture this large-scale dispersion effect, because the velocity field is reversed when the flow regime is reversed, thereby causing the large-scale dispersion process to be partially reversed. For this reason, we do not recommend the use of this test for determining dispersivity for modeling solute transport problems, except when the application involves reversing flow at the same scale as that of the test.

Two-Well Test

An alternative to radial flow tests is the two-well test, or "doublet" (Figs. 3-1e and 3-1f), wherein a pulse or step input of tracer is introduced into a recharge well and measured at a pumping well, with optional recirculation of the pumped water (containing tracer). Although complex plumbing requirements may be viewed as a disadvantage, this test is frequently employed (with recirculation) because it circumvents the problem of obtaining an independent source of water for the recharge well.

The principal problem with the use of this test lies in the interpretation of the breakthrough curve results. The analysis of the breakthrough curve is not as straightforward as that of radial flow, because along each streamline the tracer arrives at the pumping well at a different time. Consequently, only the early-time part of the doublet breakthrough curve is sensitive to dispersion, whereas the shape of the tail results from the advection pattern of the tracer. For this reason, the doublet test with a pulse input generates a breakthrough curve from which the value of dispersivity is easily determined, because the peak of the curve arrives at a time that is sensitive to dispersion. It is more difficult to determine the value of dispersivity from the doublet breakthrough curve generated by a step input, because there are only mild differences in the slopes of the initial parts of these breakthrough curves resulting from different dispersivities. If too few measurements are taken at early times in the step-input doublet test, it is difficult to ascertain the exact shape of the curve and hence the correct value of dispersivity.

The above-described problems with analyzing doublet breakthrough curves are further complicated by tests employing recirculation, where the input is routed through the aquifer several times and eventually superimposed on the original input.

SECTION 4

REVIEW OF APPROACHES TO TRACER TEST ANALYSIS

The governing equation describing the concentration of a conservative chemical tracer in a homogeneous isotropic medium is:

$$\frac{\partial c}{\partial t} = \frac{\partial}{\partial x_i}\left(D_{ij}\frac{\partial c}{\partial x_j} - u_i c\right) + D_m \frac{\partial}{\partial x_i}\left(\frac{\partial c}{\partial x_i}\right) \qquad (4\text{-}1)$$

where x_i (i = 1,2,3) are Cartesian coordinates, D_{ij} is the dispersion coefficient tensor, u_i (i = 1,2,3) are the components of the seepage velocity vector $\vec{u}$, t is time and D_m is the effective molecular diffusion coefficient. Considering only longitudinal dispersion and neglecting molecular diffusion, Eq. (4-1) is rewritten in terms of a curvilinear coordinate system as:

$$\frac{\partial c}{\partial t} + u\frac{\partial c}{\partial s} = \alpha u \frac{\partial^2 c}{\partial s^2} \qquad (4\text{-}2)$$

where s is the arc length along the direction of flow and α is the longitudinal dispersity, where the longitudinal dispersion coefficient D_{11} is assumed to be the product of a constant dispersivity $\alpha_{11} = \alpha$ and velocity $u_1 = u$. Equation (4-2) is difficult to solve analytically for non-uniform flow cases because the velocity u is a function of s.

Analytical solutions to Eq. (4-2), usually assuming uniform flow (u constant) are frequently used to evaluate data from tracer tests described in the previous section; these include Ogata and Banks (1961); Lenda and Zuber (1970) and Zuber (1974); Sauty (1977, 1978 and 1980); and Grove and Beetem (1971). These solutions are most commonly used to construct dimensionless type curves, where values of dimensionless time vs. concentration are plotted as a function of Peclet number (x/α), and the tracer test breakthrough data is matched to the type curves to obtain a best-fit value of x/α (and hence α, since the distance x is known). In many cases these solutions either have been incorrectly applied to the flow regime of interest or contain unnecessary or incorrect simplifying assumptions which contribute to error in calculating the longitudinal dispersivity value. One of the purposes here is to demonstrate the applicability of the general solution of Gelhar and Collins (1971) (which accounts for non-uniform flow effects) to the radial-flow and two-well tracer tests. Before this analysis is described in detail, however, a brief overview is given of some of the difficulties encountered in applying the "standard" solutions to tracer test results.

Some Solutions to the Advection-Dispersion Equation

1. Ogata and Banks

Ogata and Banks (1961) have presented a set of type curves for a solution to the one-dimensional advection-dispersion equation for a uniform flow field with a step input of mass. Their solution can be expressed in dimensionless form as:

$$\hat{c} = \frac{c}{c_o} = \frac{1}{2}\left\{ \operatorname{erfc}\left[\frac{1 - \hat{t}}{\left(4 \frac{\alpha}{x} \hat{t}\right)^{1/2}} \right] + \exp\left[\frac{1}{\frac{\alpha}{x}} \right] \operatorname{erfc}\left[\frac{1 + \hat{t}}{\left(4 \frac{\alpha}{x} \hat{t}\right)^{1/2}} \right] \right\} \qquad (4\text{-}3)$$

where $\hat{t}$ = dimensionless time = ut/x (x = displacement distance); $\hat{c}$ = dimensionless concentration = c/c_o, where c_o = input concentration; and x/α = Peclet number. For $\alpha/x \ll 1$, i.e., small dispersivities and/or large travel distances, the second term in (4-3) becomes insignificant, and the solution is given as:

$$\hat{c} = \frac{c}{c_o} = \frac{1}{2} \operatorname{erfc}\left[\frac{1 - \hat{t}}{\left(4 \frac{\alpha}{x} \hat{t}\right)^{1/2}} \right] \qquad (4\text{-}4)$$

Equation (4-4) is frequently used as an estimate of the non-uniform divergent radial flow solution. The solution to (4-2) for a divergent divergent radial flow field with a step input is given by Gelhar and Collins (1971) as:

$$\hat{c} = \frac{c}{c_o} = \frac{1}{2} \operatorname{erfc}\left[\frac{1 - \hat{t}}{\left(\frac{16}{3} \frac{\alpha}{R} \hat{t}^{3/2}\right)^{1/2}} \right] \qquad (4\text{-}5)$$

where R = the distance between the injection and observation wells and $\hat{t} = t/t_m$, where t_m is the average arrival time of the front. By comparing (4-4) and (4-5), it can be seen that there is a factor of $\left(\left(\frac{4}{3}\hat{t}^{1/2}\right)^{1/2}\right)$ difference between the two solutions in the denominator of the argument of the erfc function. A comparison of the two solutions is presented graphically in Figure 4-1 for several Peclet numbers. Although the difference between the two solutions decreases with increasing Peclet number, there is still a discrepancy between the two solutions even at high Peclet numbers (e.g., P = 200); therefore, if the uniform flow solution is used as an approximation of the divergent radial flow breakthrough curve, some error will result in making an estimate of longitudinal dispersivity. For large Peclet numbers the use of the one-dimensional solution, (4-5), will lead to an overestimate of the dispersivity by the factor 4/3.

2. Lenda and Zuber

The solutions to the one-dimensional advection-dispersion equation for uniform flow with an instantaneous pulse input (e.g., Crank, 1956) is given in dimensionless form as:

$$\hat{c} = \frac{c}{c_o} = \hat{t}^{-1/2} \exp\left[- \frac{(1 - \hat{t})^2}{4 \frac{\alpha}{x} \hat{t}} \right] \qquad (4\text{-}6)$$

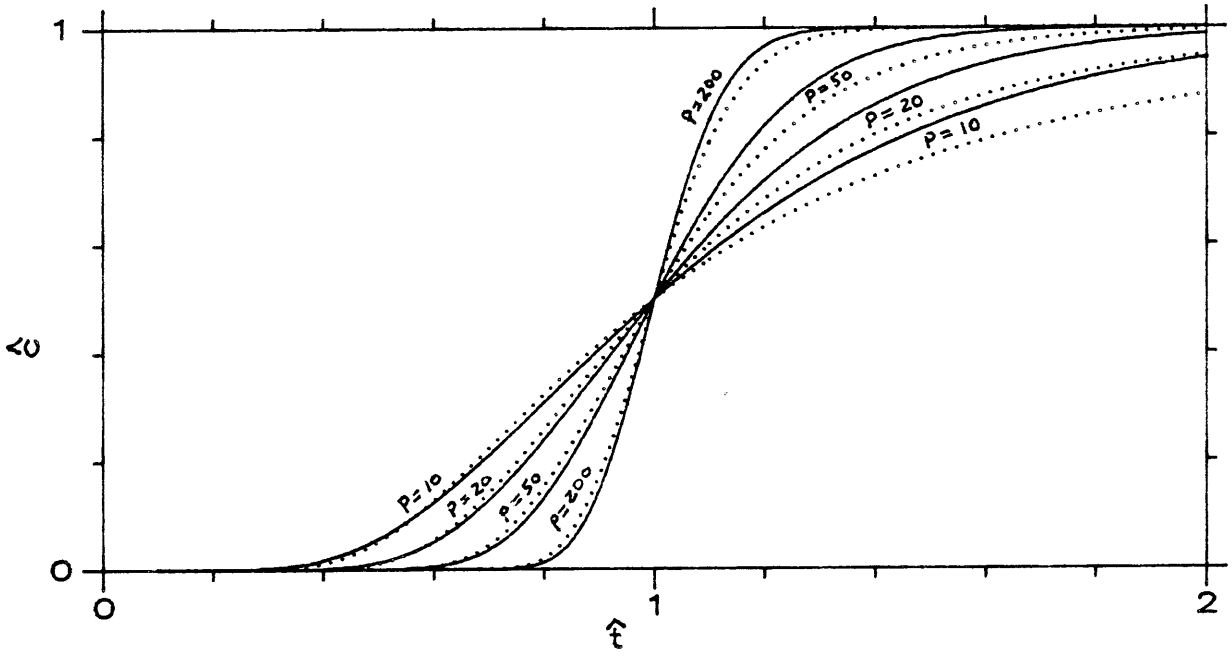

Figure 4-1. Step input in a uniform flow field (solid lines) and a divergent radial flow field (dotted lines) for P = 10, 20, 50, and 200.

where

$$c_o = \frac{M}{\rho n A x (4\pi \frac{\alpha}{x})^{1/2}} ,$$

M is the mass input of tracer, A is the cross-sectional area of the aquifer, ρ = fluid density, n = effective porosity, and x is the distance between injection and observation.

Lenda and Zuber presented an alternative solution for the one-dimensional uniform flow configuration with pulse input which they derived by taking the time derivative of the step input (Eq. 4-3). This is expressed in dimensionless form as:

$$\hat{c} = \frac{c}{c_o} = \hat{t}^{-3/2} \exp \left[\frac{-(1 - \hat{t})^2}{4 \frac{\alpha}{x} \hat{t}} \right] \qquad (4\text{-}7)$$

where

$$c_o = \frac{M}{\rho n A x (4\pi \frac{\alpha}{x})^{1/2}} ,$$

as above. They claim that Eq. (4-7) also provides a good approximation of the radial convergent flow case if the volume of water flowing through the aquifer, Axn, is replaced by $\pi x^2 bn$ where b is the aquifer thickness.

The problem with using Eq. (4-7) to estimate dispersivity is that it does not conserve mass when integrated over the space coordinate. This point is not widely recognized but was mentioned by Zuber (1974), who also remarked that, despite this fact, Equation (4-7) provides a better fit to experimental data than does Equation (4-6) when the tracer distribution in time is measured.

Unfortunately, both Equations (4-6) and (4-7), which are solutions to the advection-dispersion equation for one-dimensional uniform flow with pulse input, are often taken as approximations of the radial flow cases, and as such their use contributes to error in calculating longitudinal dispersivities. Approximate solutions for radial flow cases with pulse input which correctly account for non-uniform flow effects can be derived from Gelhar and Collins (1971) (the derivation is presented later) and are given in dimensionless form for (1) the divergent radial flow case as:

$$\hat{c} = \frac{c}{c_o} = (\frac{4}{3} \hat{t}^{3/2})^{-1/2} \exp \left[\frac{-(1 - \hat{t})^2}{\frac{16}{3} \frac{\alpha}{R} \hat{t}^{3/2}} \right] \qquad (4\text{-}8)$$

where $c_o = \frac{M}{\rho n \pi b R^2 (4 \pi \frac{\alpha}{R})^{1/2}}$, and (2) the convergent radial flow case as:

$$\hat{c} = \frac{c}{c_o} = \left[\frac{4}{3}\left(1 - (1-\hat{t})\left|1 - \hat{t}\right|^{1/2}\right)\right]^{-1/2} \exp\left[\frac{-(1-\hat{t})^2}{\frac{16}{3}\frac{\alpha}{R}\left[1 - (1-\hat{t})\left|1 - \hat{t}\right|^{1/2}\right]}\right] \quad (4\text{-}9)$$

where

$$c_o = \frac{M}{\rho n \pi b R^2 (4\pi\frac{\alpha}{R})^{1/2}} \cdot$$

It can be seen that there is a $\left(\frac{4}{3}\hat{t}^{1/2}\right)$ factor difference between Eq. (4-6) and (4-8) in the denominators of both the exponential term and in the term multiplying the exponential. The two solutions are compared in Figure 4-2; it is evident that if the uniform flow solution of Eq. (4-6) is used to model radial divergent flow, some error will result in determining a value of longitudinal dispersivity. A similar comparison is made in Figure 4-3 between Equations (4-7) and (4-9) for the uniform and radial convergent cases; again, the differences between the two solutions can be visually observed.

Note that the solutions which include the non-uniform radial flow effect (Eqs. 4-8 and 4-9) predict a greater amount of dispersion than the uniform flow solutions (Eqs. 4-6 and 4-7) for a given Peclet number. Thus if fitted to an observed breakthrough curve the uniform flow solutions will tend to overestimate the dispersivity.

3. Sauty

Sauty (1977, 1980) was the first to publish extensive work on type-curve analysis of radial-flow tracer tests. He developed a numerical solution (finite difference code) to the advection-dispersion equation to account for non-uniform flow effects, and presented his results in the form of dimensionless type curves for uniform flow, and for radial divergent and convergent flow, with both step and pulse inputs. This work is now widely used in tracer test analysis.

Sauty was unable to compare his numerical code ("RAMSES") with an analytical solution to the advection-dispersion equation for the radial flow cases with pulse input. Instead, he compared his radial flow results with analytical solutions to the one-dimensional uniform flow equation (comparable to Eqs. (4-6) and (4-7)) and claimed that since there was good agreement between the two, the uniform flow solutions could be taken as adequate approximations of the radial flow case. His comparisons from Sauty (1980) Figures 17 and 18 are presented here as Figures 4-4 and 4-5.

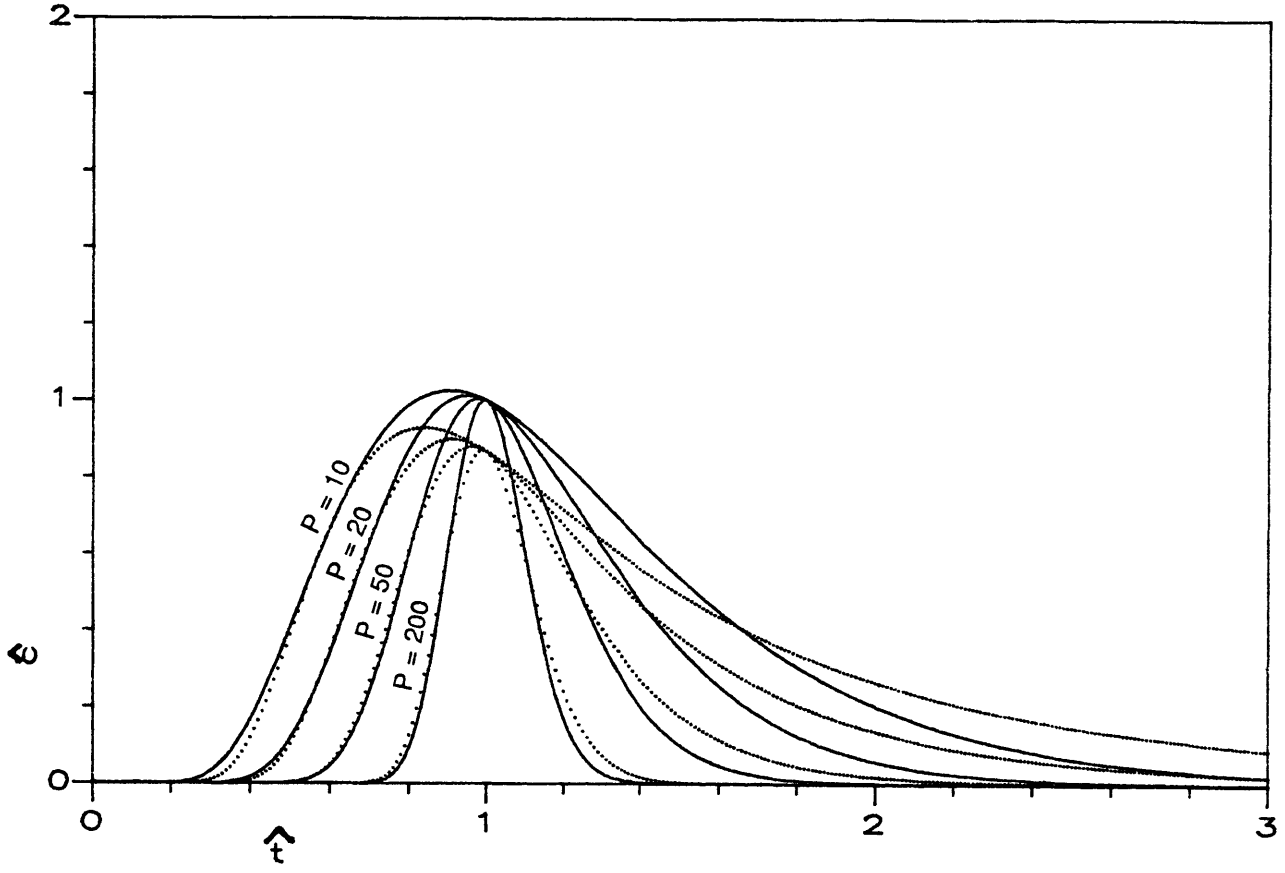

Figure 4-2. Breakthrough curves for a pulse input in uniform flow field (solid lines) after Crank, 1956 (Eq. 4-6), and a divergent radial flow field (dotted lines) after Gelhar and Collins, 1971 (Eq. 4-9) for P = 10, 20, 50, and 200.

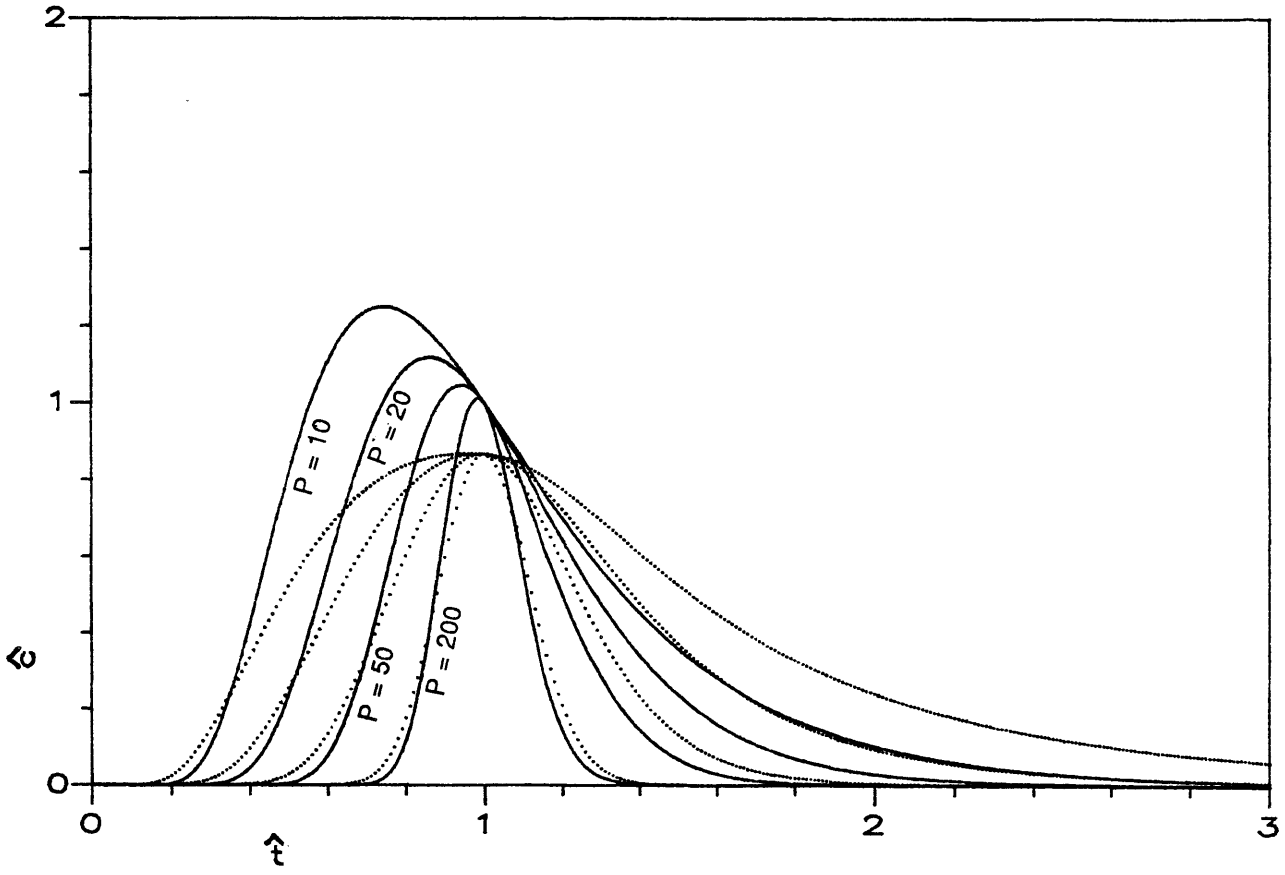

Figure 4-3. Breakthrough curves for a pulse input in a uniform flow field (solid lines) after Lenda and Zuber, 1970 (Eq. 4-7), and a convergent radial flow field (dotted lines) after Gelhar and Collins, 1971 (Eq. 4-9) for P = 10, 20, 50, and 200.

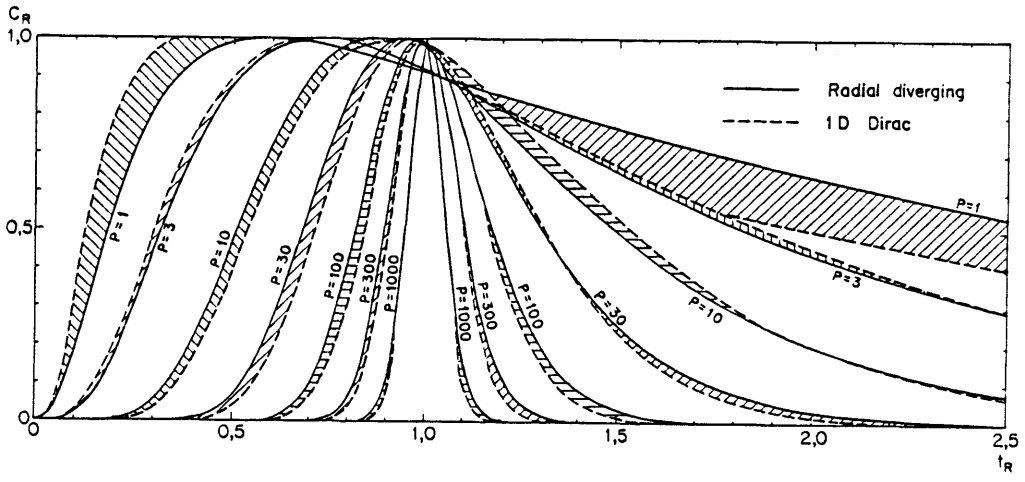

Figure 4-4. Instantaneous tracer injection in a radial divergent flow field; comparison with instaneous injection in a one-dimensional uniform flow field (from Sauty, 1980, Figure 17).

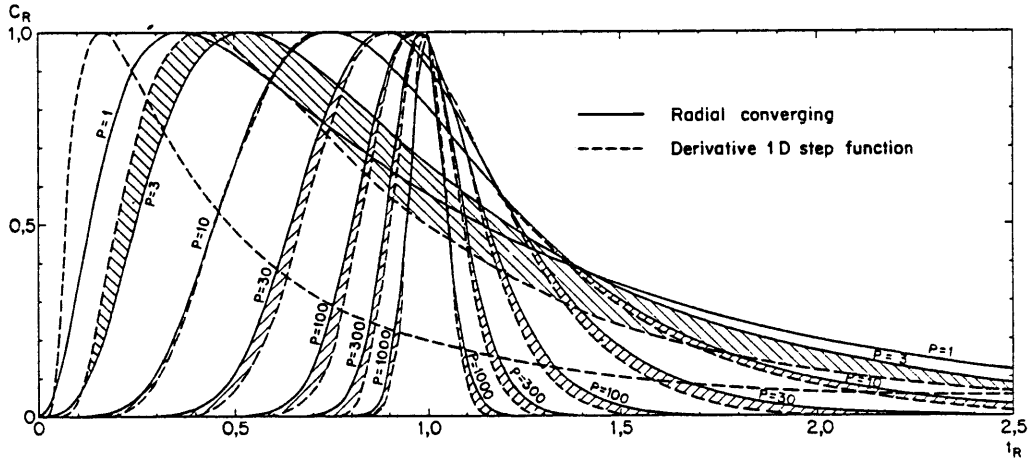

Figure 4-5. Instantaneous tracer injection in a radial convergent flow field; comparison with the derivative of an imposed step function for one-dimensional uniform flow (from Sauty, 1980, Figure 18).

If Sauty's numerical results for pulse inputs in radial flow are compared to the approximate analytical solutions for radial flow given by Equations 4-8 and 4-9 (Figures 4-6 and 4-7), it can be seen that there are significant differences between the numerical solutions and the radial flow analytical solutions, particularly in the tail regions for Peclet numbers between 10 and 100. This may be due in part to the differences in boundary conditions used in the approximate analytical solution and those implied by Sauty's numerical analysis.

Sauty was able to compare his numerical solution for a step input in radially divergent flow with approximate analytical solutions. Figure 4-8 presents a comparison between RAMSES and the analytical solution of Gelhar and Collins (Eq. 4-5) for this case. It can be seen that although there is apparent agreement for large Peclet numbers (i.e., $P \geq 100$), this is because the data were plotted in a form which does not show the high Peclet number differences. Numerical results are not available for Sauty's solution so that the difference at large P cannot be assessed. For $10 < P < 100$, differences between the two solutions are particularly surprising because earlier comparison of the analytical solution for radial flow with numerical solutions (Gelhar and Collins, 1971, Fig. 2) showed good agreement for Peclet numbers above 15. Also, Hsieh (1986) has shown excellent agreement between the approximate analytical solutions for radial flow and a numerical evalution of an exact analytical solution. His exact solution for $P = 10$ is plotted in Figure 4-8; it coincides very well with the approximate solution of Gelhar and Collins (1971). Consequently, we suspect that there are some unrecognized limitations of Sauty's numerical solution.

4. Grove and Beetem

Grove and Beetem (1971) have presented an analysis of the two-well tracer test with a step input that also allows for recirculation of the tracer. The analysis is carried out by viewing the flow field as a number of arcs or stream tubes, calculating the breakthrough curve for each stream tube (each of different length) and summing the curves to obtain a composite breakthrough curve. In this analysis, the authors assumed the velocity to be uniform in each stream tube. This is not the case: the velocity varies with travel distance along the stream tube; however, the assumption of uniform flow does not drastically affect the resulting composite breakthrough curve.

A more important concern about using this sort of tracer-test analysis to determine dispersivity is the reliability of the test itself, since only the initial part of the breakthrough curve is sensitive to dispersion. Because initial breakthrough will be at very low concentrations and usually is not resolved precisely in time, the reliability of the resulting dispersivity estimate will be low. For this reason, we do not recommend the doublet test with a step input for dispersivity determination. The two-well test with a pulse input provides breakthrough curves which are much more sensitive to

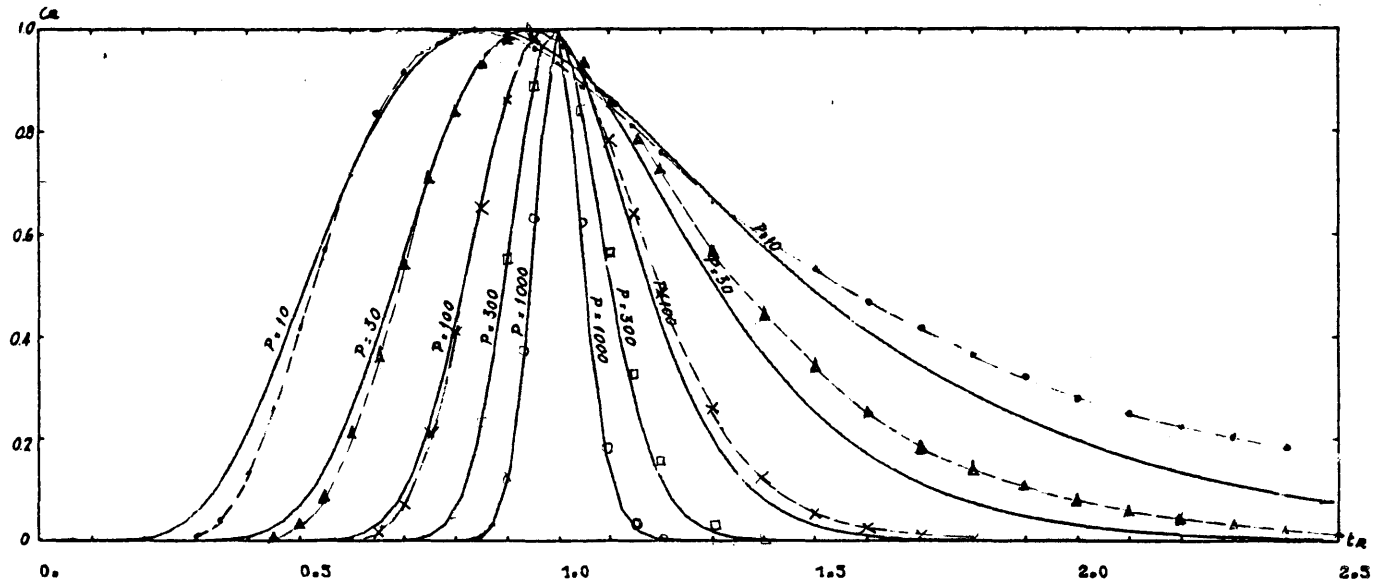

Figure 4-6. Breakthrough curves for a pulse input in a divergent radial flow field. Solid lines represent the numerical solution of Sauty (1977, 1980); dashed lines represent an analytical solution after Gelhar and Collins (1971).

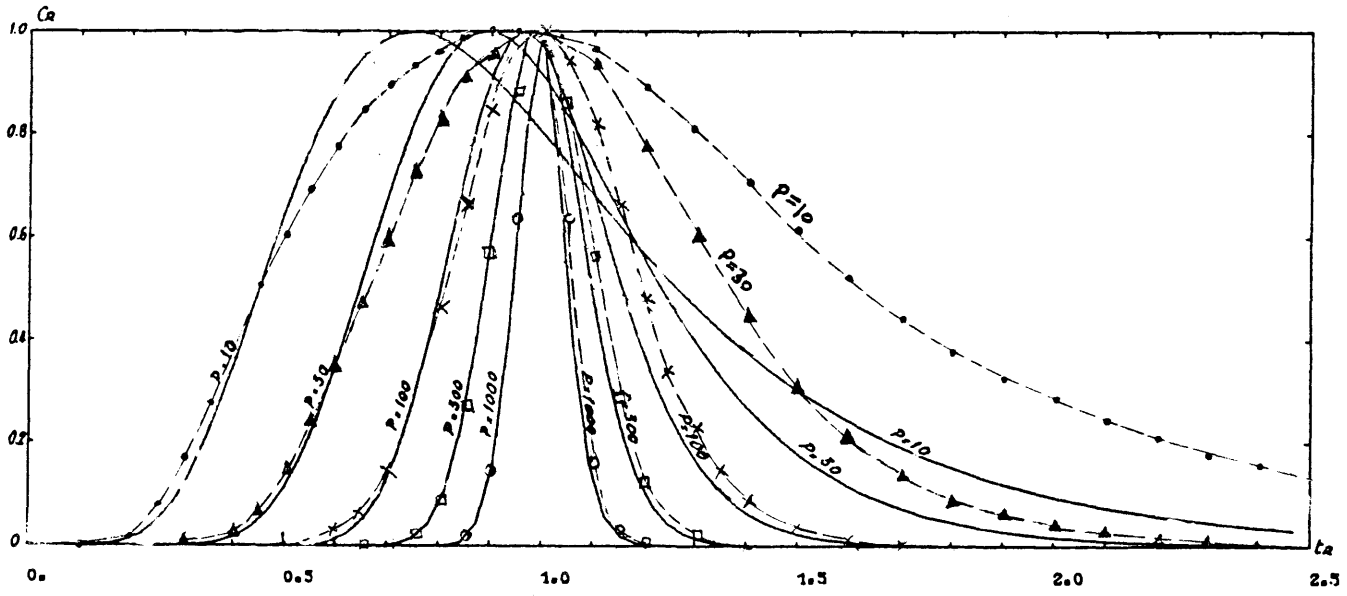

Figure 4-7. Breakthrough curves for a pulse input in a convergent radial flow field. Solid lines represent the numerical solution of Sauty (1977, 1980); dashed lines represent an analytical solution after Gelhar and Collins (1971).

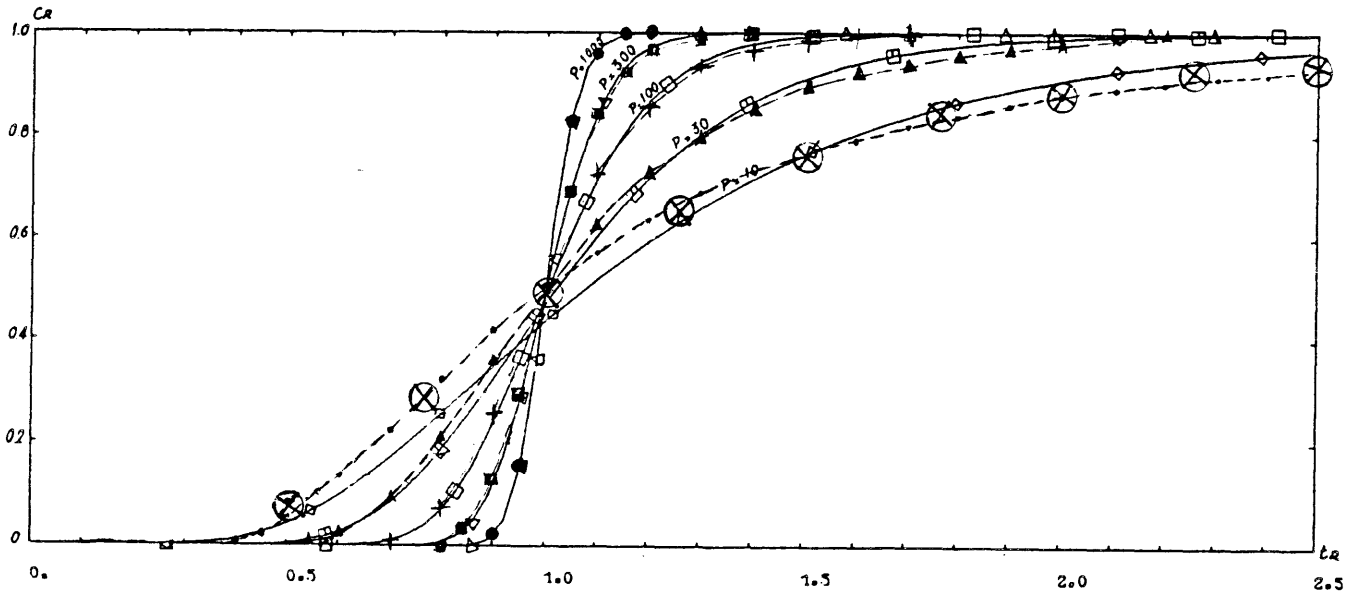

Figure 4-8. Breakthrough curves for a step input in a divergent radial flow field. Solid lines represent the numerical solution of Sauty (1977, 1980); dashed lines represent an analytical solution after Gelhar and Collins (1971). Circles with crosses indicate exact solution for P = 10 by Hsieh (1986).

dispersion. An analysis for evaluating this type of tracer test, based on Gelhar and Collins (1971), is presented in Section 5.

5. Gelhar and Collins

Gelhar and Collins (1971) developed a general analytical solution to Equation (4-2) using a boundary-layer approximation which was shown to be accurate for large P > 10. This solution fully accounts for the variable-convective velocity conditions of a steady non-uniform flow field and hence can be used to obtain an accurate estimate of longitudinal dispersivity from radial flow and two-well tracer tests for many field situations. Their general solution for a pulse input of mass (which conserves total mass of tracer in a stream tube) is given as:

$$c(s,t) = \frac{m}{\rho u(s_o)(4\pi\alpha\omega)^{1/2}} \exp\left[-\frac{\eta^2}{4\alpha\omega}\right] \qquad (4\text{-}10)$$

where

s = distance along streamline

t = time

α = longitudinal dispersivity

$\eta = \tau(s) - t$

$$\tau(s) = \int_{s_o}^{s} ds/u(s), \text{ travel time to } s$$

$$\omega(t) = \int_{s_o}^{\bar{s}} \frac{ds}{[u(s)]^2}$$

$\bar{s}(t)$ = mean location of the pulse at time t

$u(s)$ = seepage velocity

m = mass of tracer per net cross-sectional area of aquifer injected at $s = s_o$ at time $t = 0$.

The solution for a step input of mass can be derived from this result by superposition, and both solutions can be applied to convergent and divergent radial flow fields to obtain specific solutions of c as a function of the Peclet number and time for the flow field of interest. Moreover, if the general results are used in conjunction with the streamline pattern generated by a two-well flow system, specific solutions can be obtained for analysis of dispersivity from two-well tracer tests for both pulse and step inputs. Derivations of these specific solutions from the general result of Eq. (4-10), which can be used to construct type curves, will be presented later.

One problem with the use of this solution is that it is not valid very close to the input source of mass. This is due, among other things, to the limitations of the boundary-layer approximation. The analytical solution was tested against a numerical solution for the step-input radial flow case for divergent and convergent flow fields (Gelhar and Collins, 1971), and it was found that there was very good agreement for Peclet numbers greater than 100 (when the dispersed zone had traveled a distance of 100 times the dispersivity of the medium) and reasonable agreement for Peclet numbers as low as 10. However, for Peclet numbers lower than ~10 the analytical approximations will not produce very good results in most cases. However, it should be recognized that there are other complications with interpretations of breakthrough curves at low Peclet numbers which can also contribute to error in determining longitudinal dispersivity. These problems are discussed in further detail below.

Limitations of Solutions Used to Determine Dispersivity

Two points discussed above regarding problems with interpreting tracer test data bear repetition due to their frequent occurence in the analyses of tracer tests presented in the literature. First, uniform flow solutions are commonly misapplied to radial flow situations. The error incurred in determining longitudinal dispersivity from this type of analysis is illustrated in Figures 4-1 to 4-5 and discussed in the accompanying text. Secondly, uniform flow solutions such as that of Lenda amd Zuber (1974) are not mass-conserving when applied in a radial flow configuration. This may be an important consideration if such solutions are used in tracer design because the peak concentration will not be correctly predicted.

There are several other effects which are not accounted for by the above solutions. The first is the problem with interpretations of breakthrough curves at low Peclet numbers ($P < 10$). In this range, there is a problem with with non-Fickian flow effects (see Gelhar, et al., 1979) in which case the governing equation (Eq. 4-2) is not strictly applicable, and hence the solutions to it are not strictly valid. Also, in this flow region there is the complicating factor of displacement-dependent dispersivity, i.e., dispersivity increasing with displacement distance before it reaches an asymptotic constant value. All of the solutions discussed above assume that dispersivity is constant, and hence are appropriate only after the tracer has traveled a displacement distance of 10 to 100 times the dispersivity value of the medium; i.e., when the dispersivity has reached a constant value. One objective of this report is to modify the solutions of Gelhar and Collins (1971) to Eq. (4-2) to allow for dispersivity that increases linearly with distance, in order to attempt a more realistic evaluation of tracer test data from cases where the dispersivity may not have reached its asymptotic value.

A final problem concerns the interpretation of the extensive tailing exhibited by some breakthrough curves from pulse input/radial flow tests. An example of such a case is illustrated by Figure 4-9. Typically, the type curves discussed in the previous section do not fit the tail area of these breakthrough curves very well. There are several reasons for this phenomenon. First, skewness of the data will occur if the scale of the tracer test is such that non-Fickian effects and displacement-dependent dispersivity come into play. The solutions described previously do not account for these effects. Second, uniform flow solutions to the advection-dispersion equation do not exhibit as much tailing as the radial flow solutions; therefore, use of the wrong solution will contribute to a poor fit to the data. Third, in convergent radial flow tests, the tracer typically does not quickly flush out of the borehole in the form of a pulse; therefore, it would not be reasonable to expect the breakthrough curve from this test to exhibit a symmetrical pulse shape. This "borehole flushing effect" has been demonstrated for convergent radial flow tracer tests conducted in France in fractured media, where the concentration of the tracer leaving the borehole was actually measured as a function of time (Goblet, 1982). It was shown that the shape of the tracer input was approximately an exponentially decreasing function. If this function is convolved with the convergent radial flow solution for a pulse input, the shape of the long tail on the breakthrough curve for this case can be simulated. We show in the next section how the solution of Gelhar and Collins (1971) for the radial convergent case can be so modified to account for this effect.

It should be pointed out that the tracer test literature is replete with examples of tailing breakthrough curves and attendant attempts at interpretation. A review of all data from radial flow tracer tests (Gelhar, et al., 1985) reveals that in many cases the analysis of this shape of breakthrough curve is effected by superposition of two or more type curves with a resulting curve that more or less fits the data (e.g., see Figure 4-9). This superposition of type curves is often justified by attributing the breakthrough shape to several geologic layers each having a different value of dispersivity and hence a different type curve (Sauty, 1977; Ivanovitch and Smith, 1978; and Kreft and Zuber, 1979). The problem with this interpretation is that often it is not or cannot be verified by existing geologic data from the site in question. We show several examples in Section 6 where such assumptions are not needed to achieve a good fit of a type curve to the breakthrough data, if the solution used to derive the type curve accounts for the physical effects influencing the test situation.

It should be apparent from the discussion presented in this section that there are a number of problems with interpreting tracer test data to determine dispersivity. Of all the solutions presented above, Gelhar and Collins (1971) is the only one that accounts for non-uniform flow for all cases of interest. In Section 5 the general result of Gelhar and Collins as given by Eq. (4-2) will be used to obtain specific solutions and type curves for: (1) radially divergent flow with pulse and step inputs; (2) radially convergent flow with a pulse input; and (3) the two-well test with pulse and step inputs. Further, we demonstrate how the results for the radial flow cases can be adjusted to account for linearly increasing dispersivity with distance. Finally, we derive a solution for the radial convergent pulse input case that accounts for the borehole flushing effect.

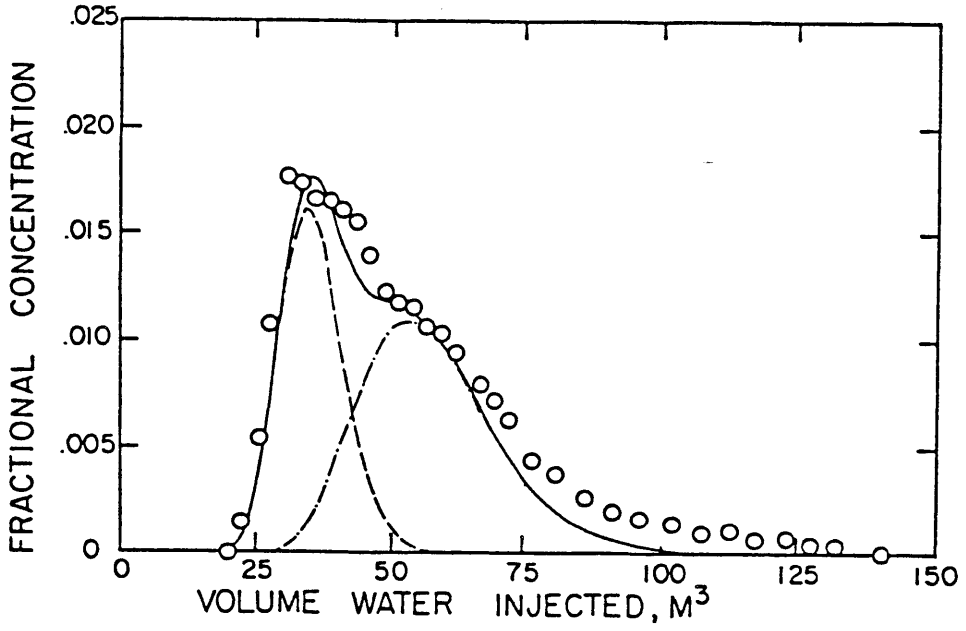

Figure 4-9. Example of a breakthrough curve from pulse injection in radially divergent flow (circles indicate observed values). Two type curves are superimposed to account for tailing (from Hoehn and Roberts, 1982).

SECTION 5

TRACER TEST ANALYSIS BASED ON GELHAR AND COLLINS (1971)

The general analytical result of Gelhar and Collins (1971), which serves as a basis for the analysis presented in this section, is given by Equation 4-10. To derive specific solutions for each case, expressions for m (for the pulse cases), $u(s_o)$, ω and η must be determined and substituted into Equation 4-10. Then either dimensionless type curves may be constructed from the solution expressed in dimensionless form, or a breakthrough-curve, dispersed-zone-width method of analysis can be carried out to determine longitudinal dispersivity from the tracer test data.

Divergent Radial Flow, Step Input

As described in Section 3, in this test a step input of tracer is injected into the recharge well and the breakthrough concentration is measured at an observation well. A cross-sectional sketch for this configuration is shown in Figure 5-1. For initial and boundary conditions given as

$c = c_o$	for	$s < s_o$	
$c = 0$	for	$s > s_o$	at $t = 0$
$c \to c_o$	as	$s \to -\infty$	
$c \to 0$	as	$s \to \infty$	for $t > 0$

the solution of the governing equation (Eq. 4-2) is given by (see Gelhar and Collins, 1971):

$$c = \frac{c_o}{2} \operatorname{erfc}\left[\frac{\eta}{(4\alpha\omega)^{1/2}}\right] \tag{5-1}$$

In radial flow the seepage velocity u(s) can be given by

$$u(s) = \frac{A}{r} \tag{5-2}$$

where

$$A = \frac{Q}{2\pi n b} \tag{5-3}$$

Q = Volumetric recharge rate
n = effective porosity
b = aquifer thickness

When (5-2) is substituted into the definition of $\omega(t)$ ($\alpha\omega$ can be viewed as a time dispersion factor) as given by Eq. 4-10, then

$$\omega(t) = \int_{s=0}^{\bar{s}} \frac{ds}{(u(s))^2} = \int_{r=r_w}^{\bar{r}} \frac{r^2 dr}{A^2} = \frac{\bar{r}^3 - r_w^3}{3A^2} \tag{5-4}$$

where $\bar{r} = \bar{s}$ = mean location of the front

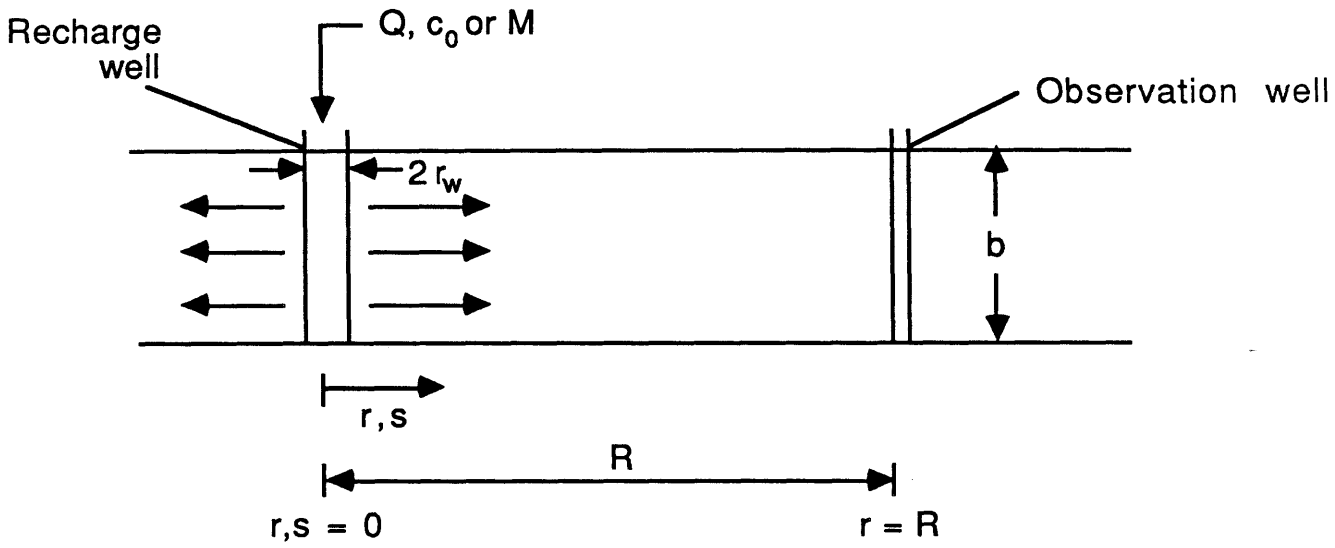

Figure 5-1. Definitional sketch for step input (c_0) or pulse input (M) in diverging radial flow.

and for negligible well radius, i.e., $r_w^3 << \bar{r}^3$,

$$\omega(t) = \frac{\bar{r}^3}{3A^2} \tag{5-5}$$

Next, evaluating $\tau(s)$, the travel time to any s, by substitution of (5-2),

$$\tau(s) = \int_{s=0}^{s} \frac{ds}{u(s)} = \int_{r=r_w}^{r} \frac{r\,dr}{A} = \frac{r^2 - r_w^2}{2A} \tag{5-6}$$

and for negligible well radius (5-6) becomes

$$\tau(s) = \frac{r^2}{2A} \tag{5-7}$$

Then, from (5-7) the average travel time to $\bar{s} = \bar{r}$, the location of the front, can be given by

$$t = \frac{\bar{r}^2}{2A} \tag{5-8}$$

Substituting (5-7) and (5-8) into the definition of η, the result is

$$\eta = \tau(s) - t = \frac{r^2 - \bar{r}^2}{2A} \tag{5-9}$$

When (5-4) and (5-9) are substituted into (5-1), the relative concentration at any point r between the injection well and observation well is given by:

$$\frac{c}{c_o} = \frac{1}{2} \operatorname{erfc} \left[\frac{r^2 - \bar{r}^2}{\left(\frac{16}{3} \alpha \bar{r}^3 \right)^{1/2}} \right] \tag{5-10}$$

This result agrees with the general result of Gelhar and Collins (1971), Eq. 37, with $r_w = 0$ and $D_m = 0$.

Breakthrough Curve-Dispersed Zone Width Method of Analysis for α Constant. The following simple analysis allows an estimate of longitudinal dispersivity to be made from a graph of the breakthrough data from a step input, divergent radial flow tracer test on the basis of Eq. (5-10). As shown in Figure 5-2 the parameters t_{50} and t must be determined graphically for the analysis. t_{50} is the time at which the $c = c_o/2$ concentration occurs; Δt is defined by drawing a line tangent to the breakthrough curve at the t_{50} point and determining the times of intersection with the lines $c = 0$ and $c = c_o$. An expression for Δt is determined from Eq. (5-10) as follows. Recall that

$$\operatorname{erfc} \xi = 1 - \operatorname{erf} \xi = 1 - \frac{2}{\sqrt{\pi}} \int_0^{\xi} e^{-u^2} du \tag{5-11}$$

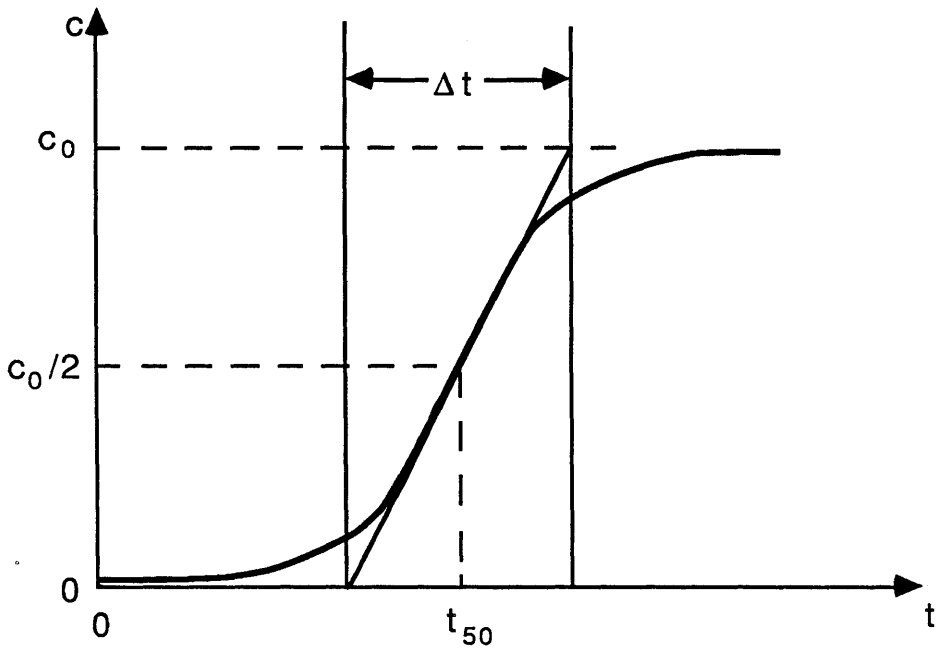

Figure 5-2. Illustration of the breakthrough-curve, dispersed-zone method of analysis for a step input in diverging radial flow.

An expression relating Δt to α then proceeds:

$$\Delta t^{-1} = \frac{\partial}{\partial t}\left(\frac{c}{c_o}\right)\Big|_{r=\bar{r}} = \frac{d\bar{r}}{dt} \cdot \frac{\partial}{\partial \bar{r}}\left(\frac{c}{c_o}\right)\Big|_{r=\bar{r}} \tag{5-12}$$

Making use of (5-11) and recognizing that $\frac{d\bar{r}}{dt} = \frac{A}{\bar{r}}$, and taking $\frac{\partial}{\partial \bar{r}}\left(\frac{c}{c_o}\right)$ at at $r = \bar{r}$, Eq. (5-12) becomes:

$$\Delta t^{-1} = \frac{1}{2}\left(\frac{-2}{\sqrt{\pi}}\right)\frac{A}{\bar{r}}\left[\frac{-2\bar{r}}{\left(\frac{16}{3}\alpha\bar{r}^3\right)^{1/2}}\right] \tag{5-13}$$

which can be written as:

$$\Delta t = \frac{\left(\frac{16}{3}\pi\alpha\bar{r}\right)^{1/2}\bar{r}}{2A} \tag{5-14}$$

Substituting $R^2 = 2At_{50}$ for $\bar{r} = R$ (in Eq. 5-8) and solving for α,

$$\alpha = \frac{3}{16}\frac{R}{\pi}\left(\frac{\Delta t}{t_{50}}\right)^2 \tag{5-15}$$

Using Δt and t_{50} determined graphically, and $\bar{r} = R$ = the distance between the recharge well and observation well, α can be estimated from (5-15). It should be noted that this analysis presumes α to be constant. Note that the result in (5-15) does not depend explicitly on the injection rate Q.

Analysis Using Dimensionless Type Curves for α Constant. In order to construct type curves for this case, Equation (5-10) must be expressed in dimensionless form and evaluated at the observation well. Taking $r = R$ and since from Eq. (5-8) $\bar{r} = (2At)^{1/2}$, Eq. 5-10 becomes:

$$\frac{c}{c_o} = \text{erfc}\left[\frac{(R^2 - 2At)}{\left(\frac{16}{3}\alpha(2At)^{3/2}\right)^{1/2}}\right] \tag{5-16}$$

Letting $t_m = \frac{R^2}{2A}$, the average travel time to $\bar{r} = R$, Eq. (5-16) can be expressed as:

$$\frac{c}{c_o} = \text{erfc}\left[\frac{\left(1 - \frac{t}{t_m}\right)}{\left(\frac{16}{3}\frac{\alpha}{R}\left(\frac{t}{t_m}\right)^{3/2}\right)^{1/2}}\right] \tag{5-17}$$

In dimensionless form, Eq. (5-17) becomes:

$$\hat{c} = \frac{1}{2}\,\mathrm{erfc}\left[\frac{(1-\hat{t})}{\left(\frac{16}{3}\frac{\alpha}{R}\hat{t}^{\,3/2}\right)^{1/2}}\right] \qquad (5\text{-}18)$$

where

$\hat{t} = \frac{t}{t_m}$ = dimensionless time

$\hat{c} = \frac{c}{c_o}$ = dimensionless concentration

$\frac{\alpha}{R} = P^{-1}$ (P = Peclet number)

Then a type curve for a chosen value of α/R is constructed by determini $\hat{c}$ as a function of $\hat{t}$ using Equation 5-18. An example set of type curves for radially divergent flow with step input is presented on log-log paper in Figure 5-3. Longitudinal dispersivity can be determined for a set of tracer test data by plotting the breakthrough curve on the same scale graph paper a matching it to the best-fitting α/R curve. Once α/R is determined from the type curve match, α can be determined directly, since R is known. It should be emphasized that, as in the previous method of analysis presented, longitudinal dispersivity is presumed to be constant in this case.

Analysis Using Dimensionless Type Curve for α Linearly Increasing with Distance. A key limiting assumption in the derivation of Eq. 5-18 is that longitudinal dispersivity is constant. Therefore, for divergent radial flow/step input tracer tests carried out in flow regimes where α is not constant (i.e., low Peclet numbers), problems may be encountered in obtainir a good fit of the breakthrough curve to the type curves given by Eq. 5-18. try to account for this effect, the derivation of Eq. 5-18 can be modified t allow for longitudinal dispersivity to increase as a function of distance. linear increase in dispersivity with distance was chosen for the analysis.

From Figure 5-4, if the average dispersivity is taken to be $\alpha = \bar{\alpha}$ at $r = R/2$, then for any distance r, $\alpha = 2\bar{\alpha}r/R$. If the theory of Gelhar and Collins (1971) is revised to reflect α as a function of distance (see notes this development in Appendix A), then the product $\alpha\omega$ is replaced by

$$\alpha\omega = \int_{r=r_w}^{\bar{r}} \alpha \frac{r^2 dr}{A^2} = \int_{r=r_w}^{\bar{r}} 2\,\bar{\alpha}\frac{r}{R}\frac{r^2}{A^2}\,dr \qquad (5\text{-}19$$

Upon integration, this gives:

$$\alpha\omega = \frac{\bar{\alpha}}{2A^2R}\left(\bar{r}^4 - \bar{r}_w^4\right) \qquad (5\text{-}20$$

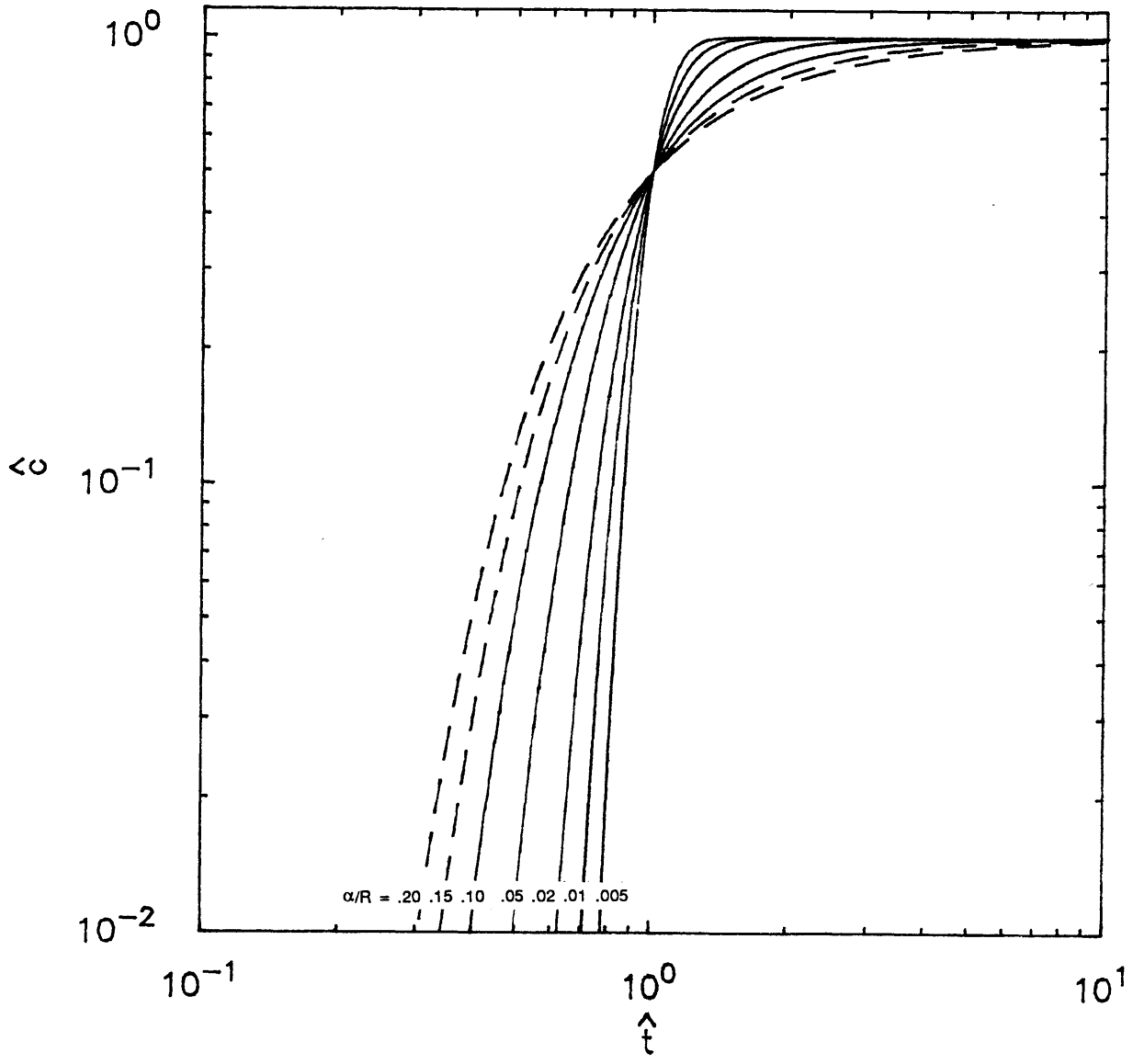

Figure 5-3. Type curves for radially divergent flow with step input, assuming constant dispersivity.

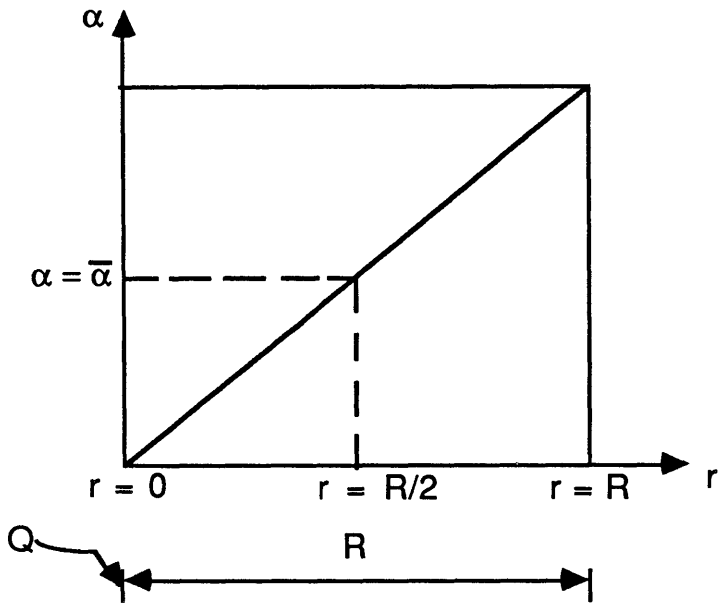

Figure 5-4. Definitional sketch of α vs. r to allow for dispersivity to increase linearly with distance for the radial diverging flow case.

When (5-9) and (5-20) are substituted into (5-1), and if $r << r_w$ the new result is:

$$\frac{c}{c_o} = \frac{1}{2} \text{ erfc } \left[\frac{(r^2 - \bar{r}^2)}{(8 \frac{\bar{\alpha}}{R} \bar{r}^4)^{1/2}}\right] \tag{5-21}$$

Substituting $r = R$ and $\bar{r}^2 = 2At$, (5-21) becomes

$$\frac{c}{c_o} = \frac{1}{2} \text{ erfc } \left[\frac{R^2 - 2At}{(8 \frac{\bar{\alpha}}{R} \cdot 4A^2t^2)^{1/2}}\right] \tag{5-22}$$

and with

$$t_m = R^2/2A \tag{5-23}$$

Eq. (5.22) becomes

$$\hat{c} = \frac{1}{2} \text{ erfc } \left[\frac{(1 - \hat{t})}{(8 \frac{\bar{\alpha}}{R} \hat{t}^2)^{1/2}}\right] \tag{5-24}$$

where $\hat{c} = c/c_o$ and $\hat{t} = t/t_m$

Type curves of $\hat{c}$ as a function of $\bar{\alpha}/R$ and $\hat{t}$ can be constructed from Eq. (5-24). An example set is presented in Figure 5-5. When Figure 5-5 is compared to Figure 5-3, it can be seen that for this case there is some discernable difference in the shape of the type curves due to linearly increasing dispersivity, but this effect is not particularly pronounced. It will be shown in the following section that the shape of the pulse input type curves is much more sensitive to this effect. This result points to the fact that it would be difficult to determine from a breakthrough curve produced by this type of tracer test whether dispersivity is increasing with distance or is in fact constant.

Divergent Radial Flow, Pulse Input

The physical configuration of this test is the same as the one previously described, except that a pulse input of tracer is introduced into the recharge well in place of a constant concentration input. For this reason, much of the analysis is similar for derivation of the concentration solution. The configuration for this case is therefore the same as for the step input (see Fig. 5-1) except that the input is given as mass M instead of as concentration c_o.

If the total mass input of tracer is given as M, then the mass input per unit area of aquifer can be expressed as:

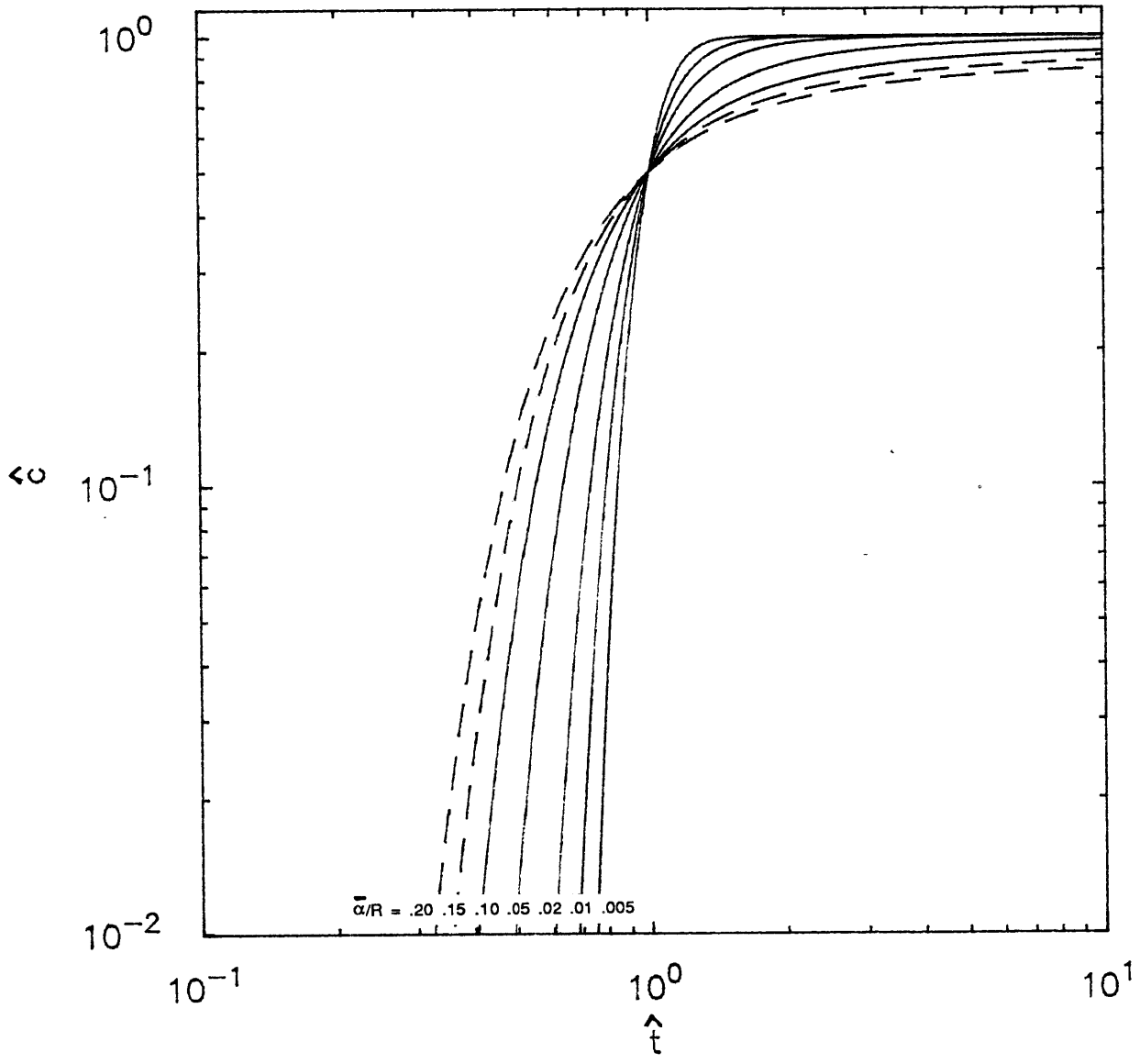

Figure 5-5. Type curves for radially divergent flow with step input, assuming dispersivity increasing linearly with distance.

$$m = \frac{M}{2\pi nbr} \tag{5-25}$$

where n = the effective porosity and r = r_w for the divergent radial flow case. Expressions for u(s), $\omega(t)$ and η are identical to those of the step input case for the divergent radial flow regime, and are given by Eqs. (5-2), (5-5) and (5-9), respectively. When these expressions are substituted into the general solution for a pulse input given by Eq. 4-10 (again assuming $r_w << r$), with $u(s_o) = \frac{A}{r_w}$ the result is:

$$c = \frac{M}{\rho 2\pi nb}\left(\frac{3}{4\pi\alpha\bar{r}^{-3}}\right)^{1/2} \exp\left[\frac{-(r^{-2}-\bar{r}^{-2})^2}{\frac{16}{3}\alpha\,\bar{r}^{-3}}\right] \tag{5-26}$$

Taking r = R, and $\bar{r} = (2At)^{1/2}$ from Eq. 5-8, Eq. 5-26 becomes:

$$c = \frac{M}{\rho 2\pi nb}\left[\frac{3}{4\pi\alpha\,(2At)^{3/2}}\right]^{1/2} \exp\left[\frac{-(R^2 - 2At)^2}{\frac{16}{3}\alpha\,(2At)^{3/2}}\right] \tag{5-27}$$

Letting $\hat{t} = t/t_m$ with $t_m = R^2/2A$, i.e., the average travel time to $\bar{r} = R$, Eq. 5-27 can be expressed as:

$$c = \frac{M}{\rho 2\pi nb}\left[\frac{3}{4\pi\alpha R^3(\hat{t})^{3/2}}\right]^{1/2} \exp\left[\frac{-(1-\hat{t})^2}{\frac{16}{3}\frac{\alpha}{R}(\hat{t})^{3/2}}\right] \tag{5-28}$$

Breakthrough-Curve, Pulse-Width Method of Analysis for α Constant. The longitudinal dispersivity for a set of tracer test data can be estimated using Equation (5-28) by considering the time width of the breakthrough curve at the e^{-1} concentration level relative to the peak concentration, c_m, at time t_m. When $\alpha/R << 1$ the peak occurs at t_m and the pulse is practically symmetric, in which case, from Eq. 5-28,

$$\left(1 - \frac{t}{t_m}\right) = \pm\left[\frac{16}{3}\frac{\alpha}{R}\left(\frac{t}{t_m}\right)^{3/2}\right]^{1/2} \tag{5-29}$$

at the e^{-1} level. Solving for t,

$$t = t_m \pm t_m\left[\frac{16}{3}\frac{\alpha}{R}\left(\frac{t}{t_m}\right)^{3/2}\right]^{1/2} \tag{5-30}$$

Letting $t_1 = t_m - t_m\left[\frac{16}{3}\frac{\alpha}{R}\left(\frac{t_1}{t_m}\right)^{3/2}\right]^{1/2}$ (5-31a)

and $$t_2 = t_m + t_m \left[\frac{16}{3}\frac{\alpha}{R}\left(\frac{t_2}{t_m}\right)^{3/2}\right]^{1/2} \qquad (5\text{-}31b)$$

then $$\Delta t = t_2 - t_1 = t_m \left[\frac{16}{3}\frac{\alpha}{R}\right]^{1/2}\left[\left(\frac{t_2}{t_m}\right)^{3/4} + \left(\frac{t_1}{t_m}\right)^{3/4}\right] \qquad (5\text{-}32)$$

For small α/R, $t_1 \simeq t_2 \simeq t_m$ on the right side of (5-32) and then

$$\alpha = \frac{3R}{64}\left(\frac{\Delta t}{t_m}\right)^2 \qquad (5\text{-}33)$$

Equation (5-33) can be used to determine longitudinal dispersivity from a set of tracer test data for pulse input in radially divergent flow once Δt and t_m are determined for the data set (see Figure 5-6). It is noted that Eq. (5-33) is strictly valid only if α is constant and for relatively small α/R. This expression can be used for initial estimates of dispersivity but a type curve analysis which uses all of the data is needed for accurate analysis when α/R is not small.

Analysis Using Dimensionless Type Curves for α Constant. Type curves may be constructed for this case by expressing Eq. (5-28) in dimensionless form and evaluating it at the observation well as follows:

$$\hat{c} = (\hat{t}^{3/2})^{-1/2} \exp\left[\frac{-(1-\hat{t})^2}{\frac{16}{3}\frac{\alpha}{R}\hat{t}^{3/2}}\right] \qquad (5\text{-}34)$$

where

$\hat{t} = t/t_m$ = dimensionless time

$\hat{c} = \dfrac{c\rho 2\pi nbR^2\left(\frac{4}{3}\pi\frac{\alpha}{R}\right)^{1/2}}{M}$ = dimensionless concentration

$\alpha/R = P^{-1}$ (P = Peclet number)

Type curves for this case may be constructed by graphing $\hat{c}$ as a function of $\hat{t}$ for a chosen α/R, using Eq. 5-34. An example set of type curves for radially divergent flow with pulse input is shown on log-log paper in Figure 5-7. Longitudinal dispersivity may then be determined by matching the observed breakthrough curve with a type curve. Again, it is emphasized that α was assumed to be constant for the above derivation.

Analysis Using Dimensionless Type Curves for α Linearly Increasing with Distance. Equation (5-26) may be modified to allow for dispersivity to increase with distance in an analogous fashion to the step input case for divergent radial flow. Using Figure 5-4 again as a definitional sketch, the expression for $\alpha\omega$ is exactly the same for this case. If u(s), η and $\alpha\omega(t)$ are expressed by Eqs. (5-2), (5-9), and (5-20), respectively (and assuming negligible well radius), substitution into Eq. 4-10 gives as a new result:

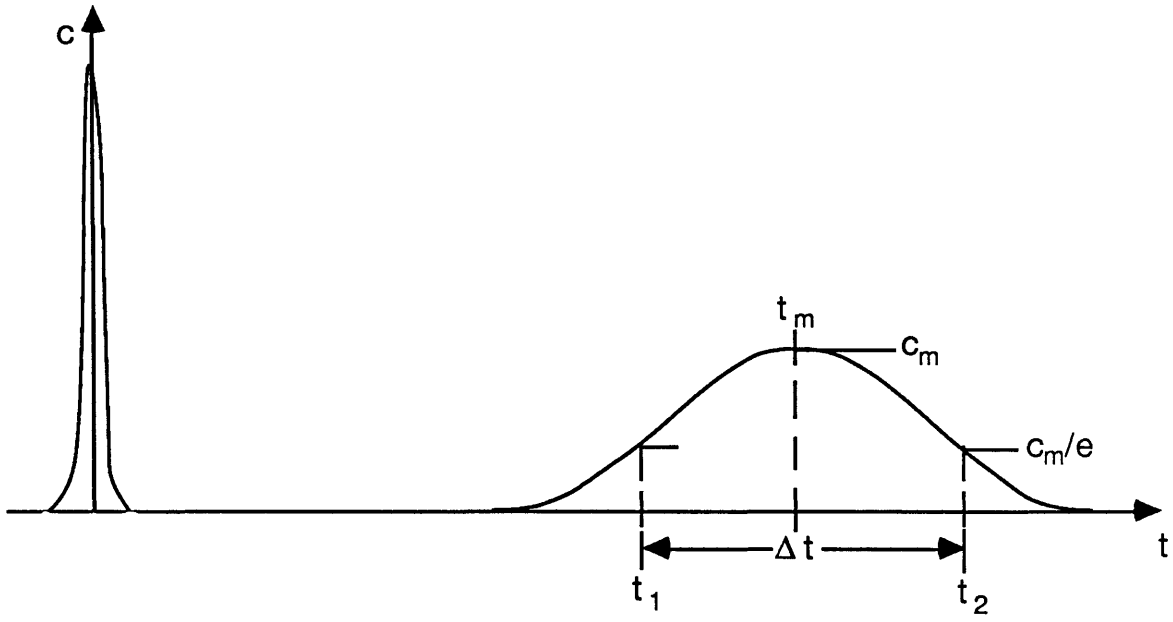

Figure 5-6. Illustration of the breakthrough-curve, pulse-width method of analysis.

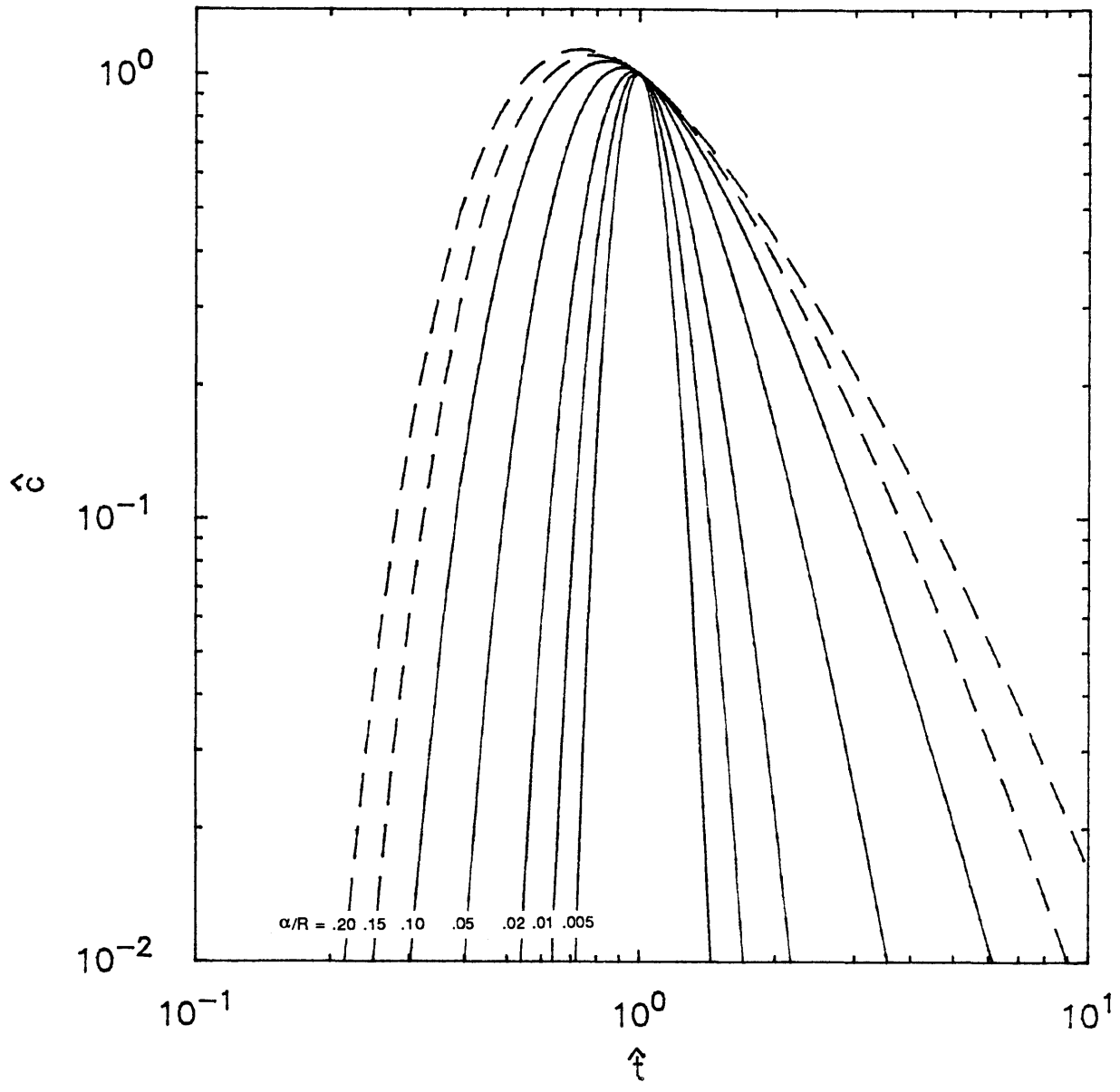

Figure 5-7. Type curves for radially divergent flow with pulse input, assuming constant dispersivity.

$$c = \frac{M}{\rho 2\pi nb}\left(\frac{2\pi\bar{\alpha}\bar{r}^4}{R}\right)^{-1/2} \exp\left[\frac{-(r^2 - \bar{r}^2)^2}{8\frac{\bar{\alpha}}{R}\bar{r}^4}\right] \qquad (5\text{-}35)$$

Substituting $r = R$ and $\bar{r}^2 = 2At$, (5-35) becomes:

$$c = \frac{M}{\rho 2\pi nb}\left(\frac{2\pi\bar{\alpha}4A^2t^2}{R}\right)^{-1/2} \exp\left[\frac{-(R^2 - 2At)^2}{(8\frac{\bar{\alpha}}{R})(4A^2t^2)}\right] \qquad (5\text{-}36)$$

With $t_m = R^2/2A$, Eq. 5-36 becomes

$$c = \frac{M}{\rho 2\pi nb}\left(2\pi\bar{\alpha}R^3\frac{t^2}{t_m^2}\right)^{-1/2} \exp\left[\frac{-(1 - \frac{t}{t_m})^2}{8\frac{\bar{\alpha}}{R}(\frac{t}{t_m})^2}\right] \qquad (5\text{-}37)$$

And in dimensionless form the final solution is:

$$\hat{c} = \left(\frac{3}{2}\right)^{-1/2}\hat{t}^{-1} \exp\left[\frac{-(1 - \hat{t})^2}{8\frac{\bar{\alpha}}{R}\hat{t}^2}\right] \qquad (5\text{-}38)$$

where $\hat{c} = \dfrac{c\rho 2\pi nbR^2\left(\frac{4}{3}\pi\frac{\bar{\alpha}}{R}\right)^{1/2}}{M}$

and $\hat{t} = t/t_m$.

A set of type curves constructed from Eq. (5-38) is presented in Figure 5-8. When Figure 5-7 is compared to Figure 5-8, it can be seen that the tailing exhibited by the type curves in the latter case is much more pronounced. This is a direct result of allowing the dispersivity to increase linearly with distance in the derivation of the solution to the governing equation. This sort of type curve may be used to achieve a better fit of some data from radially divergent flow cases that exhibit long tails and do not fit well to the type curves presented in the previous section for the case where α is presumed to be constant.

Converging Radial Flow, Pulse Input

The breakthrough curve for this case is generated by injecting a mass input of tracer into an observation well and measuring the concentration at a pumping well; Figure 5-9 illustrates this configuration. The velocity u(s) is given by Eq. (5-2) and the mass input per unit aquifer area, m, is given by Eq. (5-25) with r=R. Expressions for $\omega(t)$ and η must be derived for this flow regime and together with (5-2) and (5-25) be substituted into (4-10) to derive an expression for concentration at the recharge well.

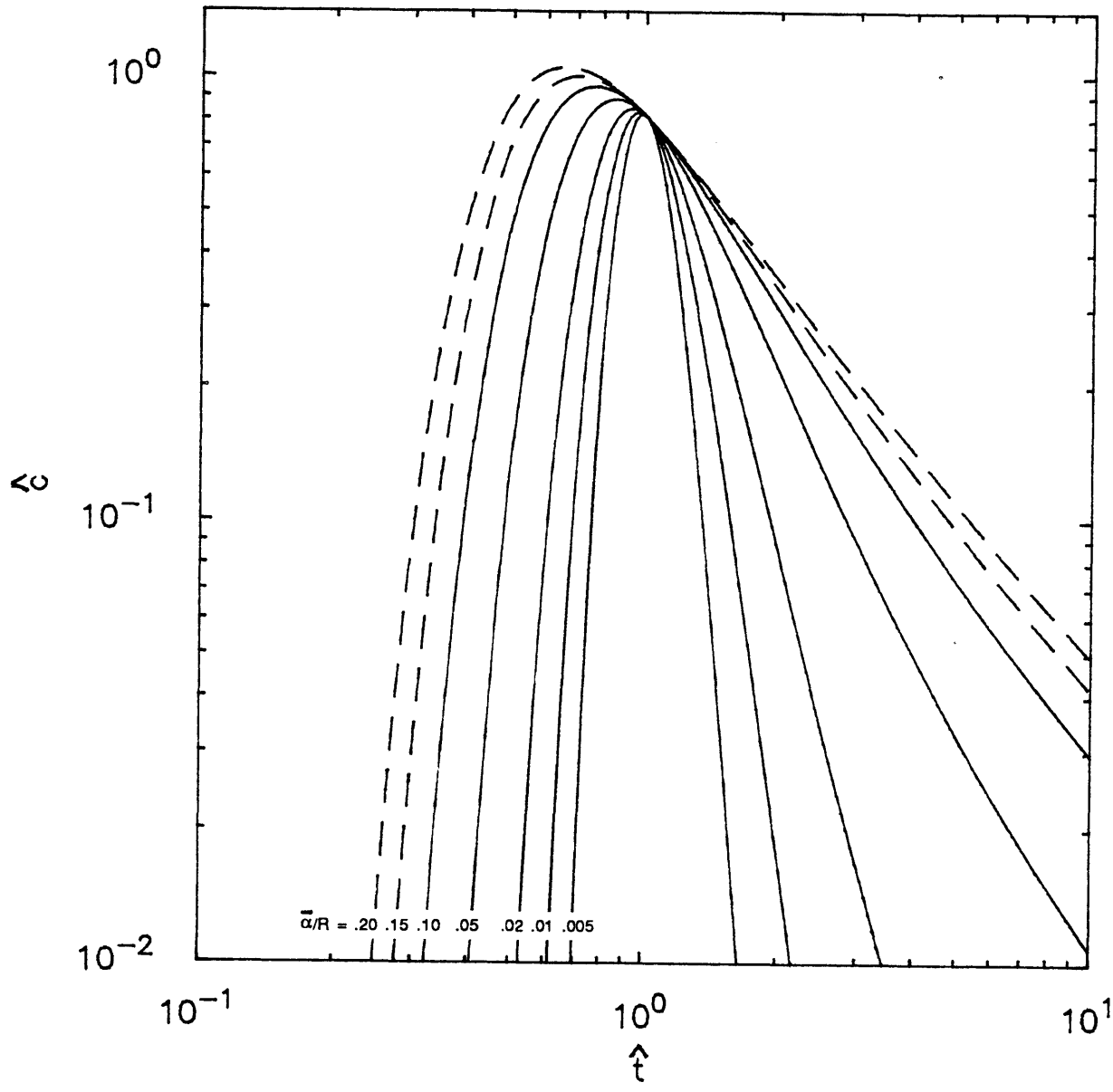

Figure 5-8. Type curves for radially divergent flow with pulse input, assuming dispersivity increasing linearly with distance.

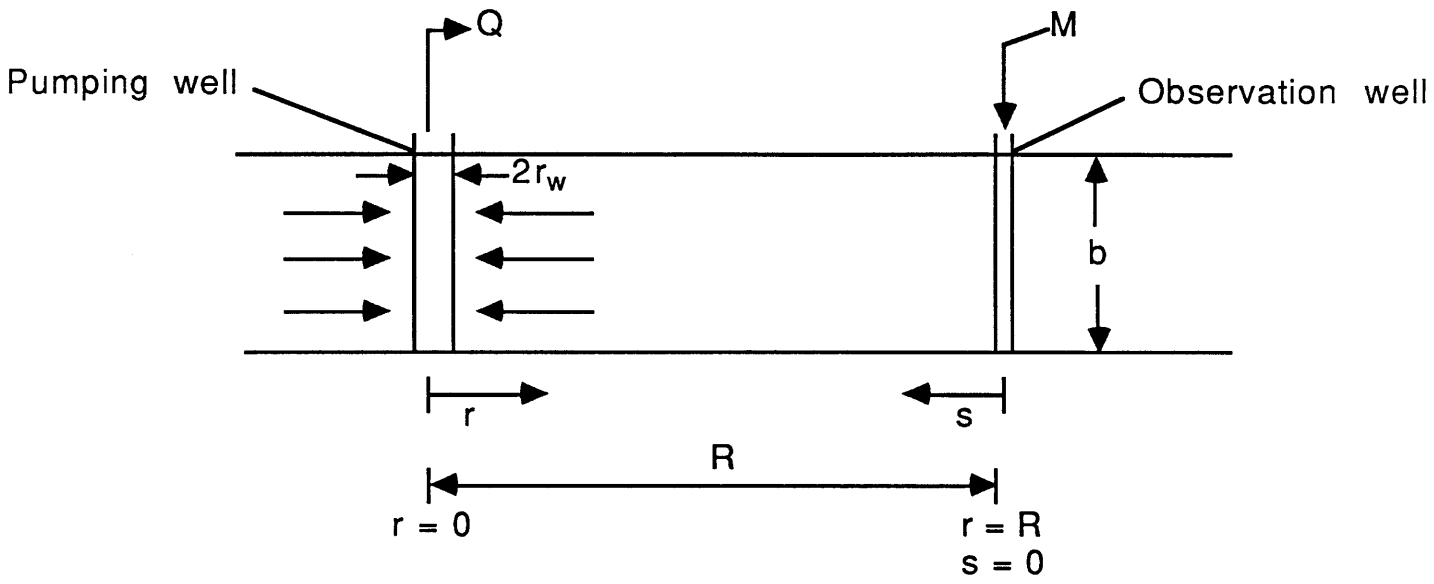

Figure 5-9. Definitional sketch for pulse input (M) in a converging radial flow field.

By definition, $\omega(t) = \int_{s=0}^{\bar{s}} \frac{ds}{(u(s))^2}$. For the convergent radial flow case, and using (5-2), $\omega(t)$ can be written as

$$\omega(t) = \int_{r=\bar{r}}^{R} \frac{r^2 dr}{A^2} = \frac{R^3 - \bar{r}^3}{3A^2} \tag{5-39}$$

The travel time to any s, $\tau(s)$ in conjunction with Eq. (5-2) is given by:

$$\tau(s) = \int_{s=0}^{s} \frac{ds}{u} = - \int_{r=R}^{r} \frac{r\, dr}{A} = \frac{R^2 - r^2}{2A} \tag{5-40}$$

The average travel time t to $\bar{s} = \bar{r}$, the location of the front, can be deduced from (5-40) to be

$$t = \frac{R^2 - \bar{r}^2}{2A} \tag{5-41}$$

Substituting (5-40) and (5-41) into the definition of η, the result is

$$\eta = \tau(s) - t = \frac{r^2 - \bar{r}^2}{2A} \tag{5-42}$$

When the values of m, $\omega(t)$ and η are given by Eqs. (5-25), (5-39) and (5-42), respectively, and these substitutions are made along with $u(s_o)=A/R$ into the general pulse solution given by Eq. 4-10, the result is:

$$c = \frac{M}{\rho 2\pi nb\left(\frac{4}{3}\pi\alpha(R^3 - \bar{r}^3)\right)^{1/2}} \exp\left[\frac{-(r^2 - \bar{r}^2)^2}{\frac{16}{3}\alpha\,(R^3 - \bar{r}^3)}\right] \tag{5-43}$$

Evaluating (5-43) at the pumping well, i.e., at r = 0, and from Eq. (5-41) $\bar{r}^2 = R^2 - 2At$ and $\bar{r} = \left|R^2 - 2At\right|^{1/2}$, Eq. (5-43) becomes: (5-44)

$$c = \frac{M}{\rho 2\pi nb\left[\frac{4}{3}\pi\alpha(R^3-(R^2-2At)\left|R^2-2At\right|^{1/2}\right]^{1/2}} \cdot$$

$$\exp\left[\frac{-(R^2 - 2At)^2}{\frac{16}{3}\alpha\left(R^3-(R^2-2At)\left|R^2-2At\right|^{1/2}\right)}\right]$$

Letting $\hat{t} = t/t_m$ with $t_m = R^2/2A$, the average travel time to $\bar{r} = 0$, Eq. 5-44 can be expressed as:

$$c = \frac{M}{\rho 2\pi nbR^2\left(\frac{4}{3}\pi\frac{\alpha}{R}\right)^{1/2}\left[1-(1-\hat{t})\left|1-\hat{t}\right|^{1/2}\right]^{1/2}} \cdot \exp\left[\frac{-(1-\hat{t})^2}{\frac{16}{3}\frac{\alpha}{R}\left[1-(1-\hat{t})\left|1-\hat{t}\right|^{1/2}\right]}\right] \qquad (5\text{-}45)$$

Breakthrough-Curve Pulse-Width Method of Analysis for α Constant. Following the same method presented for the divergent radial flow case with pulse input (see Figure 5-6), consideration of the pulse width of the breakthrough concentration defined by Eq. 5-45 at the e^{-1} level gives:

$$\left(1-\frac{t}{t_m}\right) = \pm\left[\frac{16}{3}\frac{\alpha}{R}\left(1-(1-\frac{t}{t_m})\left|1-\frac{t}{t_m}\right|^{1/2}\right)\right]^{1/2} \qquad (5\text{-}46)$$

solving for t,

$$t = t_m \pm t_m\left[\frac{16}{3}\frac{\alpha}{R}\left(1-(1-\frac{t}{t_m})\left|1-\frac{t}{t_m}\right|^{1/2}\right)\right]^{1/2} \qquad (5\text{-}47)$$

Letting

$$t_1 = t_m - t_m\left[\frac{16}{3}\frac{\alpha}{R}\left(1-\frac{t}{t_m}\right)\left|1-\frac{t}{t_m}\right|^{1/2}\right)\right]^{1/2} \qquad (5\text{-}48a)$$

and

$$t_2 = t_m + t_m\left[\frac{16}{3}\frac{\alpha}{R}\left(1-(1-\frac{t}{t_m})\left|1-\frac{t}{t_m}\right|^{1/2}\right)\right]^{1/2} \qquad (5\text{-}48b)$$

then

$$\Delta t = t_2 - t_1 = t_m\left[\frac{16}{3}\frac{\alpha}{R}\right]^{1/2}\left\{\left[1-(1-\frac{t_2}{t_m})\left|1-\frac{t_2}{t_m}\right|^{1/2}\right]^{1/2} - \left[1-(1-\frac{t_1}{t_m})\left|1-\frac{t_1}{t_m}\right|^{1/2}\right]^{1/2}\right\} \qquad (5\text{-}49)$$

If $t_m \cong t_1 \cong t_2$, then the $\{\ \}$ term in (5-49) is ≈ 2 and solving (5-49) for α gives:

$$\alpha = \frac{3R}{64}\left(\frac{\Delta t}{t_m}\right)^2 \qquad (5\text{-}50)$$

This is the same approximate result as obtained for the divergent radial flow case. Eq. (5-50) can then be used to determine longitudinal dispersivity from a set of tracer test data for pulse input in a radially convergent flow field, if it can be assumed that α is constant and α/R is relatively small.

Analysis Using Dimensionless Type Curves for α Constant. Type curves may be constructed for the pulse input radial convergent flow case by expressing Eq. (5-45) in dimensionless form and evaluating it at the recharge well as follows:

$$\hat{c} = \left[1 - (1 - \hat{t})\left|1 - \hat{t}\right|^{1/2}\right]^{-1/2} \exp\left[\frac{-(1 - \hat{t})^2}{\frac{16}{3}\frac{\alpha}{R}\left[1 - (1 - \hat{t})\left|1 - \hat{t}\right|^{1/2}\right]}\right] \qquad (5\text{-}51)$$

where $\hat{t} = t/t_m$ = dimensionless time

$\hat{c} = c\rho 2\pi nbR^2(4\pi/3 \cdot \alpha/R)^{1/2}/M$ = dimensionless concentration

α/R = inverse dimensionless distance (inverse Peclet number)

A set of type curves generated using Eq. 5-51 is presented in Figure 5-10. Assuming that longitudinal dispersivity is constant, α can be determined for a set of tracer test data plotted on the same scale graph paper by matching with these type curves.

Analysis Using Dimensionless Type Curves for α Linearly Increasing with Distance. To modify Eq. (5-43) to allow for variable dispersivity, using the definitional sketch presented in Figure 5-11 and $\alpha = 2\bar{\alpha}s/R$, the expression for $\alpha\omega$ is revised as follows:

$$\alpha\omega = \int_{s=0}^{\bar{s}} \frac{\alpha(s)}{u^2(s)} = \int_{r=\bar{r}}^{R} 2\bar{\alpha}\frac{s}{R}\frac{r^2}{A^2}\,dr \qquad (5\text{-}52)$$

Using the relationship $r + s = R$, $\alpha\omega$ is found to be:

$$\alpha\omega = \frac{2\bar{\alpha}}{A^2}\left[\frac{(R^3 - \bar{r}^3)}{3} - \frac{(R^4 - \bar{r}^4)}{4R}\right] \qquad (5\text{-}53)$$

Then with η and $\alpha\omega(t)$ expressed by Eqs. (5-42) and (5-53), respectively, the general pulse solution given by Eq. 4-10 becomes:

$$c = \frac{M}{\rho 2\pi nbR\left(\frac{8\pi\bar{\alpha}}{R^2}\left[\frac{(R^3-\bar{r}^3)}{3} - \frac{(R^4-\bar{r}^4)}{4R}\right]\right)^{1/2}} \exp\left[\frac{-[(r^2 - \bar{r}^2)/2A]^2}{\frac{8\bar{\alpha}}{A^2}\left[\frac{(R^3-\bar{r}^3)}{3} - \frac{(R^4-\bar{r}^4)}{4R}\right]}\right] \qquad (5\text{-}54)$$

Substituting $r = 0$ and $r = R - 2At$, $r = \left|R - 2At\right|$, Eq. (5-54) becomes:

$$c = \frac{M}{\rho 2\pi nbR\left(\frac{8\pi\bar{\alpha}}{R^2}\left[\frac{R^3 - (R^2 - 2At)\left|R^2 - 2At\right|^{1/2}}{3} - \frac{(R^4 - (R^2 - 2At)^2}{4R}\right]\right)^{1/2}} \cdot$$

$$\exp\left[\frac{-(R^2 - 2At)^2}{32\bar{\alpha}\left[\frac{1}{3}\left(R^3 - (R^2 - 2At)\left|R^2 - 2At\right|^{1/2}\right) - \frac{1}{4R}\left(R^4 - (R^2 - 2At)^2\right)\right]}\right] \qquad (5\text{-}55)$$

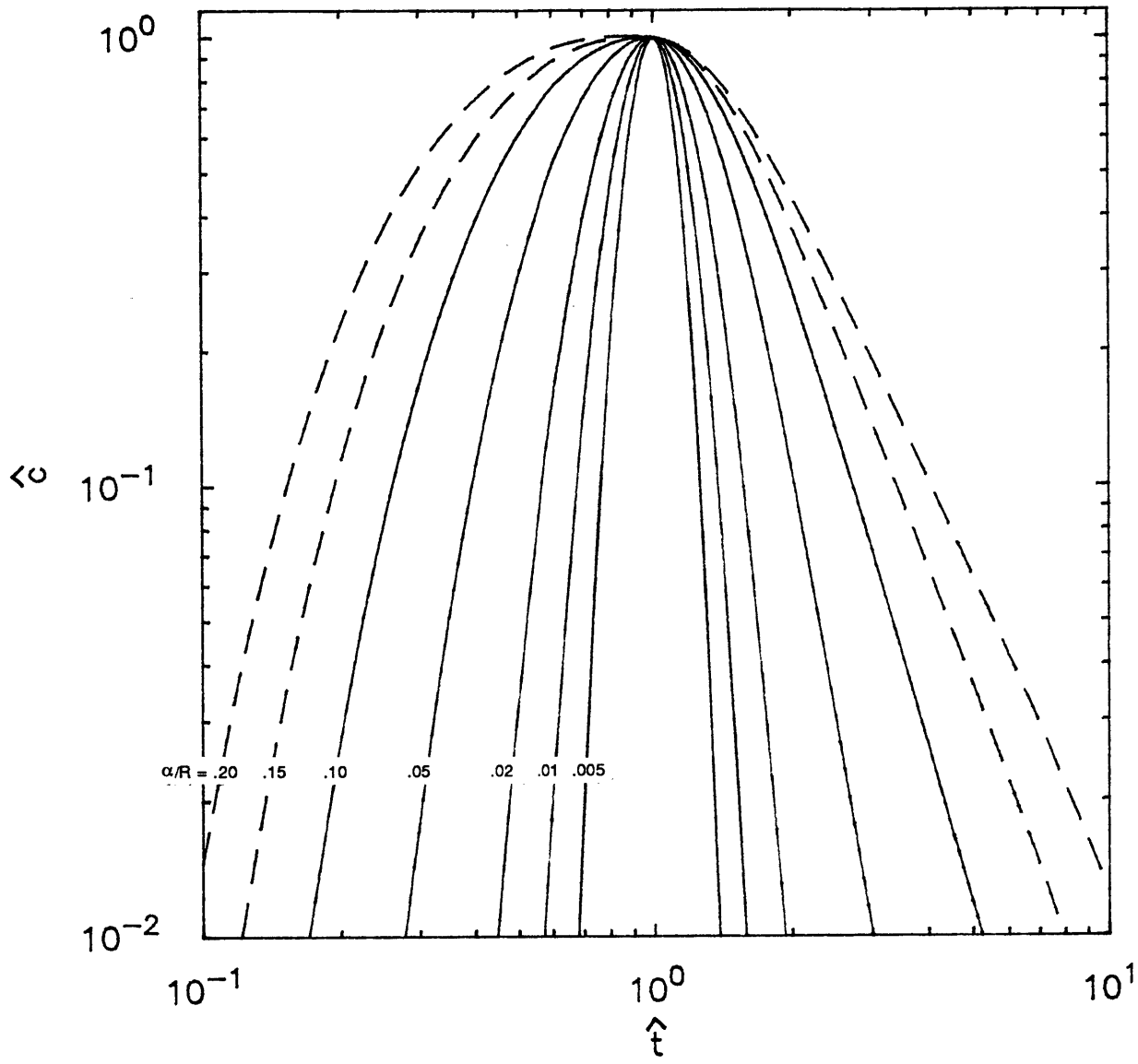

Figure 5-10. Type curves for radially convergent flow with pulse input, assuming dispersivity constant.

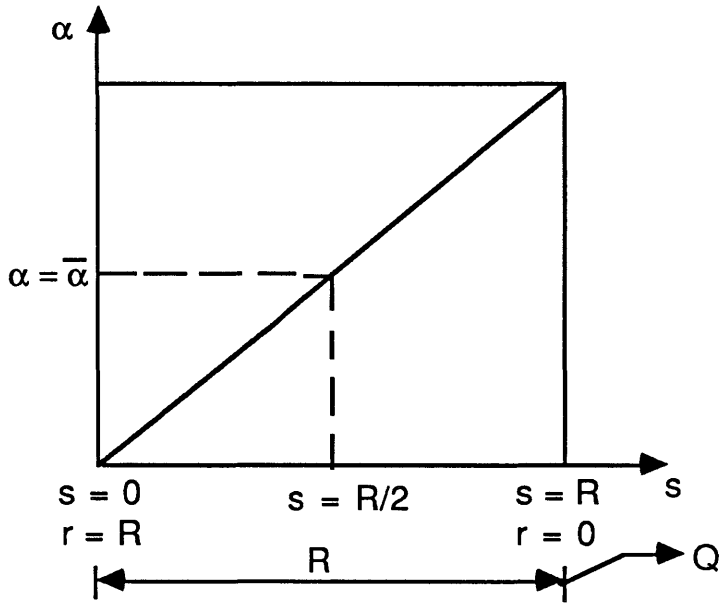

Figure 5-11. Definitional sketch of α vs. s to allow for dispersivity to linearly increase with distance for the radial converging flow case.

with $t_m = R^2/2A$, and

$$\hat{c} = \frac{c\rho 2\pi nbR^2\left(\frac{4}{3}\pi\frac{\bar{\alpha}}{R}\right)^{1/2}}{M}$$

$$\hat{t} = t/t_m \qquad (5\text{-}56)$$

in dimensionless form the final solution is:

$$\hat{c} = \left[2\left(1 - (1-\hat{t})\left|1-\hat{t}\right|\right)^{1/2} - \frac{3}{2}\left(1 - (1-\hat{t})^2\right)\right]^{-1/2} \cdot$$

$$\exp\left[\frac{-(1-\hat{t})^2}{\frac{16}{3}\frac{\bar{\alpha}}{R}\left[2\left(1-(1-\hat{t})\left|1-\hat{t}\right|^{1/2}\right) - \frac{3}{2}\left(1-(1-\hat{t})^2\right)\right]}\right] \qquad (5\text{-}57)$$

A set of type curves constructed using Eq. (5-57) is presented in Figure 5-12. When compared to Figure 5-10, the increased tailing in Figure 5-12 is apparent. This is a direct result of the above analysis which allows for dispersivity to increase as a linear function of distance. Use of this set of type curves for some tracer test data from radially convergent flow cases may provide a better fit to the breakthrough data in cases where increasing dispersivity contributes to the effect of an elongated tail.

Analysis Accounting for Borehole Flushing Effect for α Constant. As depicted by Figure 5-13, in some cases the long tails exhibited by the breakthrough curves from "pulse" input convergent radial flow cases may be due to slow departure of the slug input from the borehole. If the borehole is treated as an ideal mixer and assumed to intercept flow from a width twice its diameter, then with the radial specific discharge given by $q_r = Q/2\pi rb$, the volumetric flow rate intercepted by the borehole is:

$$Q_b = 2dbq_r = \frac{Qd}{\pi R} \qquad (5\text{-}58)$$

where d is the diameter of the borehole and R is the distance between the borehole and the pumping well. The rate of mass input (mass/time) leaving the borehole can then be expressed as

$$\frac{d}{dt}(\rho V_b c) = -\rho Q_b c \qquad (5\text{-}59)$$

where V_b is the volume of the fluid in the borehole.

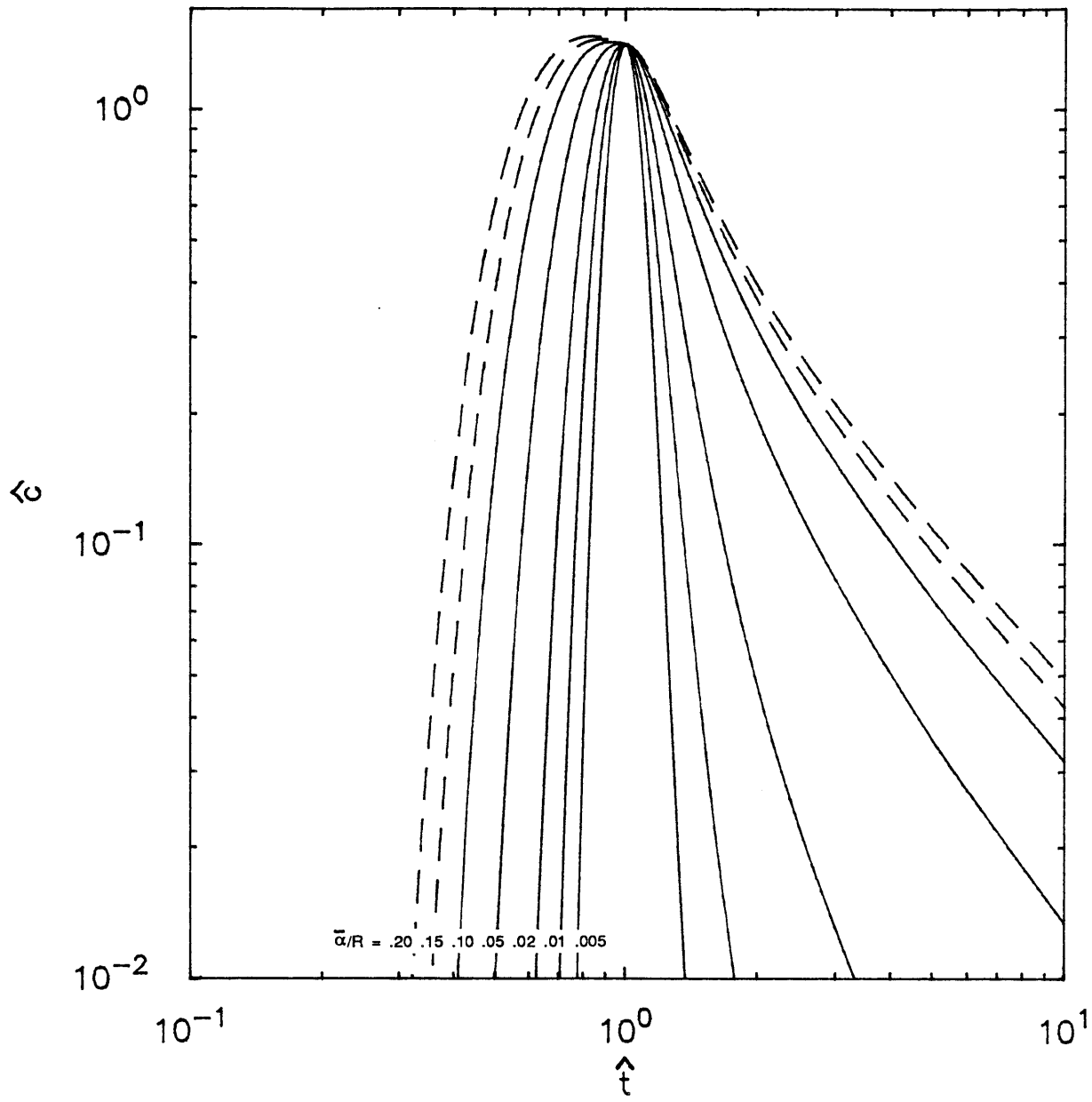

Figure 5-12. Type curves for radially convergent flow with pulse input, assuming dispersivity increasing linearly with distance.

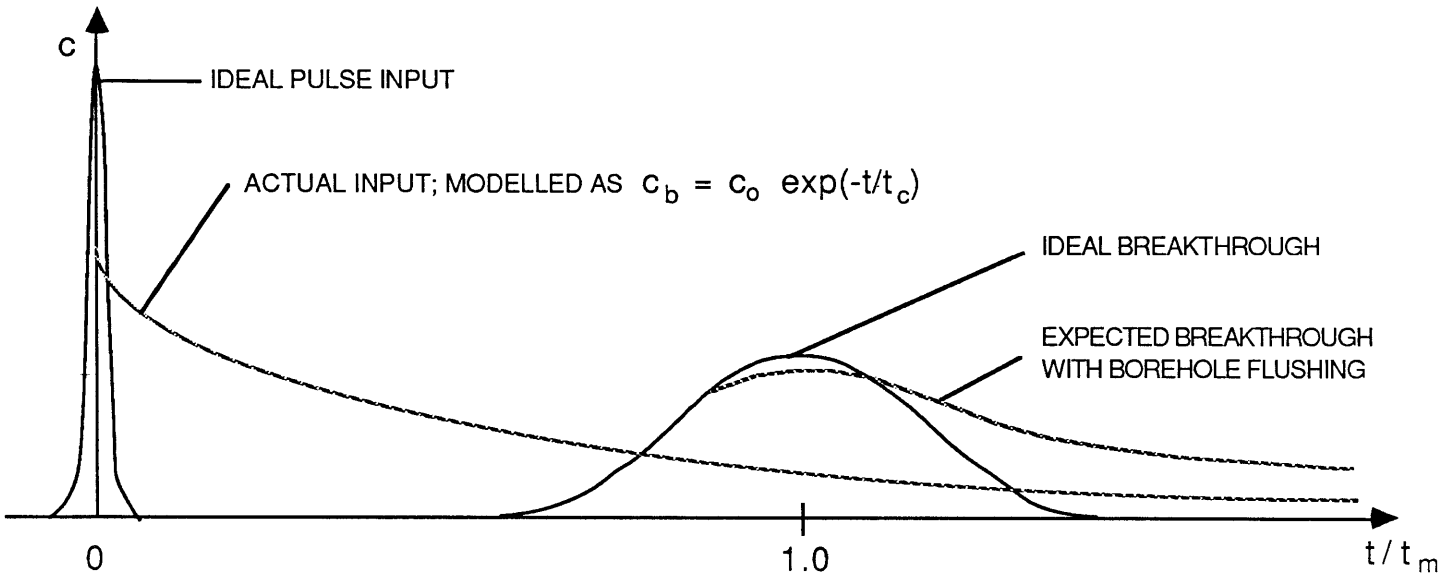

Figure 5-13. Effect of exponentially decreasing concentration input on the shape of the breakthrough curve in the converging radial flow test.

This can be rearranged to give

$$\frac{dc}{c} = -\frac{Q_b}{V_b}\, dt \qquad (5\text{-}60)$$

If t_c is defined as V_b/Q_b, and (5-60) is integrated using the initial condition that $c = c_o$ at $t = 0$, then (5-60) becomes:

$$\ln c = -\frac{t}{t_c} + \ln c_o \qquad (5\text{-}61a)$$

Or equivalently,

$$\frac{c}{c_o} = e^{-t/t_c} \qquad (5\text{-}61b)$$

where $$t_c = \frac{V_b}{Q_b} = \frac{\pi^2 dbR}{4Q} \qquad (5\text{-}62)$$

and

$$c_o = \frac{M}{\rho V_b} \qquad (5\text{-}63)$$

Eq. 5-61 gives the input concentration from the borehole as a function oftime. Convolution of this input concentration with the pulse solution given by Eq. (5-45) for the convergent radial flow case can be used to find the breakthrough curve with the borehole flushing effect as follows. Since the tracer mass input rate from the borehole is a function of time, i.e., $\rho Q_b c = f(t)$, then the incremental mass input is $\Delta M = f(\tau)\Delta\tau$ at time $t = \tau$. If this is convolved with the pulse input solution for $M = 1$, i.e., $c_1(r,t)$, then the breakthrough concentration can be expressed as

$$c = \sum c_1(t - \tau)f(\tau)\Delta\tau \qquad (5\text{-}64a)$$

or

$$c = \int_{\tau=0}^{t} c_1(t - \tau)f(\tau)\, d\tau \qquad \text{as } \Delta\tau \to 0 \qquad (5\text{-}64b)$$

which can be written equivalently as

$$c = \int_{\tau=0}^{t} c_1(\tau)f(t - \tau)\, d\tau \qquad (5\text{-}64c)$$

With M = 1, $c_1(r,t)$ is given at the pumping well by:

$$c_1 = \frac{1}{\rho 2\pi nbR^2 \left[\frac{4}{3}\pi\frac{\alpha}{R}\left[1 - (1 - \frac{t}{t_m})\left|1 - \frac{t}{t_m}\right|^{1/2}\right]^{1/2}\right]} \cdot$$

$$\exp\left[\frac{-(1 - \frac{t}{t_m})^2}{\frac{16}{3}\frac{\alpha}{R}(1 - \frac{t}{t_m})\left|1 - \frac{t}{t_m}\right|^{1/2}}\right] \qquad (5\text{-}65)$$

which in dimensionless form is:

$$\hat{c}_1 = c_1 \rho 2\pi nbR^2 \left(\frac{4}{3}\pi\frac{\alpha}{R}\right)^{1/2} \qquad (5\text{-}66)$$

$f(\tau)$ is given by substituting Eqs. (5-61b), (5-62) and (5-63):

$$f(\tau) = \rho Q_b C = \rho Q_b c_o e^{-\tau/t_c}$$

$$= \rho Q_b \frac{M}{\rho V_b} e^{-\tau/t_c}$$

$$= \frac{1}{t_c} M e^{-\tau/t_c} \qquad (5\text{-}67)$$

which with $\hat{\tau} = \tau/t_m$ is

$$f(\tau) = \left(\frac{M}{t_c}\right) e^{-\hat{\tau}(t_m/t_c)} \tag{5-68}$$

Substituting (5-66) and (5-68) into (5-64b), the dimensionless concentration at the well can then be specified by:

$$\hat{c} = \frac{c\rho 2\pi nbR^2\left(\frac{4}{3}\pi\frac{\alpha}{R}\right)^{1/2}}{M} = \int_{\hat{\tau}=0}^{\hat{t}} \hat{c}_1(\hat{t}-\hat{\tau})\left(\frac{t_m}{t_c}\right) e^{-\hat{\tau}(t_m/t_c)} d\hat{\tau} \tag{5-69}$$

Letting $\theta = \frac{t_m}{t_c}$, the final result in general form is:

$$\hat{c}\left(\hat{t};\frac{\alpha}{R},\theta\right) = \int_{\hat{\tau}=0}^{\hat{t}} \hat{c}_1(\hat{t}-\hat{\tau})\ \theta\ e^{-\theta\hat{\tau}}\ d\hat{\tau} \tag{5-70}$$

or equivalently

$$\hat{c}\left(\hat{t};\frac{\alpha}{R},\theta\right) = \int_{\hat{\tau}=0}^{\hat{t}} \hat{c}_1(\hat{\tau})\ \theta\ e^{-\theta(\hat{t}-\hat{\tau})}\ d\hat{\tau} \tag{5-71}$$

With the full expression for $\hat{c}_1(\hat{\tau})$ substituted into (5-71), $\hat{c}$ is given as:

$$\hat{c}(\hat{t};\ \frac{\alpha}{R},\theta) = \int_{\hat{\tau}=0}^{\hat{t}} \left[1 - (1-\hat{t})\left|1 - \hat{t}\right|^{1/2}\right]^{-1/2} \theta \cdot$$

$$\exp -\left\{\left[\frac{(1-\hat{\tau})^2}{\frac{16}{3}\frac{\alpha}{R}\left(1 - (1-\hat{\tau})\left|1-\hat{\tau}\right|^{1/2}\right)}\right] + \left[\theta(\hat{t}-\hat{\tau})\right]\right\} d\hat{\tau} \qquad (5\text{-}72)$$

where $\hat{t} = \frac{t}{t_m}$

$\hat{\tau} = \frac{\tau}{t_m}$

$\theta = \frac{t_m}{t_c} = \frac{4Rn}{\pi d}$

$\hat{c} = \frac{c\rho 2\pi nbR^2(\frac{4}{3}\pi\frac{\alpha}{R})^{1/2}}{M}$ (c is defined by Eq. 5-64)

The integral expression given by (5-72) can be evaluated numerically to yield type curves as a function of the two parameters α/R and θ. A FORTRAN code to do the numerical integration, and values of $\hat{c}$ and $\hat{t}$ so generated to construct the type curves given in Figure 5-14, are listed in Appendix B.

To effect type curve matching, θ should first be estimated based on the known diameter of the borehole, the porosity of the medium, and the distance between the borehole and pumping well. Then a family of curves of various α/R's can be derived based on this value of θ. Figure 5-14 presents a set of type curves for different values of θ given one value of α/R (= 0.05), in order to illustrate the effect of θ on the shape of the type curve for one value of dispersivity. As $\theta \to \infty$, influence of the borehole flushing effect on the shape of the type curve diminishes; the type curve for θ = 100 falls nearly on top of the standard convergent radial flow case for α/R = 0.05 presented in Figure 5-10. On the other hand, as θ becomes small (<5), the effect becomes pronounced. From the definition of θ ($\theta = nR/\pi d$), the borehole flushing phenomenon is therefore most important in low-porosity geologic settings (e.g., fractured media), and/or for situations of small distance between injection well and borehole, and/or large borehole diameter.

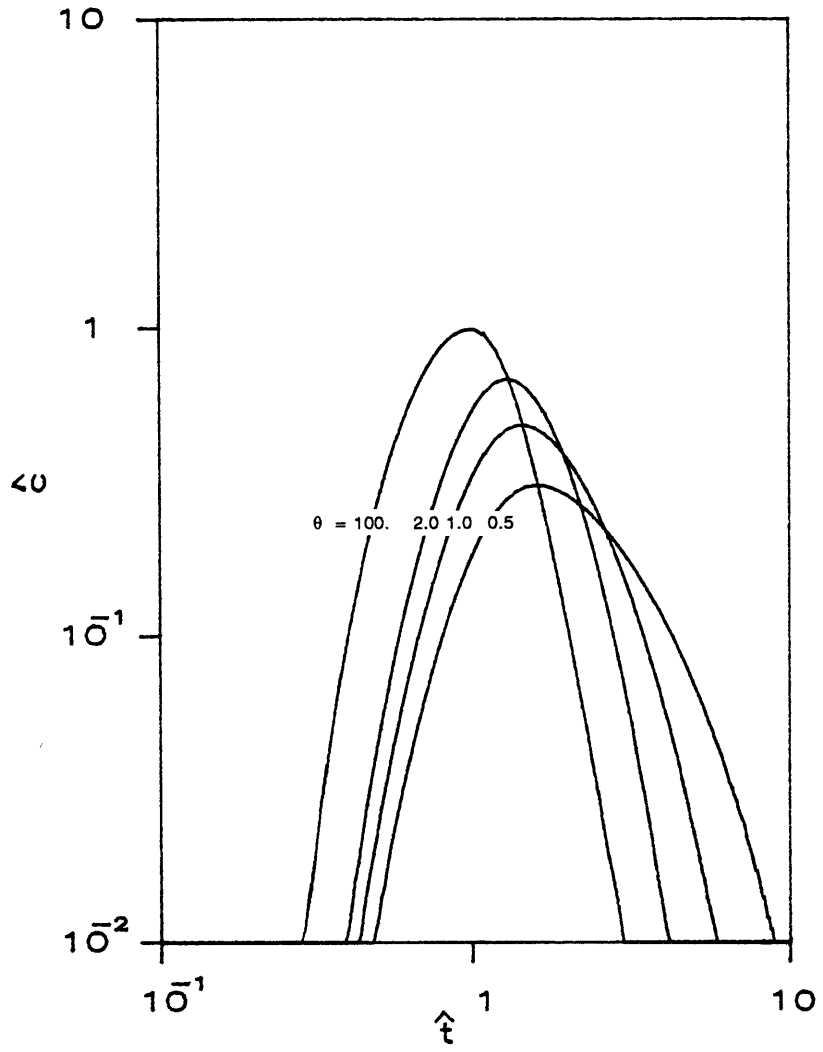

Figure 5-14. Type curves for a pulse input in radial convergent flow with constant α and borehole flushing effect for $\alpha/R = 0.05$.

Analysis Accounting for Borehole Flushing Effect for α Linearly Increasing with Distance. Following the analyses presented previously for the convergent radial flow case to allow for linearly increasing dispersivity, the convolution solution for the borehole flushing effect given by Eq. (5-72) can be similarly modified. Using the definitional sketch presented in Figure 5-11, the expression for $\hat{c}_1$ in 5-71 is replaced by Eq. (5-57). Combining this with the general dimensionless convolution solution given by Eq. (5-71), the dimensionless expression for $\hat{c}$ is then:

$$\hat{c}\ (\hat{\tau};\ \frac{\bar{\alpha}}{R},\theta) = \int_{\hat{\tau}=0}^{\hat{t}} \left[2(1 - (1-\hat{t})\left|1 - \hat{t}\right|^{1/2}) - \frac{3}{2}((1 - (1-\hat{t})^2)\right]^{-1/2} \theta \cdot$$

$$\exp -\left\{ \frac{(1 - \hat{\tau})^2}{\frac{16}{3}\frac{\bar{\alpha}}{R}\left[2\ (1 - (1-\hat{t})\left|1 - \hat{t}\right|^{1/2}) - \frac{3}{2}(1 - (1-\hat{t})^2)\right]} + [\theta(\hat{t} - \hat{\tau})] \right\} d\hat{\tau} \quad (5\text{-}73)$$

for the concentration at the pumping well in convergent radial flow for α linearly increasing with distance and borehole flushing. The dimensionless variables have the same definitions as those of Eq. (5-72). A set of type curves generated from this solution (using a program for numerical integration) for $\bar{\alpha}/R = 0.05$ and various values of θ is presented in Figure 5-15. When Figure 5-15 is compared to Figure 5-14 (the α constant case), it can be seen that there is increased tailing in the latter case produced by the linearly increasing dispersivity. Thus in instances when the combined effect of linearly increasing dispersivity and borehole flushing are responsible for producing long tails on breakthrough curves, these type curves will be useful for estimating α.

Two-Well Tests

Pulse Input, α Constant

The breakthrough curve of this tracer test is generated when a pulse of mass is injected into a recharge well and measured at a pumping well of a two-well flow system (see Figure 5-16). Mathematical analysis of this case is carried out by applying the general theoretical result of Gelhar and Collins given by Eq. 4-10 along each streamline indentified by the stream function ψ. This case has previously been presented in detail by Gelhar (1982) and will therefore only be summarized here.

At the pumping well, the velocity $u(s_o)$ is given by:

$$u(s_o) = Q_r/(2\pi r_w n b) \quad (5\text{-}74)$$

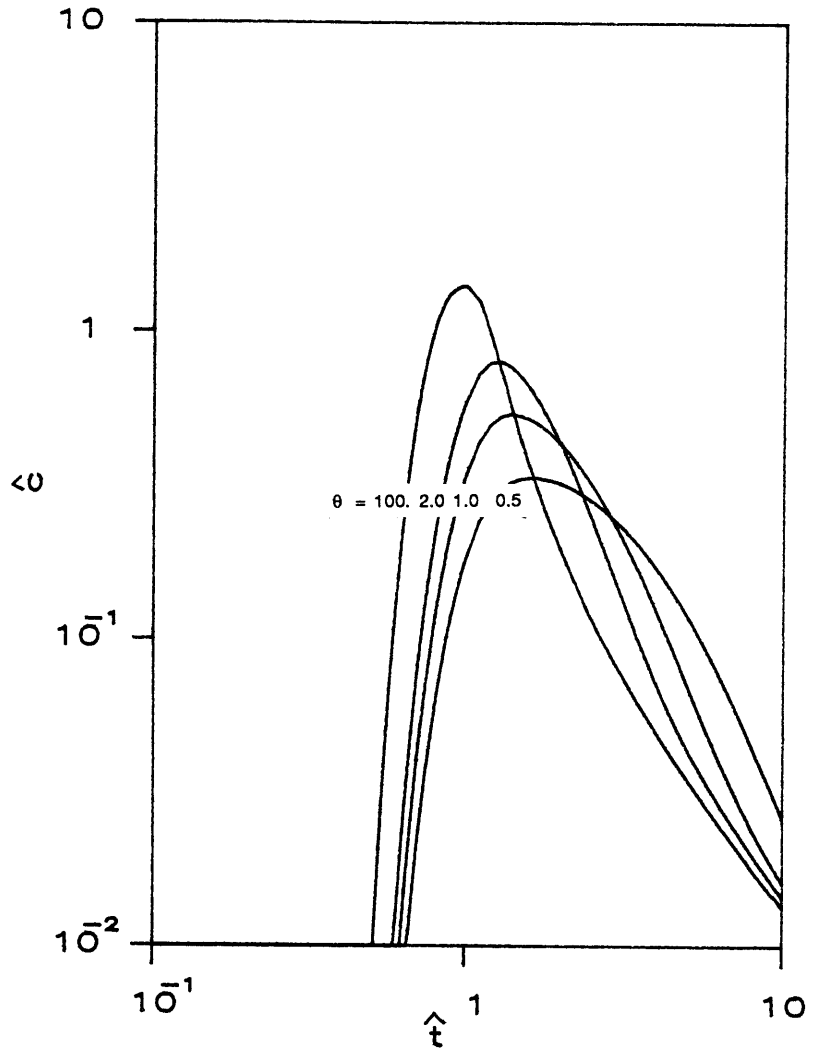

Figure 5-15. Type curves for radial convergent flow with pulse input and borehole flushing effect for α linearly increasing with distance and $\bar{\alpha}/R = 0.05$.

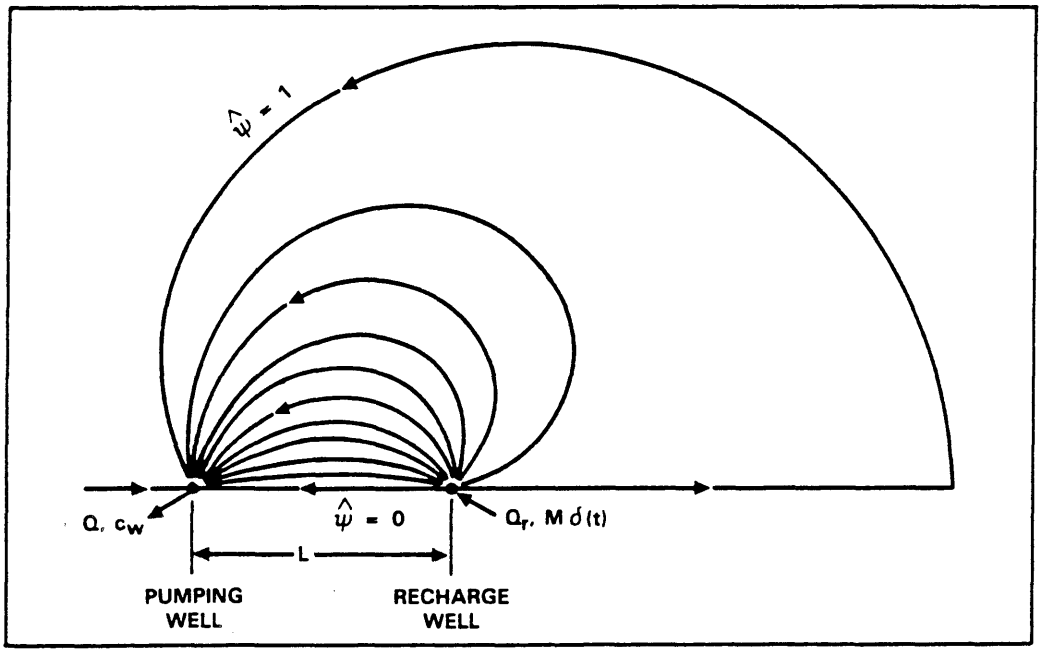

Figure 5-16. Streamline pattern for two-well flow system with Q/Q_r = 2/3. (Note that L = distance between the two wells).

where

Q_r = recharge rate
r_w = well radius
n = effective porosity
b = aquifer thickness
$m = M/2\pi r_w nb$
M = Mass of tracer injected

and therefore

$$\frac{m}{u(s_o)} = \frac{M}{Q_r} \tag{5-75}$$

The flow-weighted concentration at the pumping well can then be determined from the following integral:

$$c_w = \frac{2H}{Q} \int_{\phi=0}^{Q/2b} \left(\frac{M}{\beta Q}\right)(4\pi\alpha\omega)^{-1/2} \exp\left[\frac{-(\tau - t)^2}{4\alpha\omega}\right] d\phi \tag{5-76}$$

where β reflects the ratio of the flow rate of the recharge well to the flow rate at the pumping well (i.e., $\beta = Q_r/Q$). Since the velocity u is dependent on the value of the stream function ϕ, then τ and ω (defined by Eq. 4-10) in this integral also depend on the value of ϕ, i.e., $\tau(s,\phi)$ and $\omega(t,\phi)$. Gelhar (1982) evaluated the integral in (5-76) numerically. The resulting type curves for the equal-flow case are presented in Figure 5-17.

In this analysis, Gelhar assumed transverse dispersion to be negligible for $\alpha/L < 0.1$ because dispersion occurs primarily along the direct streamlines between the two wells, where the solute pulse fronts will be nearly perpendicular to the streamlines. Goblet (1984) tested the validity of this assumption by comparing the analytical results for $\alpha/L = .05$ and $\alpha/L = .02$ with simulations calculated by a numerical finite element code ("METIS") where $\alpha_T = 0.1\ \alpha_L$ was used. The numerical results were in very good agreement with the analytical results, thereby confirming the weak role of transverse dispersivity in the spreading of the solute in this tracer test. A comparison of the analytical and numerical results is shown in Figure 5-18.

Step Input, α Constant. In this two-well test, the breakthrough curve is generated by injecting a constant concentration of tracer continuously into a recharge well and measuring the breakthrough concentration at the pumping well. The solution for the concentration at the well is found by convolution of the pulse-input result with a constant input function of tracer over time.

Type curves generated by numerical integration of the pulse type curves (Fig. 5-17) are given in Figure 5-19. The resulting curves illustrate the relatively weak effect of longitudial dispersivity on the shape of breakthrough curves generated by this test. This causes difficulty in accurately determining the value of α/R when matching breakthrough data to these type curves. For this reason, we do not recommend this test for determining dispersivity. The type curves generated by the pulse input (Fig. 5-17) are much more sensitive to the value of dispersivity and therefore type curve matching for the pulse input case can be more easily carried out.

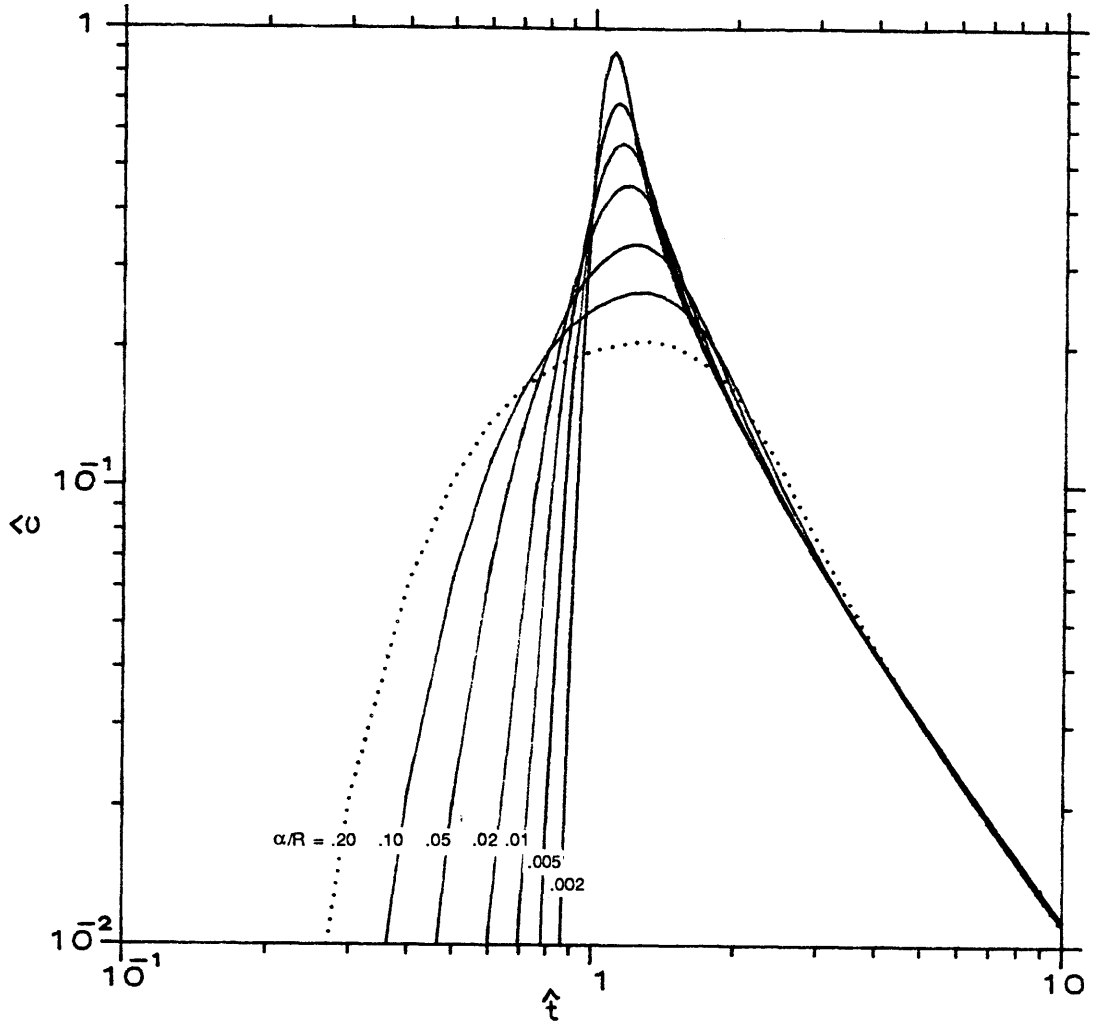

Figure 5-17. Type curves for two-well pulse input test with equal flow (from Gelhar, 1982, Figure 6).

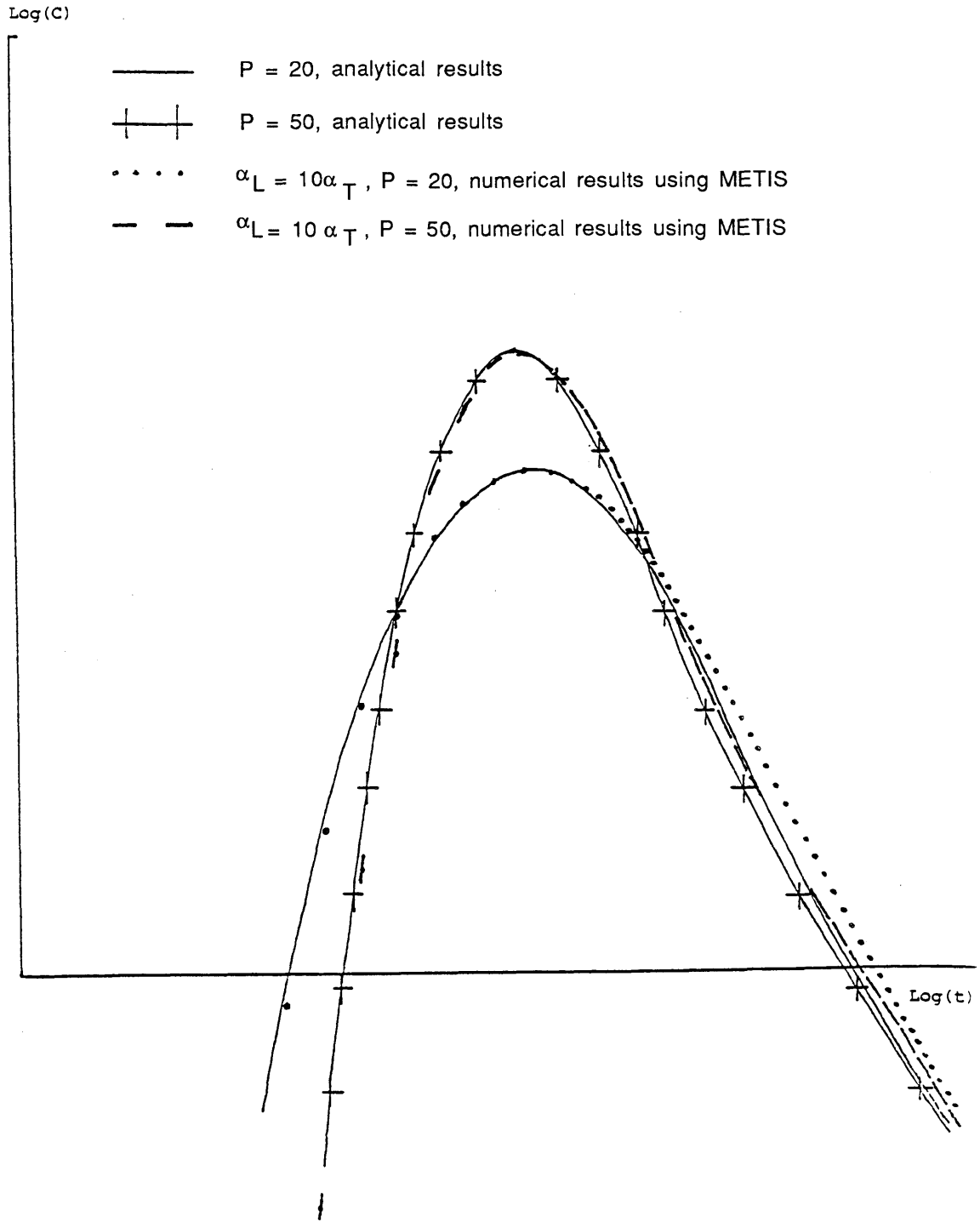

Figure 5-18. Comparison of analytical results and numerical results (using METIS) for two-well tracer test with pulse input (Goblet, 1984).

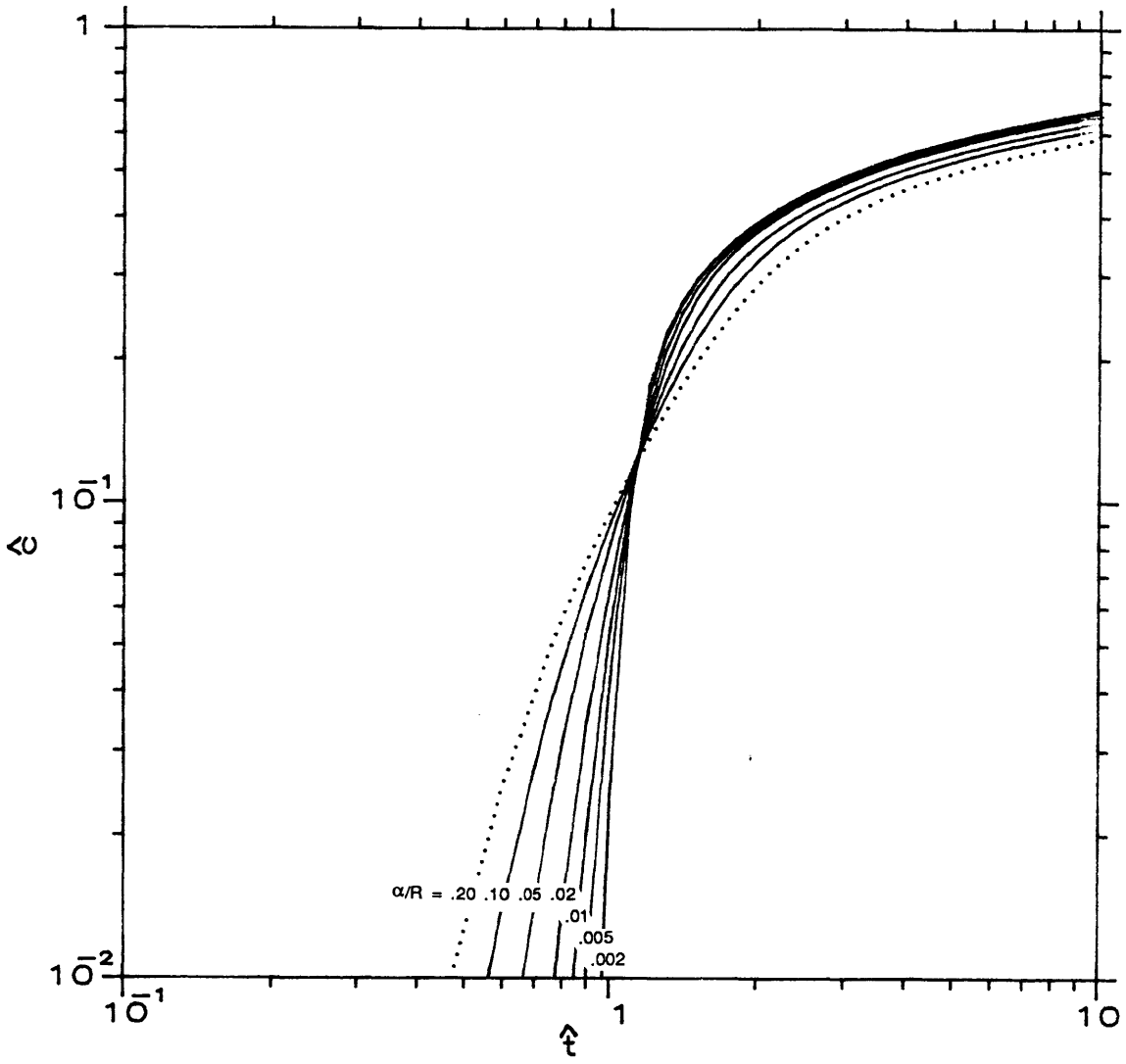

Figure 5-19. Type curves for two-well step input test with equal flow.

SECTION 6

APPLICATION OF THE ANALYTICAL RESULTS TO FIELD-SCALE TRACER TEST DATA

In this section, we illustrate the use of the analytical results presented in Section 5 for determining longitudinal dispersivity from field data. In most cases, the field data have been previously evaluated using other techniques. What we present are alternative methods of analysis and discussion of the merits of both. As will be seen, in some cases there are difficulties in interpreting the tracer test data due to ambiguities in reported results or due to errors in running the tracer tests. It is emphasized that careful design of such tests and complete and accurate reporting of results are essential for achieving the best interpretation of the data possible.

Corbas, France -- Pulse Input in Radial Convergent Flow

This tracer test was performed in a sand and gravel aquifer approximately 12 m thick in France, using iodide as the tracer. An analysis of the data for longitudinal dispersivity using a finite element code was previously presented by Sauty (1977). The data from this test are particularly interesting because observations of breakthrough concentration were taken at three distances from the injection borehole (25, 50 and 150 m), thus providing an opportunity to examine this influence of distance on the shape of the breakthrough curve and hence on the value of dispersivity. The field data are presented in Figure 6-1.

Breakthrough-Curve, Pulse-Width Method of Analysis. Applying the method discussed in Section 5 to Figure 6-1, results for longitudinal dispersivity are calculated and presented in Table 6-1. Note that for this analysis Δt is defined by $c_m/2$ instead of c_m/e, and therefore Eq. (5-50) becomes

$$\alpha = \frac{3R}{64\ln 2}\left(\frac{\Delta t}{t_m}\right)^2 \qquad (6\text{-}1)$$

It can be seen from the results presented in Table 6-1 that the value obtained for α increases with distance from the injection borehole, with an approximately constant Peclet number.

Type-Curve Matching. To use the method of analysis presented in Section 5, the field data are plotted on log-log paper, then aligned with either Figure 5-10 or Figure 5-12 until the best fit is achieved. When type curve matching is attempted using the breakthrough data from the 25 m and 50 m tests (Figs. 6-2 through 6-5) good fits cannot be achieved with either set of type curves. This indicates that some other phenomenon is influencing the shape of the breakthrough curves (i.e., non-Fickian flow effects and/or borehole flushing), thus reinforcing the difficulties encountered in interpreting data from this type of test when run at short distances. Unfortunately, the borehole flushing effect cannot be evaluated for this set of data because the effective porosity and diameters of the boreholes are unknown.

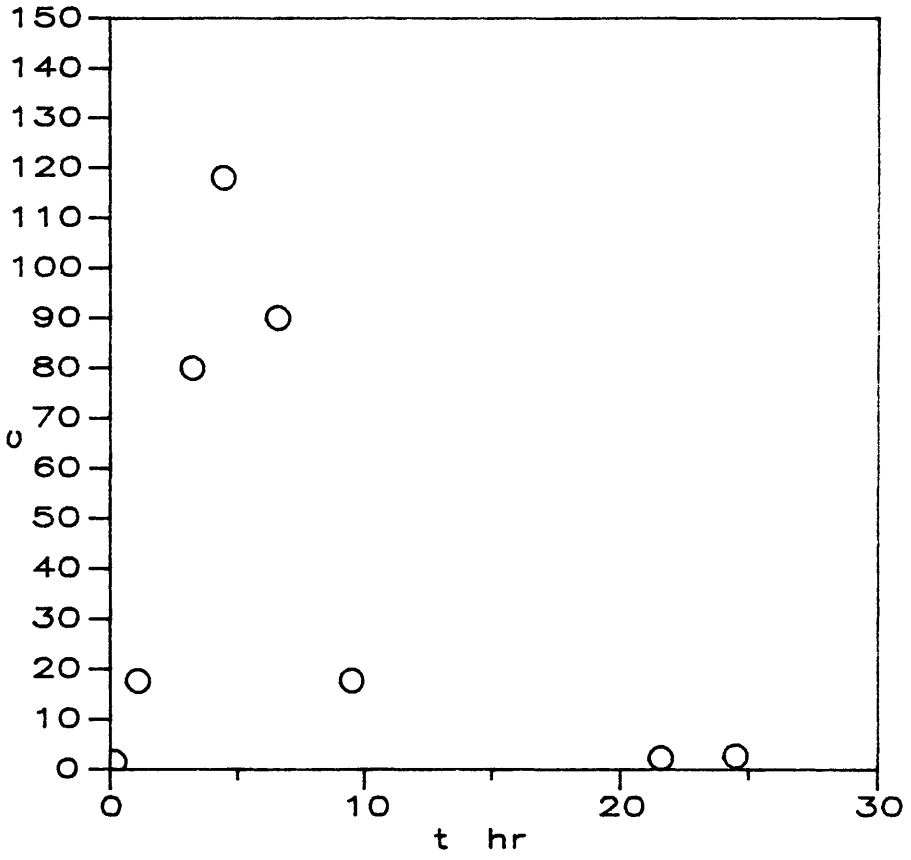

Figure 6-1a. Breakthrough curve at 25 m from a pulse input in a radially convergent flow field at Corbas, France (from Sauty, 1977).

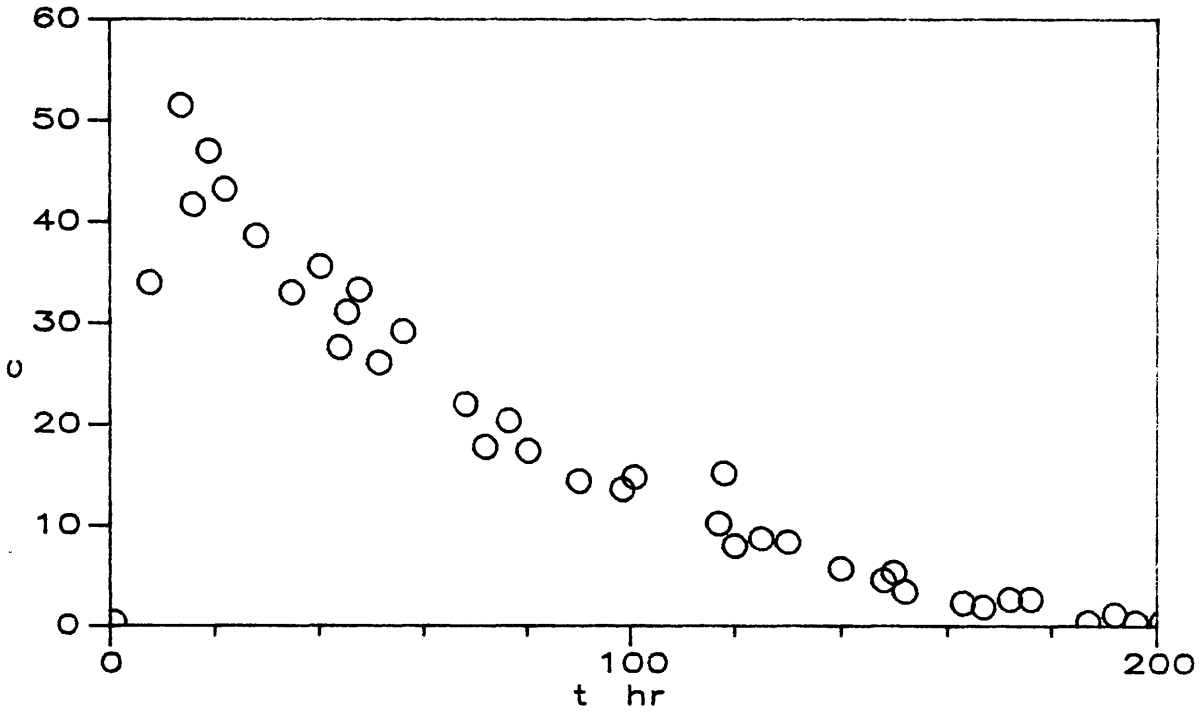

Figure 6-1b. Breakthrough curve at 50 m from a pulse input in a radially convergent flow field at Corbas, France (from Sauty, 1977).

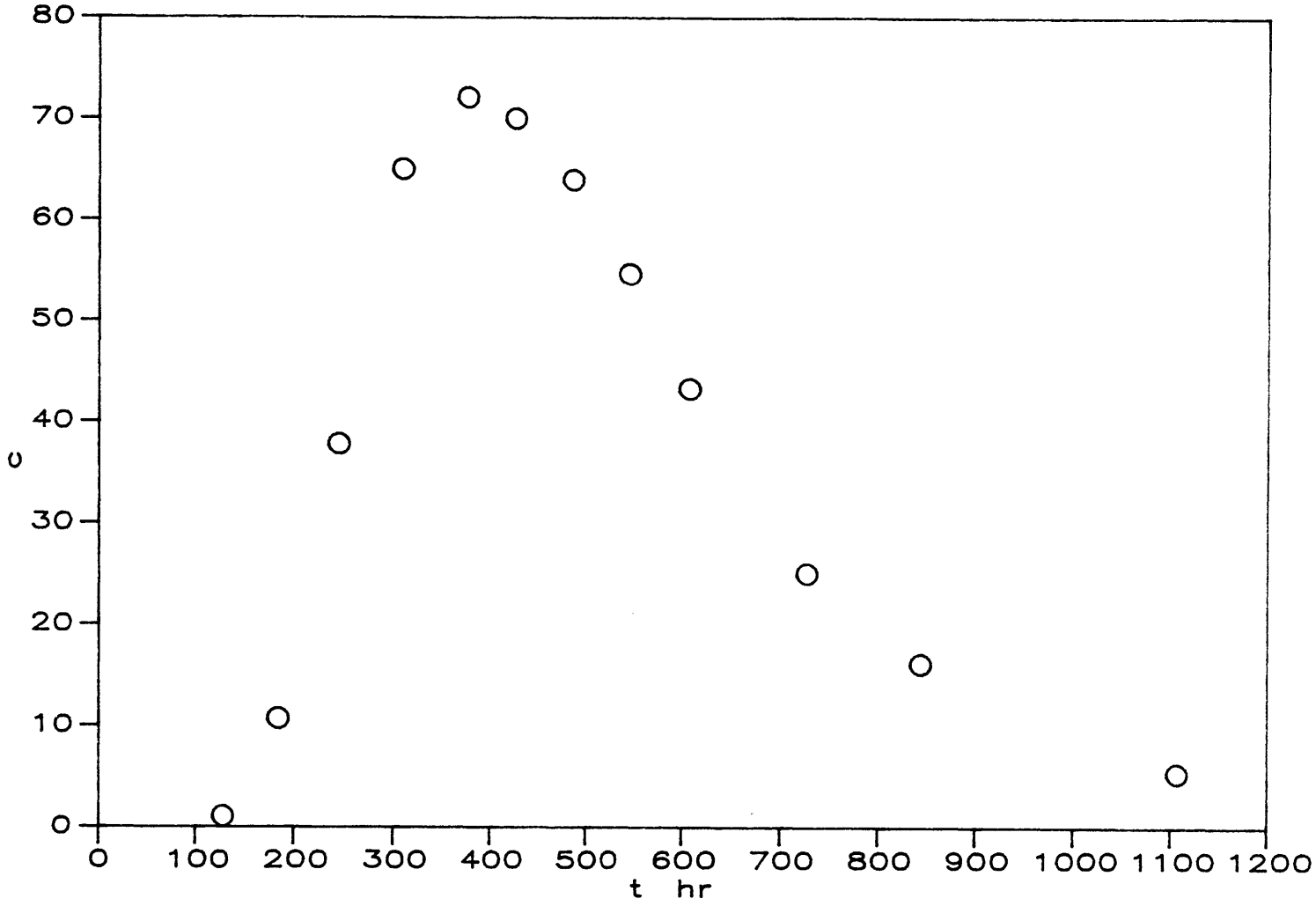

Figure 6-1c. Breakthrough curve at 150 m from a pulse input in a radially convergent flow field at Corbas, France (from Sauty, 1977).

TABLE 6-1

Values of longitudinal dispersivity, determined from the breakthrough-curve, pulse-width method of analysis for a radially convergent flow tracer test (Corbas, France) at three distances from the injection borehole.

R (m)	Δt (hr)	t_m (hr)	$\frac{\alpha}{R}$	α (m)	$\frac{t_m}{t_o}$	$\frac{nb}{Q}$ (hr/m^2)
150	410	400	.07	10.5	.96	.0059
50	20*	17	.092	4.6	.93	.0023
25	6	5	.095	2.4	.93	.0027

* twice rise time.

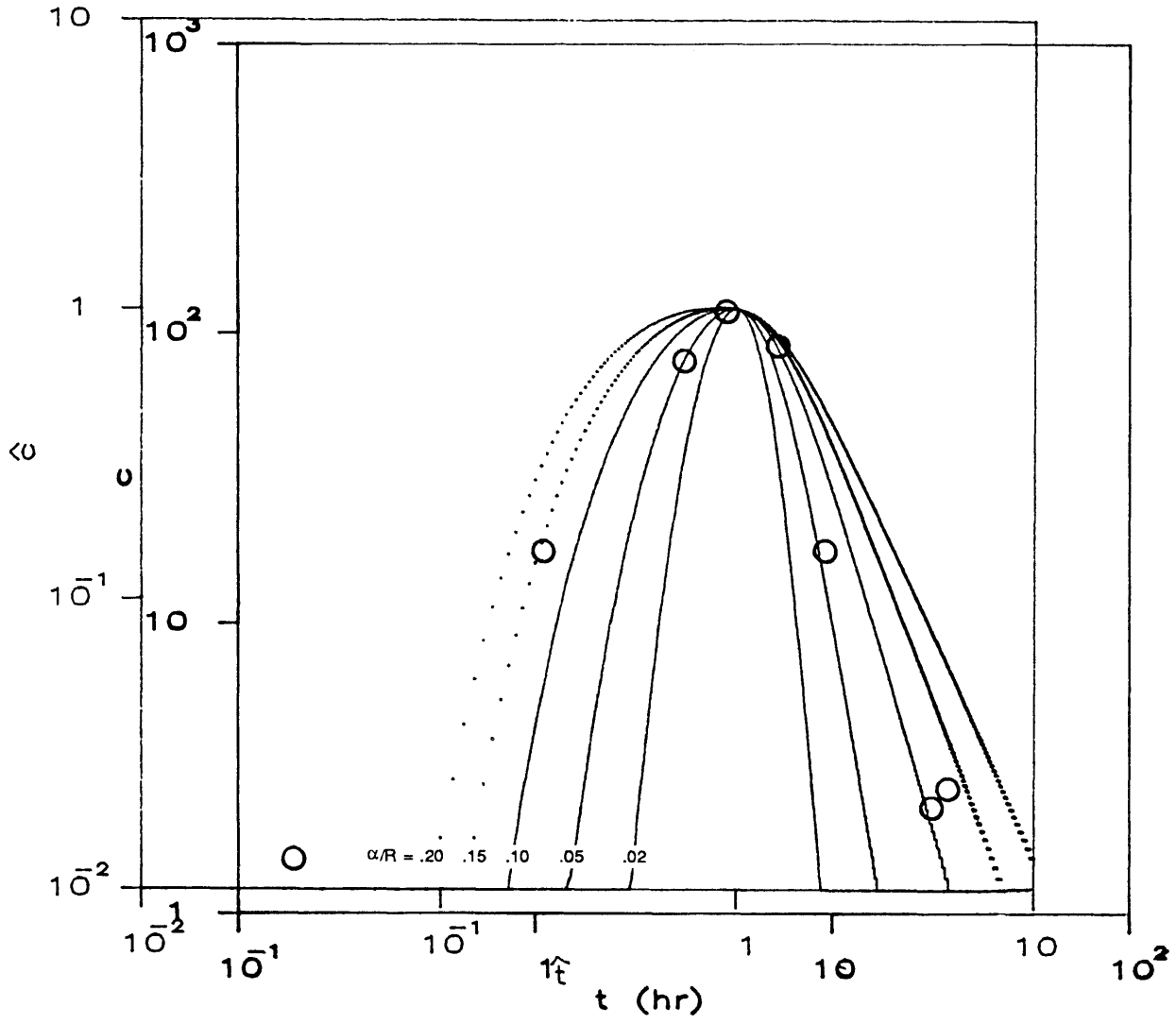

Figure 6-2. Breakthrough curve for R = 25 m at Corbas, France matched with type curves for α constant.

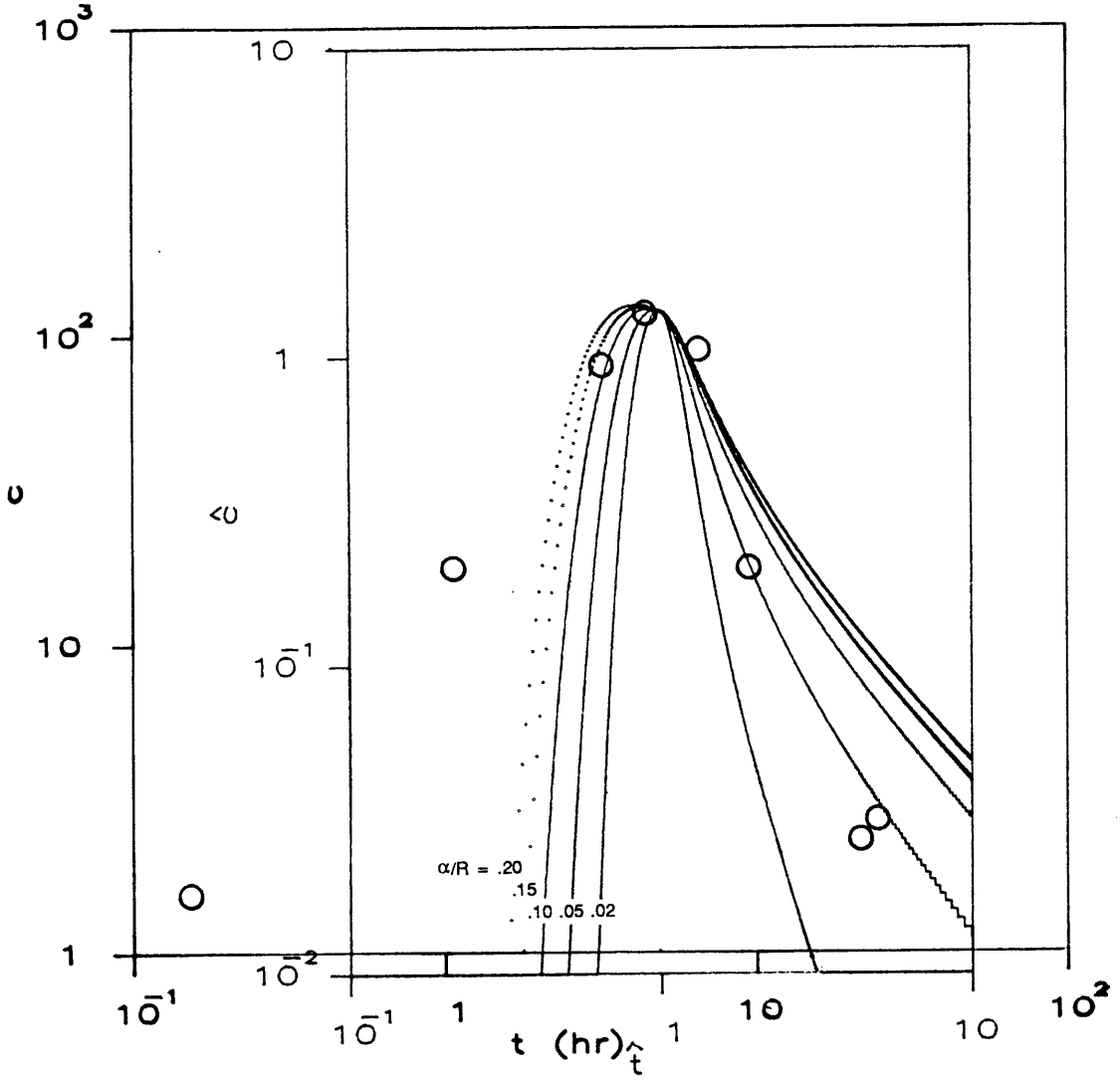

Figure 6-3. Breakthrough curve for R = 25 m at Corbas, France matched with type curves for α linearly increasing with distance.

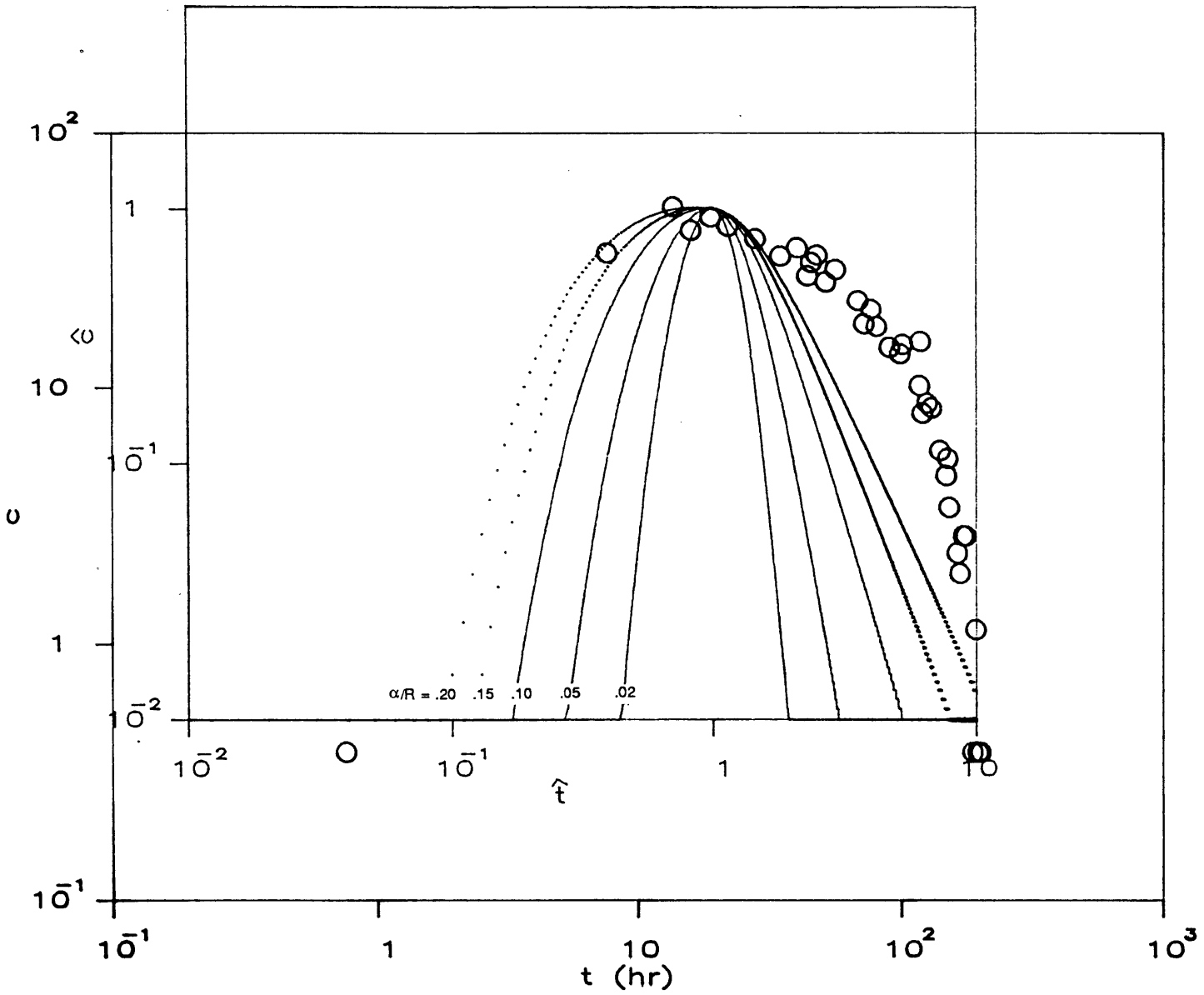

Figure 6-4. Breakthrough curve for R = 50 m at Corbas, France matched with type curves for α constant.

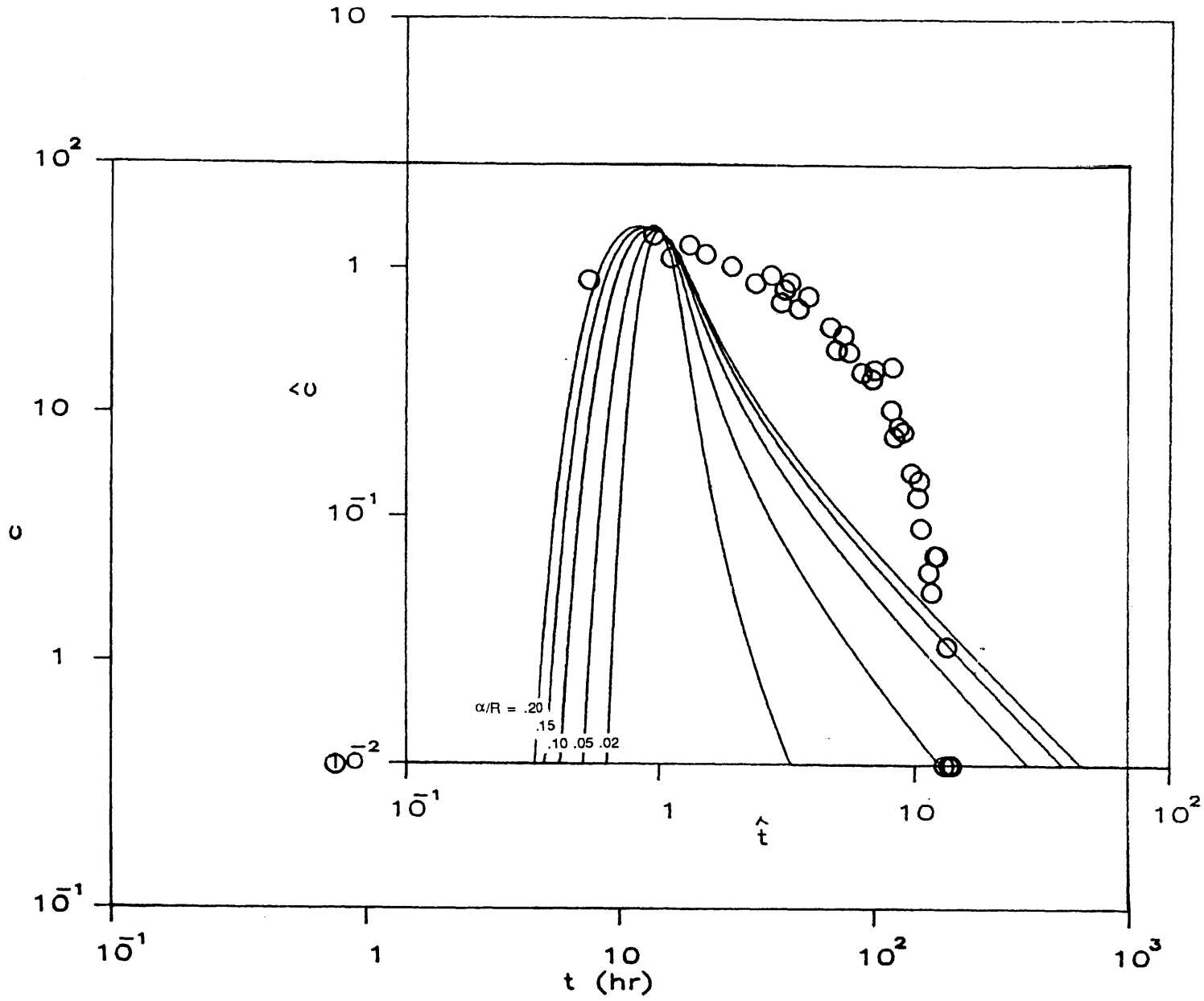

Figure 6-5. Breakthrough curve for R = 50 m at Corbas, France matched with type curves for α linearly increasing with distance.

When the data from the 150 m test are aligned with the type curve for α constant (Fig. 6-6), a good fit is achieved yielding $.10 < \alpha/R < .05$. The dispersivity is therefore $15m < \alpha < 7.5$ m. This is in good agreement with the the result determined using the pulse-width method where a value of $\alpha = 10.5$ m was found for this case.

From the type curve match at $\hat{t} = t/t_m = 1.0$, $t = 410$ hr, so using $t_m = 410$ hr $= \pi R^2 nb/Q$, $nb/Q = 0.0058$ hr/m^2. This compares well with the value of 0.0059 hr/m^2 found using the pulse-width method. If Q were known, with b = 12m, n could be calculated.

It is interesting to note that when the same data for R = 150 m are aligned with the type curve for α linearly increasing with distance (Fig. 6-7), the fit is not nearly as good as with Fig. 6-6. This may indicate that, at a distance of 150 m in this aquifer, the longitudinal dispersivity has reached a constant value, and hence the better fit to the set of type curves where α is presumed to be constant.

Comparison with Previously Reported Results. In order to determine values for dispersivity for the breakthrough curves, Sauty (1977) used a two-layer scheme to fit his type curves to the breakthrough curves at R = 25 m and 50 m (Fig. 6-8). This assumption was not supported by geologic evidence of two distinct layers for this site. Using this analysis, Sauty found that $\alpha = 11.0$ m and 1.25 m for R = 25 m, and $\alpha = 25$ m and 6.25 m for R = 50 m, with the two values implying two layers. He was able to fit the data at R = 150 m well to a single type curve, with the result that $\alpha = 12.5$ m.

Our results are in reasonable agreement with Sauty's results for R = 150 m ($\alpha = 10.5$ m from the pulse-width method and $15 \text{ m} < \alpha < 7.5$ m from type curve matching). We do not attempt to make any inferences about α for R = 25 m and 50 m type curves, because the data simply do not fit. Using a simple pulse-width method of analysis, we found α to increase with distance -- i.e., $\alpha = 2.4$, 4.6, and 10.5 m at 25, 50, and 150 m, respectively. This result agrees with other field observations regarding the behavior of dispersivity over distance.

Palo Alto Baylands, California -- Pulse Input in Radial Divergent Flow

This tracer test was conducted in a sand and gravel aquifer 1-2 m thick in Palo Alto Baylands, California, using ^{82}Br and ^{3}H as tracers. Breakthrough curves were measured at 7.6 m and 16.8 m from the injection well. An analysis of the data to determine longitudinal dispersivity was previously presented by Hoehn and Roberts (1982). Only the results from the tritium test are re-evaluated here. The field data are shown in Figure 6-9.

Breakthrough-Curve, Pulse-Width Method of Analysis. When the method described in Section 5 is applied to Figure 6-9, dispersivities may be calculated, and the results are presented in Table 6-2. Note that as in the

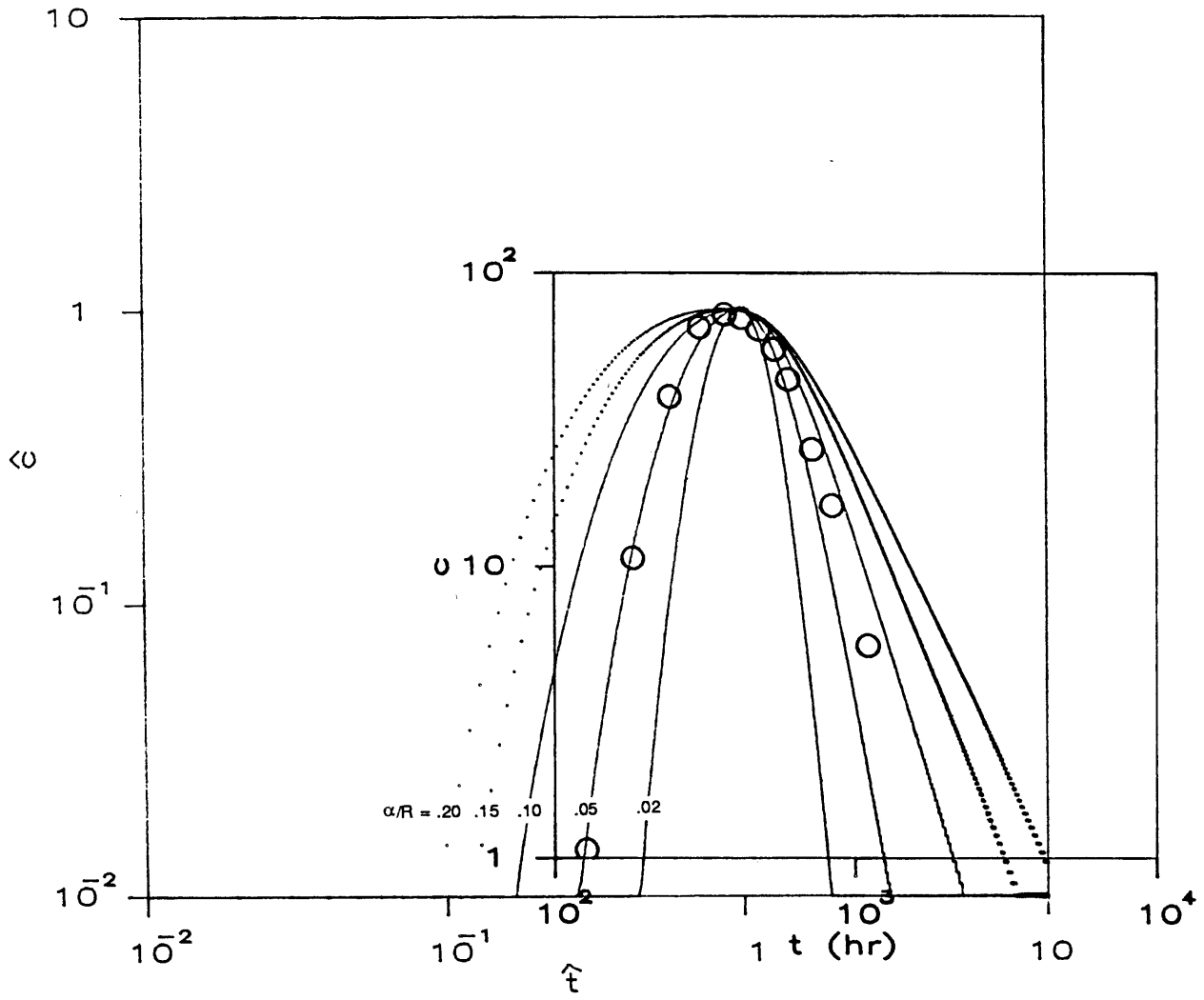

Figure 6-6. Type curve matching to breakthrough curve data for R = 150 m at Corbas, France, where α is assumed to be constant.

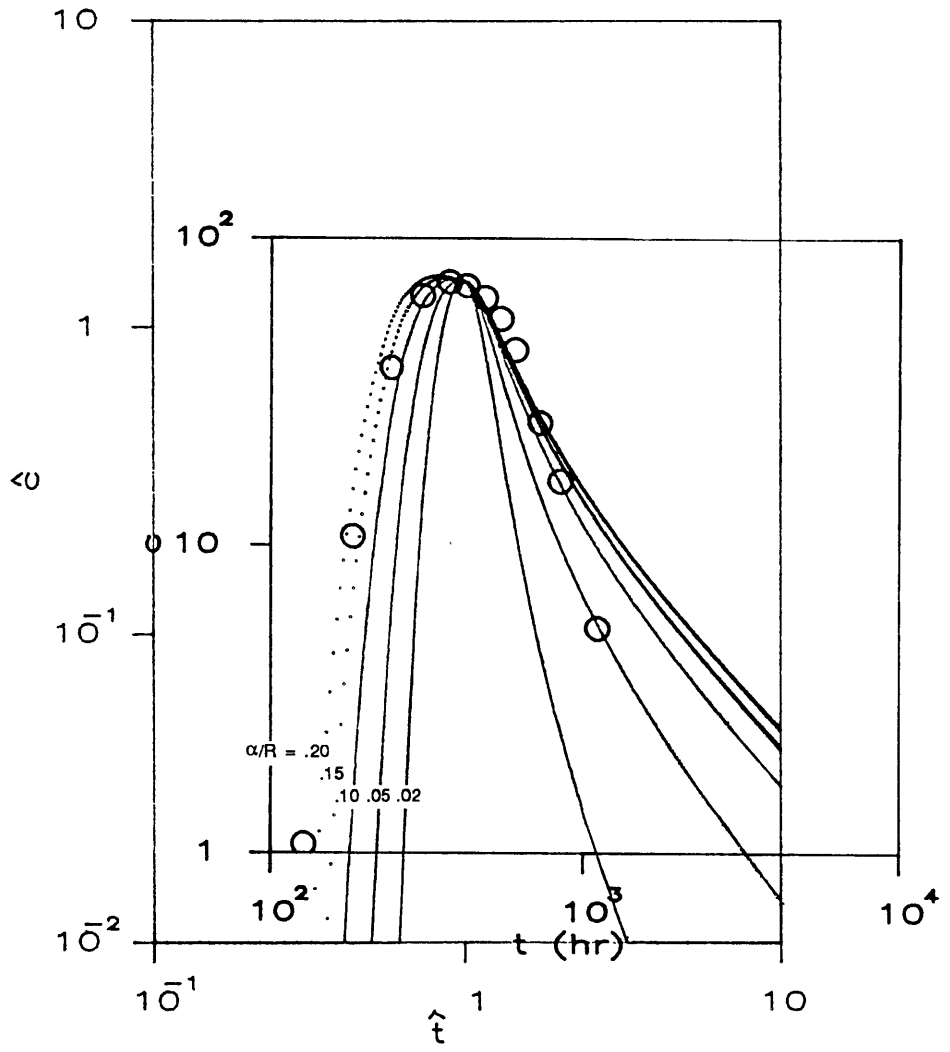

Figure 6-7. Type curve matching to breakthrough curve data for R = 150 m at Corbas, France for α linearly increasing with distance.

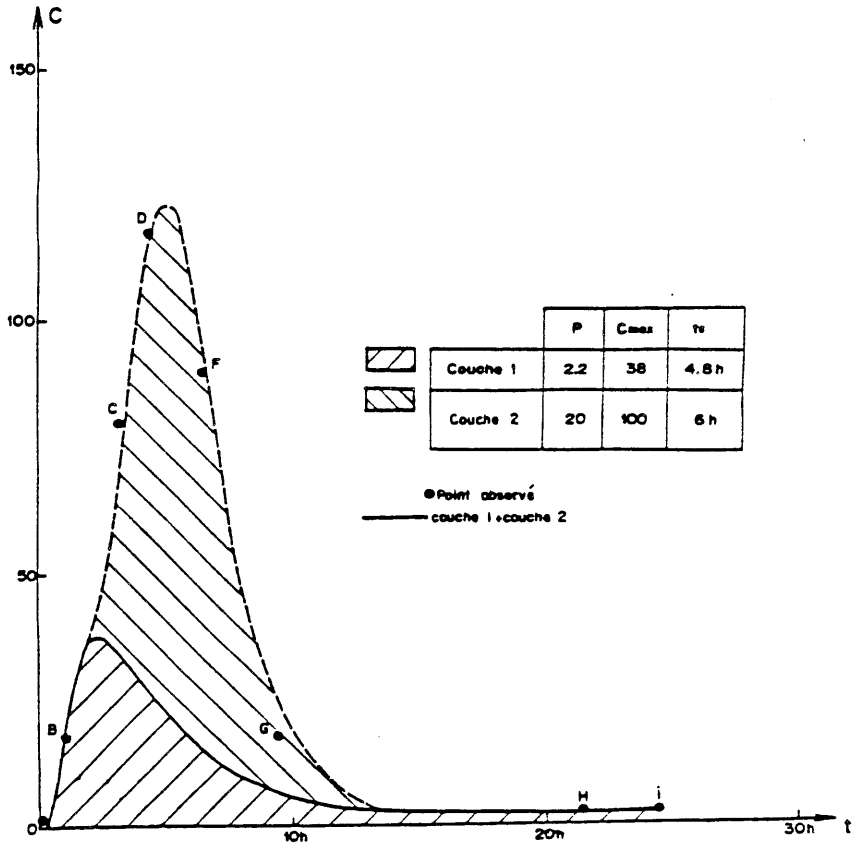

Figure 6-8a. Type curve matching to breakthrough curve data for R = 25 m at Corbas, France, assuming a two-layer model.

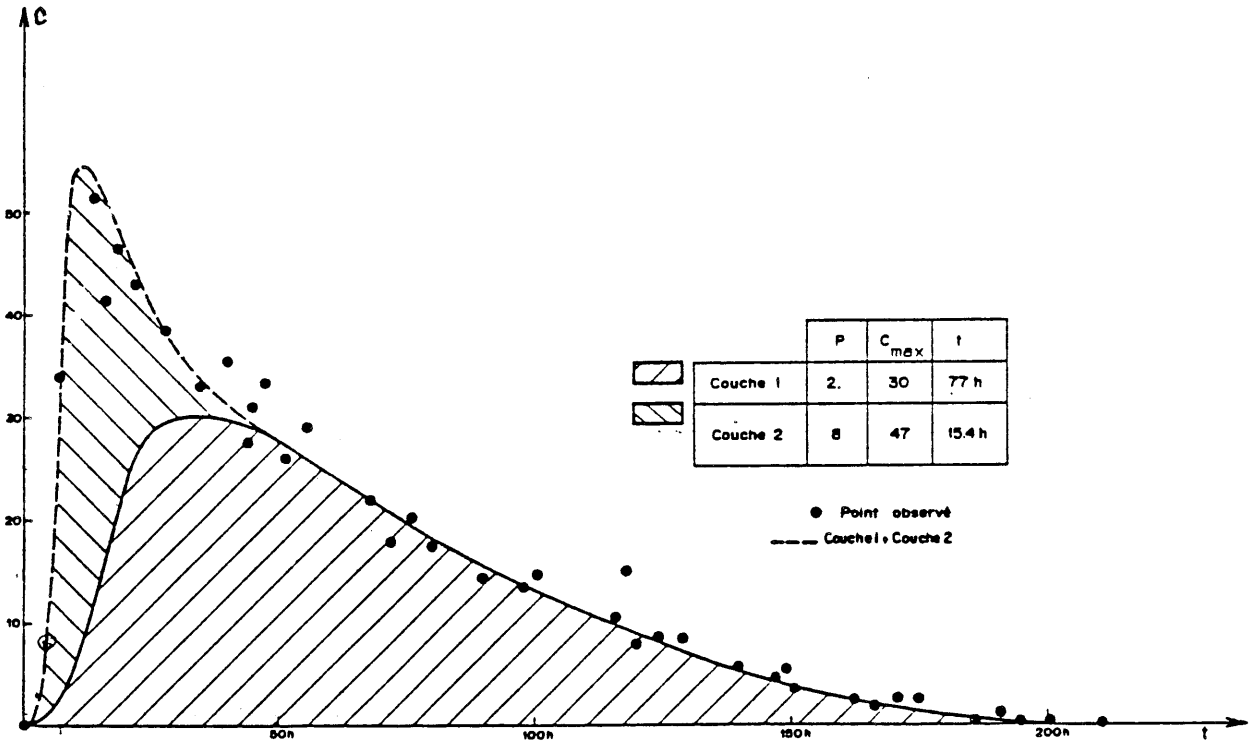

Figure 6-8b. Type curve matching to breakthrough curve data for R = 50 m at Corbas, France, assuming a two-layer model.

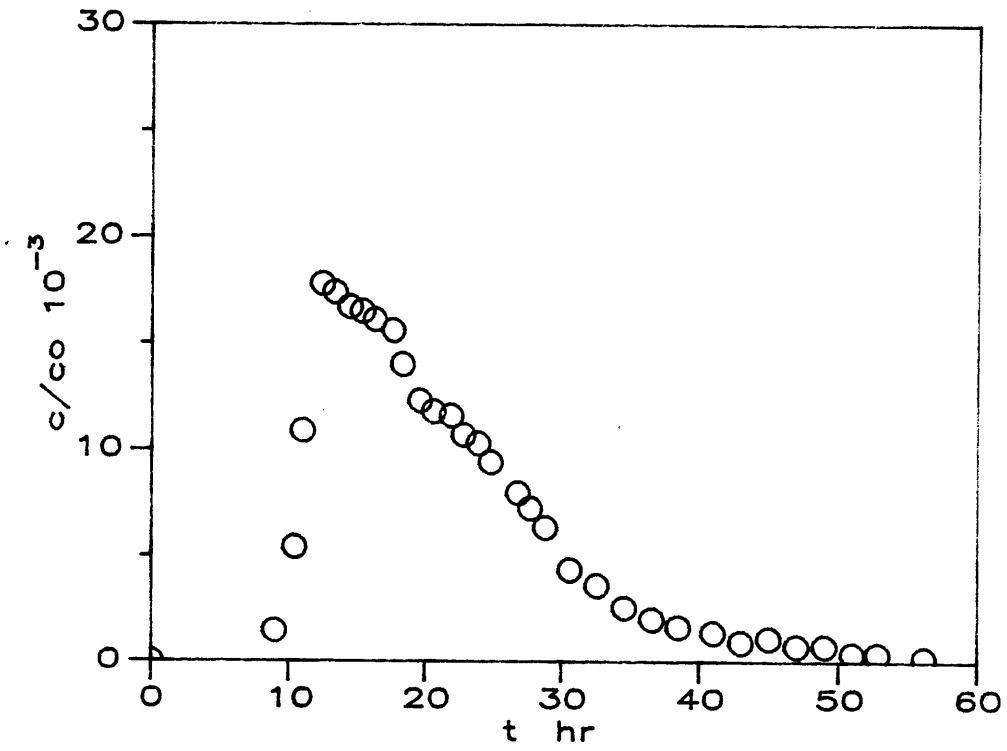

Figure 6-9a. Breakthrough curve at 7.6 m from a pulse input in a radially divergent flow field at Palo Alto Baylands, California (Hoehn and Roberts, 1982).

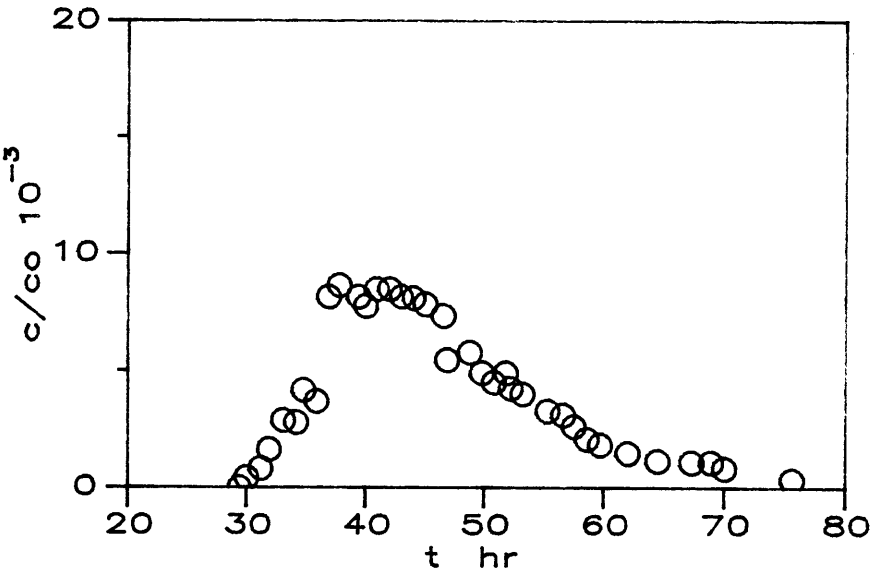

Figure 6-9b. Breakthrough curve at 16.8 m from a pulse input in a radially divergent flow field at Palo Alto Baylands, California (Hoehn and Roberts, 1982).

TABLE 6-2

Values of longitudinal dispersivity, determined from the breakthrough-curve, pulse-width method of analysis for a radially divergent flow tracer test (Palo Alto Baylands, California) at two distances from the injection borehole.

R (m)	Δt (hr)	t_m (hr)	$\frac{\alpha}{R}$	α (m)
7.6	15.0	12.4	.099	0.75
16.8	17.5	37.8	.014	0.24

previous section, Δt is defined here by $c_m/2$ instead of c_m/e, thus Eq. (5-33) becomes

$$\alpha = \frac{3R}{64\ln 2} \left(\frac{\Delta t}{t_m}\right)^2 \qquad (6\text{-}2)$$

This yields the result that the calculated dispersivity is lower at a further distance from the injection point, which is contrary to what would be expected physically.

Type-Curve Matching. To use the methods presented in Section 5, the field data are plotted on log-log paper and aligned with Figures 5-7 and 5-8 until the best fits are achieved. Figures 6-10 and 6-11 illustrate type-curve matching of the 7.6 m breakthrough curves with Figures 5-7 and 5-8; Figures 6-12 and 6-13 illustrate type-curve matching of the 16.8 m breakthrough curve with these same type curves. The results of the type curve matching are presented in Table 6-3.

For the 7.6 m well, it can be seen that neither set of type curves fits the data very well, which is not surprising, given the complications due to non-Fickian flow which typically occur at short distances from the injection point. The range of values given in Table 6-3 for α is based on the best match with the rising limb and peak of the breakthrough curve.

For the 16.8 m well, the shape of the type curve is in much better agreement with the shape of the breakthrough curve; of the two sets, the shape of the type curve for α linearly increasing with distance provides the better fit.

Comparing the values of α determined for the two wells, the analysis using the type curves for α linearly increasing with distance yields values of α determined for the 16.8 m well that are greater than those determined for the 7.6 m well, whereas the analysis using the type curves for α constant yields approximately the same range of α for the two observation radii. From this information it could be concluded that the type curves for α linearly increasing with distance fit the data better. That the dispersivity of the aquifer has reached an asymptotic constant value by R = 16.8 m cannot be clearly demonstrated.

Comparison with Previously Reported Results. The analysis previously presented for this data (Figure 6-14 and Table 6-4) used a two-domain model to fit the breakthrough curves (Hoehn and Roberts, 1982). While the values of dispersivity from that analysis and the one presented here do not differ drastically, the previous analysis depends on the use of a model which has no physical meaning for the geologic site in question, i.e., the assumption of two distinct geologic zones. Moreover, even using this assumption the composite breakthrough curve composed of the two sub-curves does not fully

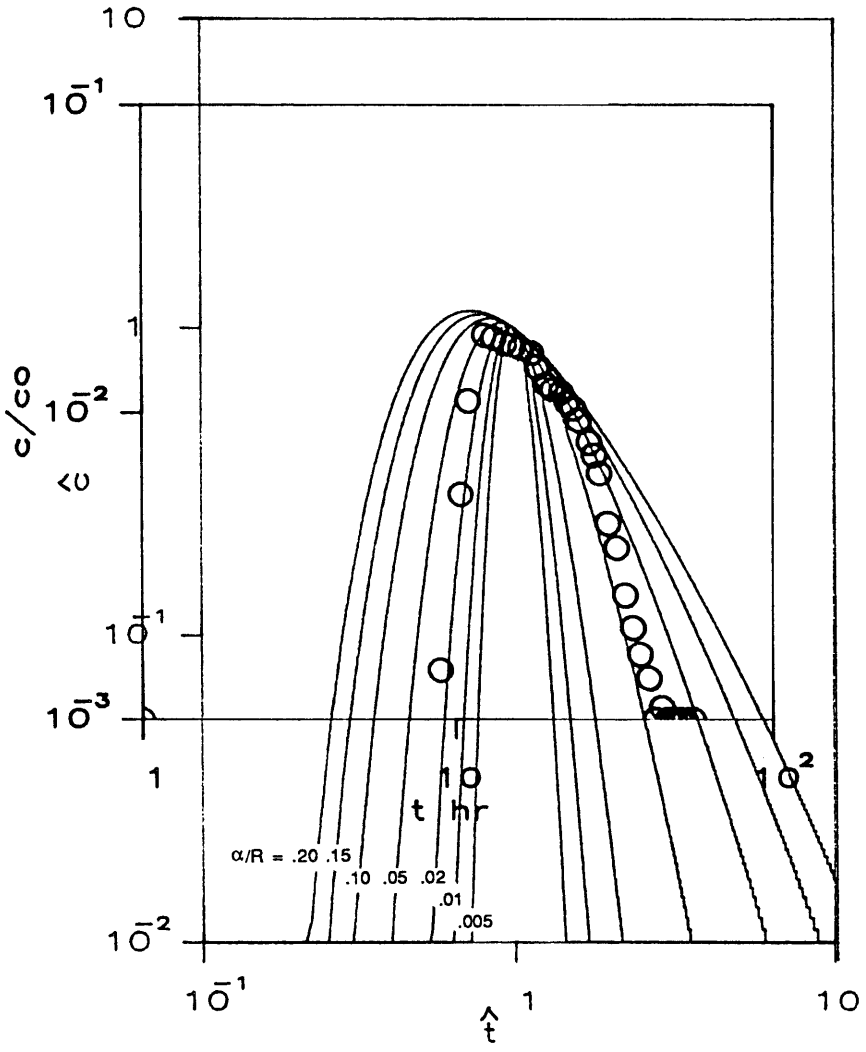

Figure 6-10. Type curve matching to breakthrough curve data for R = 7.6 m at Palo Alto Baylands, California, where α is assumed to be constant.

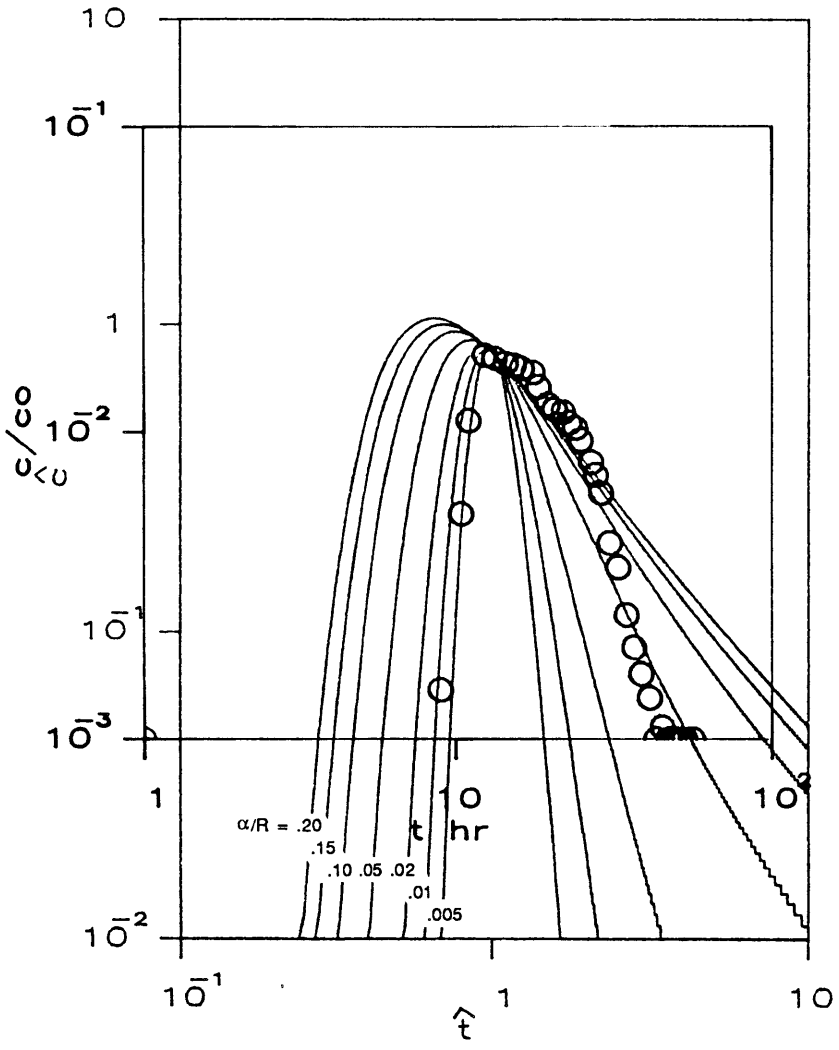

Figure 6-11. Type curve matching to breakthrough curve data for R = 7.6 m at Palo Alto Baylands, California, for α linearly increasing with distance.

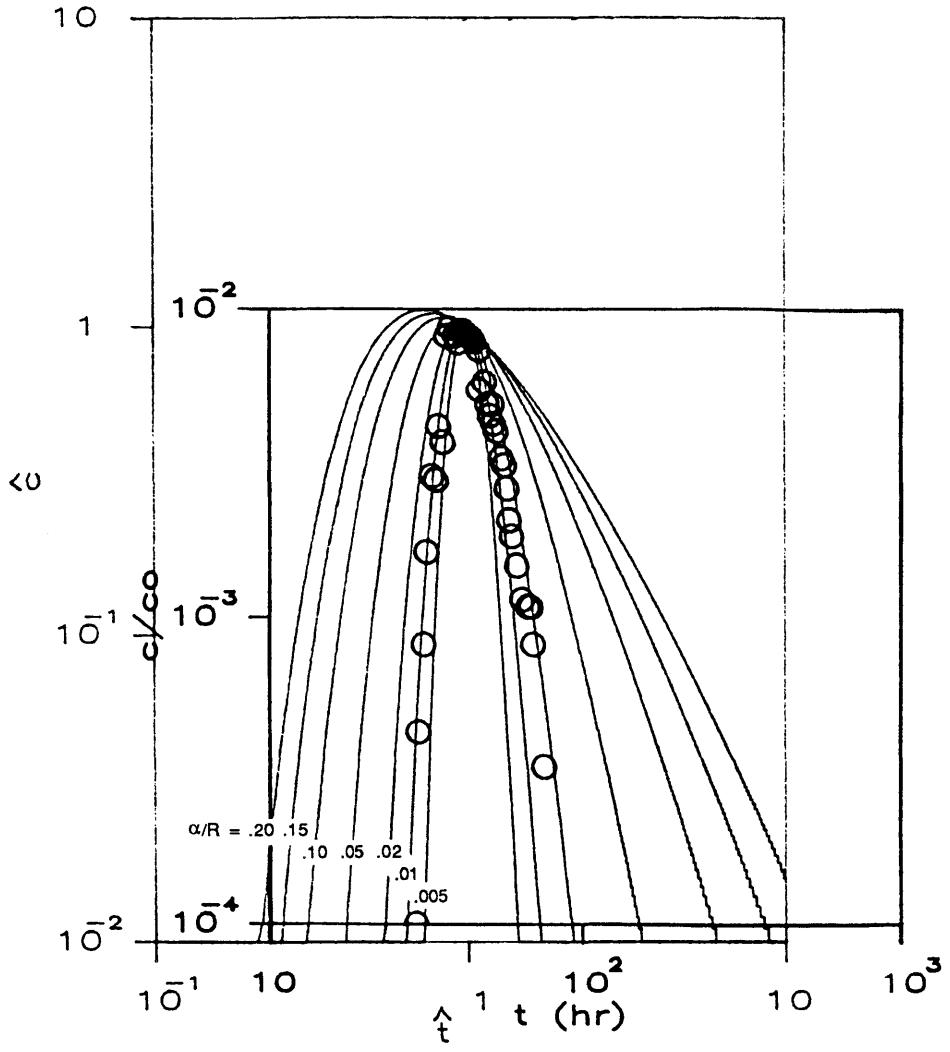

Figure 6-12. Type curve matching to breakthrough curve data for R = 16.8 m at Palo Alto Baylands, California, where α is assumed to be constant.

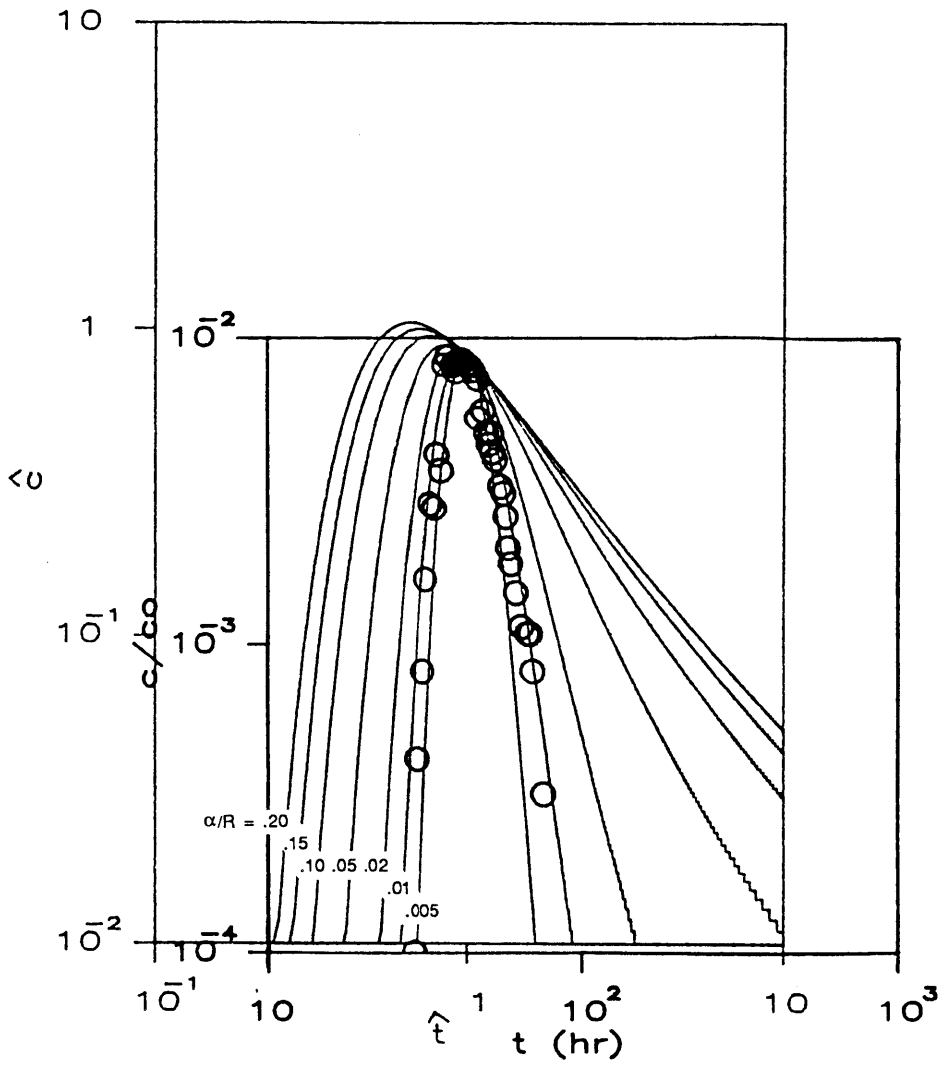

Figure 6-13. Type curve matching to breakthrough curve data for R = 16.8 m at Palo Alto Baylands, California, for α linearly increasing with distance.

TABLE 6-3

Values of longitudinal dispersivity, determined from type curve matching with radially divergent flow tracer-test breakthrough curves from Palo Alto Baylands, California.

R (m) (Fig. 4.7)	$\frac{\bar{\alpha}}{R}$ for α const (m)	$\bar{\alpha}$ for α const. (m)	$\frac{\bar{\alpha}}{R}$ for α lin. inc. (Fig. 4-8)	$\bar{\alpha}$ for α lin.inc. (m)
7.6	.02 - .05	.15 - .38	.01 - .02	.076 - .15
16.8	.007 - .02	.12 - .34	.007 - .02	.12 - .34

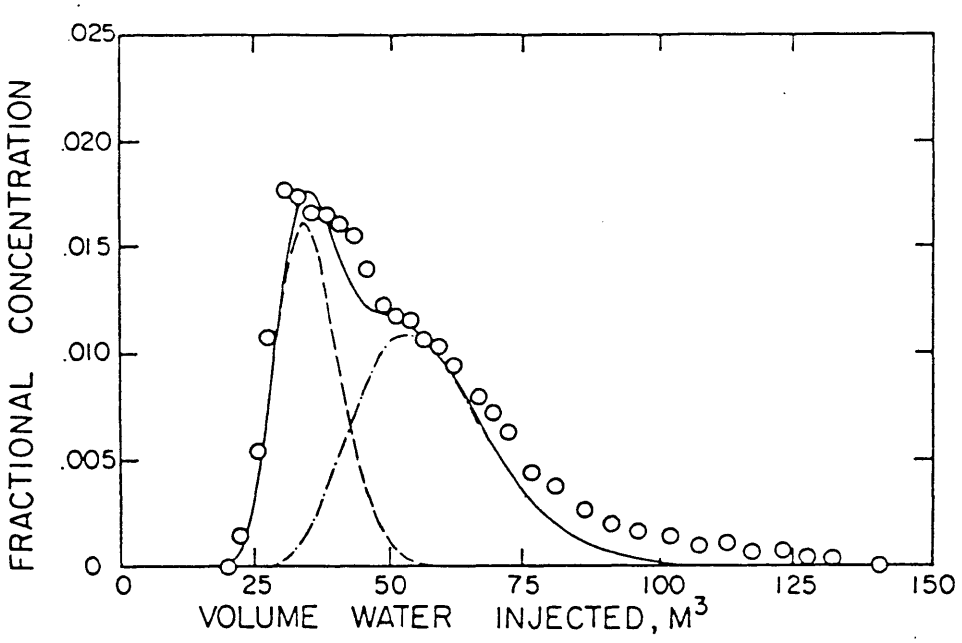

Figure 6-14a. Breakthrough curve analysis of Palo Alto data at R = 7.6 m using a "two-domain" model (from Hoehn and Roberts, 1982).

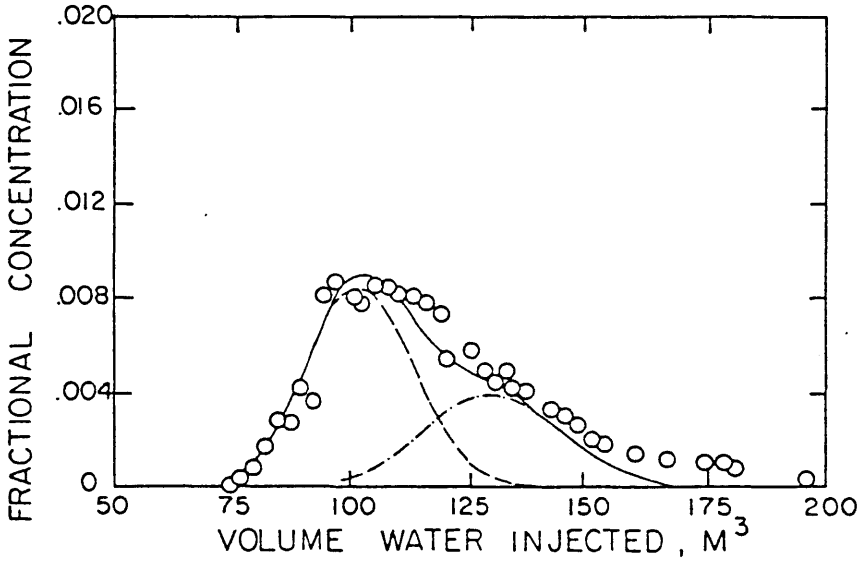

Figure 6-14b. Breakthrough curve analysis of Palo Alto data at R = 16.8 m using a "two-domain" model (from Hoehn and Roberts, 1982).

TABLE 6-4

Results reported by Hoehn and Roberts (1982) for divergent radial flow tracer test conducted at Palo Alto Baylands, California.

MORE PERMEABLE DOMAIN			LESS PERMEABLE DOMAIN	
R (m)	Peclet Number	α (m)	Peclet Number	α (m)
7.6	100	.08	53	.14
16.8	220	.08	220	.08

account for the tailing, both for R = 7.8 m and R = 16.8 m. On the other hand, the type curve analysis presented here does not depend on artificial assumptions about the physical situation, and provides results which appear to be physically plausible -- i.e., that the dispersivity is increasing with distance for an approximately constant Peclet number.

Savannah River Plant, Georgia -- Pulse Input in Doublet with Recirculation

This tracer test was carried out in fractured media (crystalline schist and gneiss), with a pulse input of tritium injected over a 76 m thickness. The breakthrough concentration was measured at a pumping well 538 m distant from the injection well, and recirculation was employed. The data (Figure 6-15) were previously analyzed by Webster, Procter and Marine (1970) using a Grove and Beetem (1971) type of analysis.

We re-evaluated the portion of the breakthrough curve before recirculation using the analytical results presented in Section 5. From type-curve matching with Figure 5-17 (Figure 6-16) a value of $\alpha/R = 0.08$ was determined, yielding $\alpha = 47$ m. Choosing a match point of $\hat{t} = 1.0$ and $\hat{t} = 235$ d, and since $t = Qt/n\pi b^2$, with $Q = 7.9$ gpm $= 43$ m^3/d, a value of porosity of $n = 0.00046$ was calculated. While these results are smaller than the originally reported results of $\alpha = 134$ m and $n = 0.0008$ by factors of approximately 3 and 2, respectively, we have more confidence in the results based on the Gelhar and Collins solution, because the methodology completely accounts for non-uniform flow effects and is not complicated by recirculation. When the type curve for $\alpha/R = 0.08$ is replotted against the original data (Figure 6-17, dashed line), it can be seen that there is a much better fit to the rising portion of the breakthrough curve than the solution presented by Webster, Procter and Marine. Therefore, we believe that the value of $\alpha = 47$ m and $n = 0.00046$ better characterize the longitudinal dispersivity and porosity at this site.

Hanford, Washington -- Pulse Input in Doublet without Recirculation

This tracer test consisted of a pulse input of ^{131}I in a doublet, where the recharge and pumping wells were 17.1 m (56 ft) apart. The breakthrough curve data and analysis using the solution based on Gelhar and Collins (Section 5) are discussed in detail in Gelhar, 1982. The match of the data to the type curves similar to Figure 5-17 but modified for unequal injection and withdrawal flow rates is reproduced here as Figure 6-18. The results of the type curve match yield $\alpha/L = 0.035$ and therefore $\alpha = 0.60$ m (1.96 ft). This type curve match also yields $t = 1.18$ hr for $\hat{t} = Qt/nbL^2 = 1$, and since $Q = 3.42$ gal/min and $L = 56$ ft, an effective thickness of $nb = .00037$ m (0.105 ft) is calculated. These data and calculations illustrate the usefulness of conducting the doublet test -- note that the peak concentration is well defined and that dispersivity may easily be determined from the shape of the breakthrough curve.

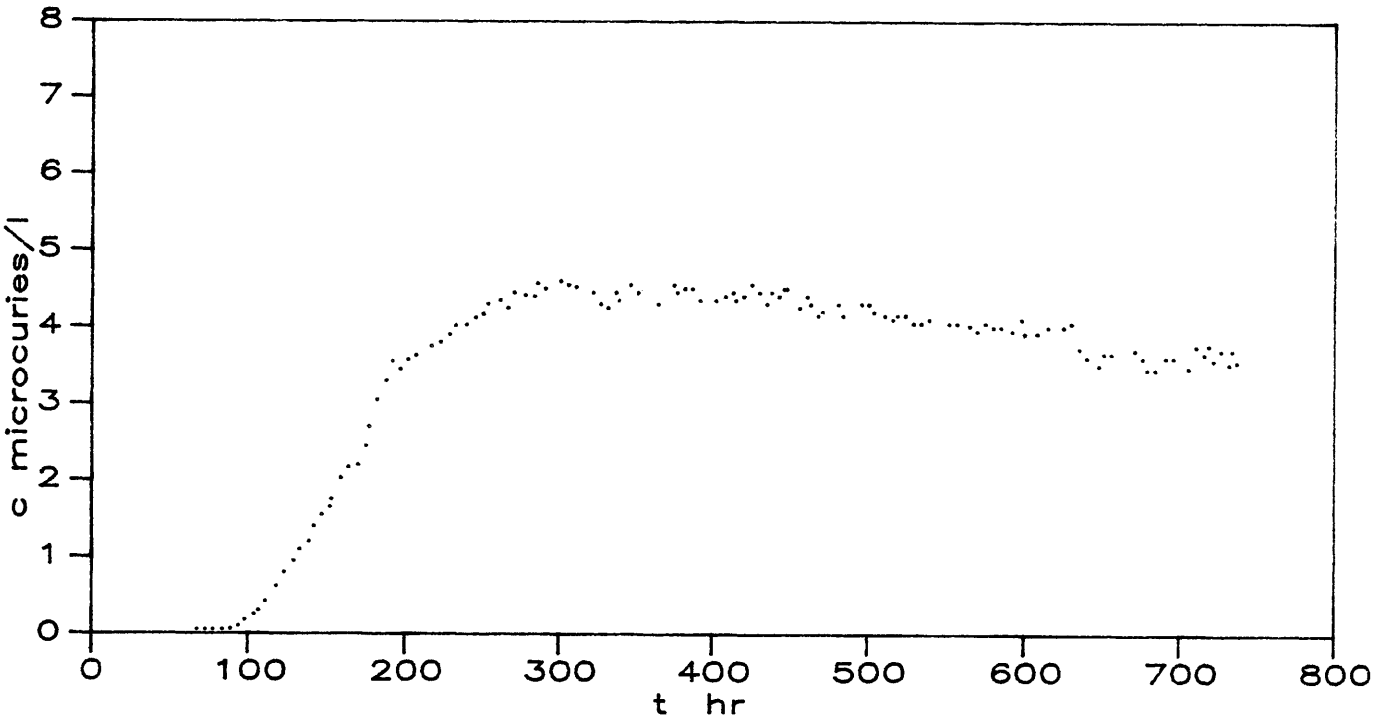

Figure 6-15. Breakthrough curve from pulse input in a doublet, with recirculation, near Savannah River Plant, Georgia (from Webster, Procter and Marine, 1970).

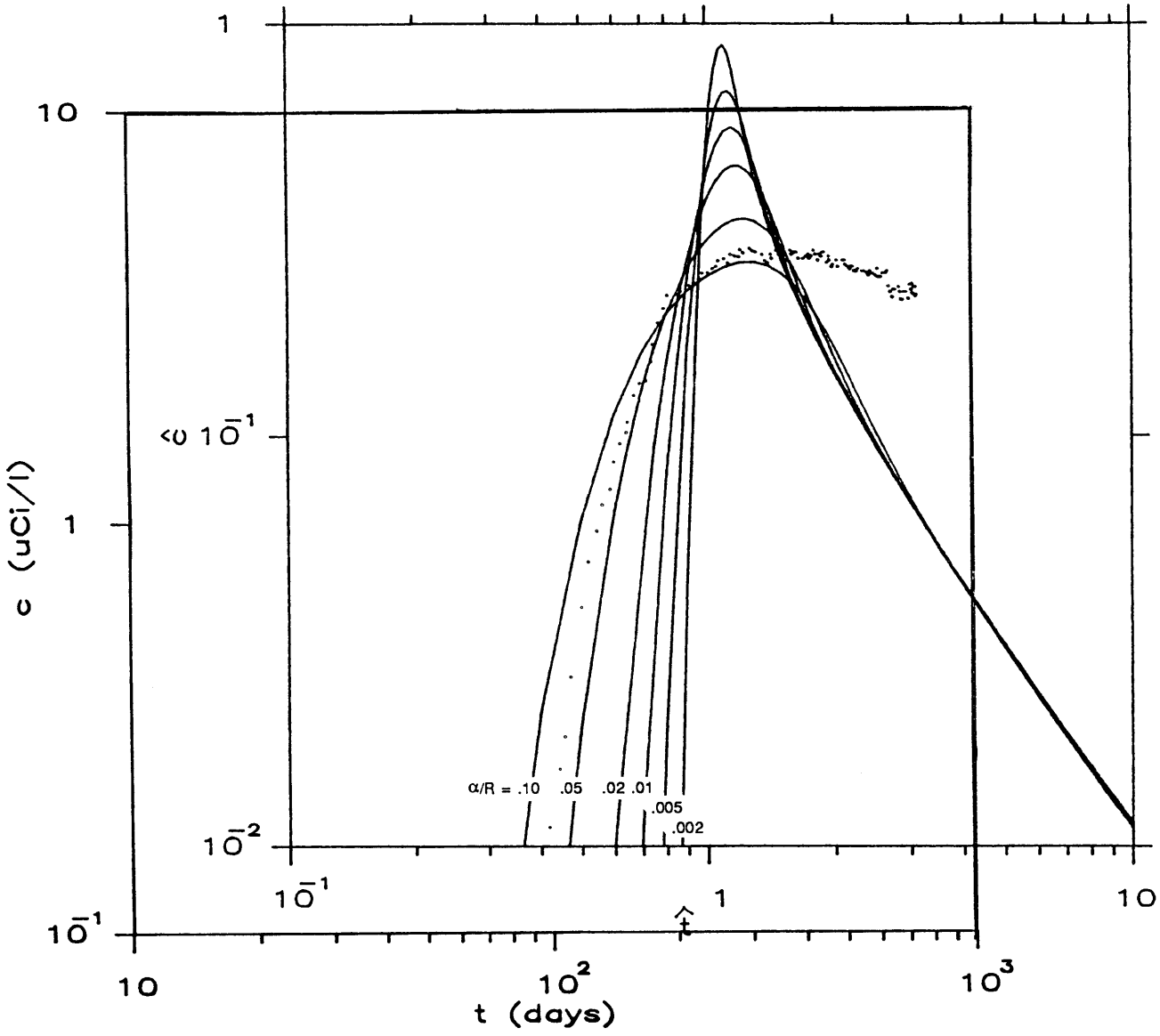

Figure 6-16. Type curve matching to breakthrough curve data from the two-well pulse test at Savannah River Plant, Georgia.

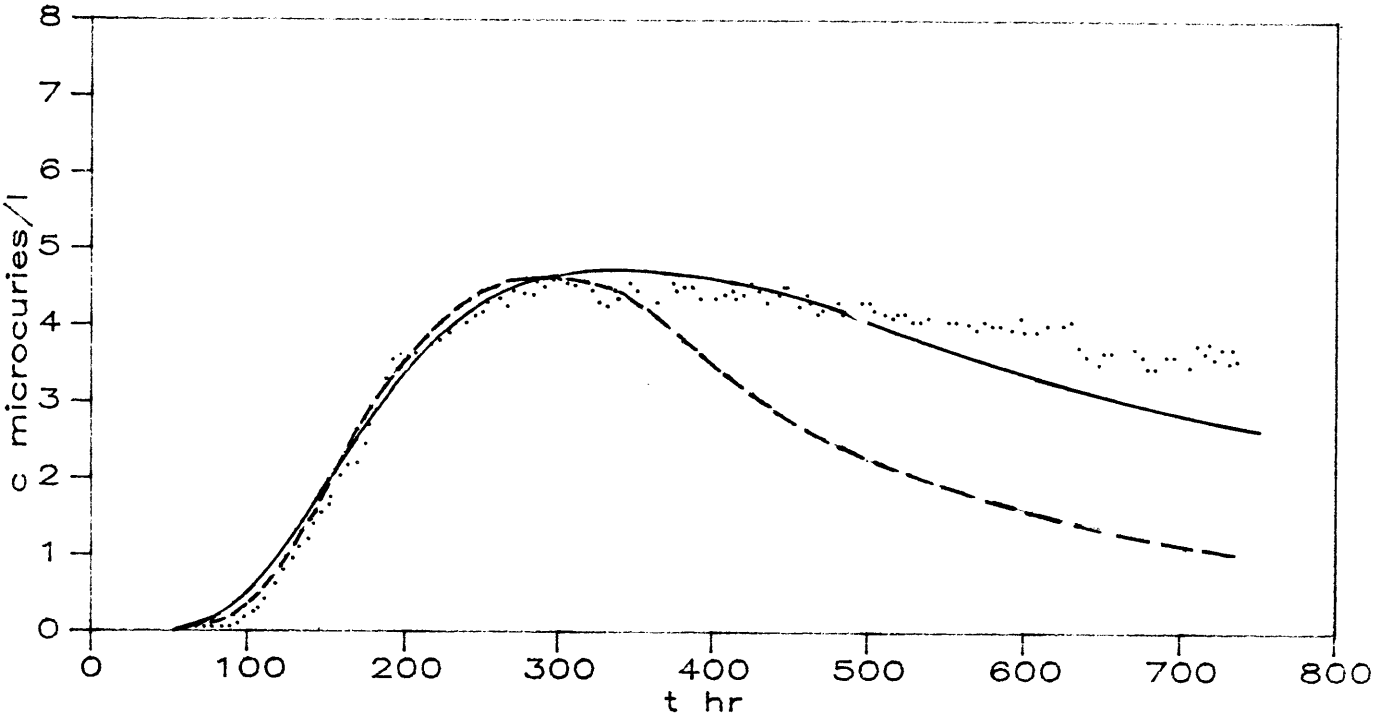

Figure 6-17. Breakthrough curve data (points) with superimposed theoretical curve derived by Webster, Procter and Marine (solid line) and type curve from Gelhar, 1982 (dashed line).

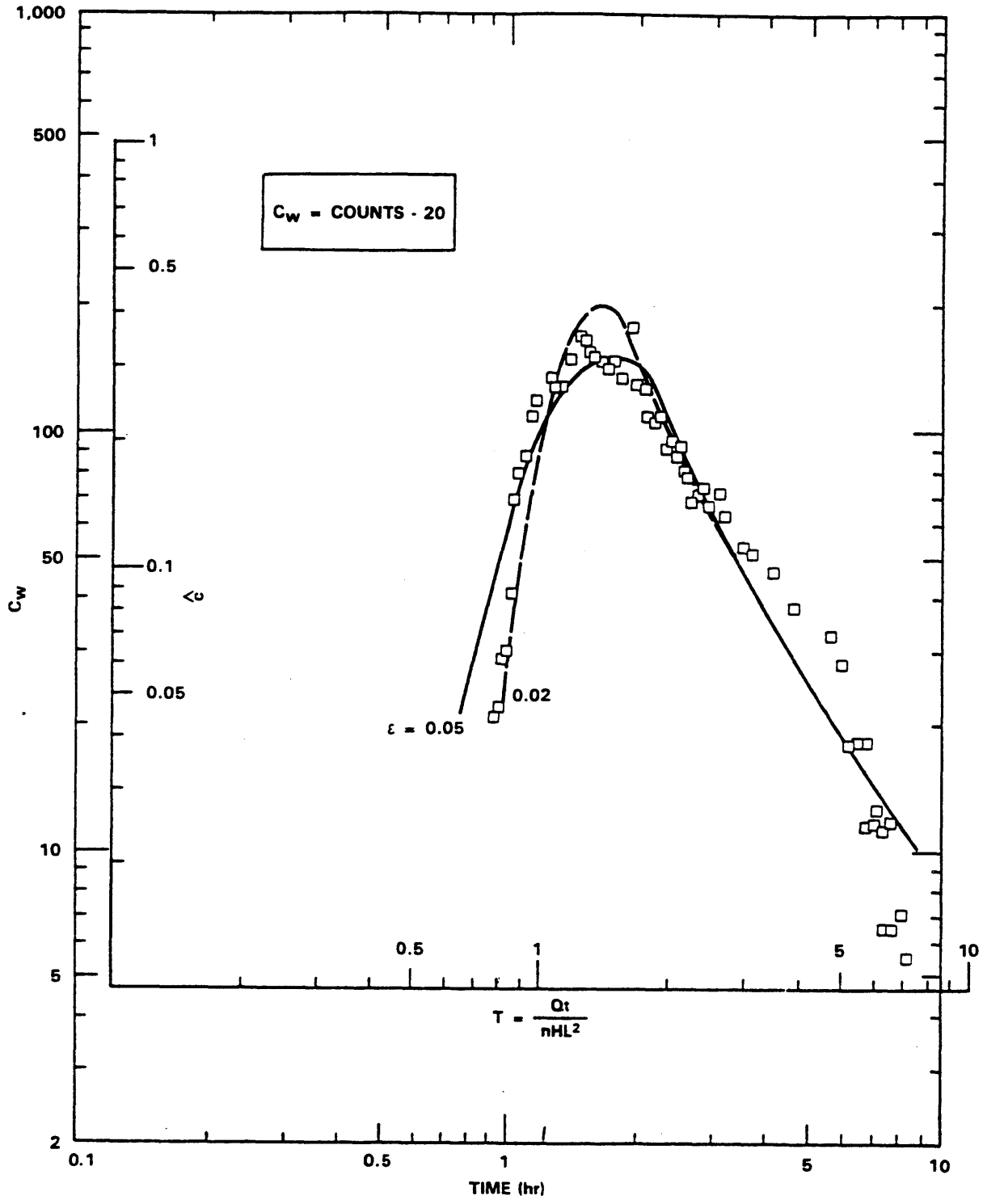

Figure 6-18. Breakthrough curve and type curve matching for pulse input of ^{131}I in a doublet (from Gelhar, 1982).

Tucson, Arizona -- Step Input in a Doublet without Recirculation

This tracer test was carried out in unconsolidated sand, silt and gravel with continuous input of chloride into a doublet, with the recharge and discharge wells separated by a distance of 79.2 m. Simultaneous injection and withdrawal were carried out for 14 days, followed by a 9-day period of pumping after injection was stopped. A total of 3.0×10^6 gallons of water were injected, yielding an average injection rate of 811 m^3/d. The chloride breakthrough data at the pumping well are reproduced as Figure 6-19, and have previously been evaluated to determine longitudinal dispersivity by Robson (1974), using a Grove and Beetem (1971) type of analysis.

When these data are plotted on log-log paper and aligned with the type curves presented in Figure 5-18, an estimate of $\alpha/L = 0.015$ is obtained, yielding $\alpha = 1.2$ m (see Figure 6-20). From matching the abscissas, the effective thickness is found to be nb = .71 m. (Porosity cannot be determined since the actual thickness is not known.)

Robson previously reported a value of longitudinal dispersivity of $\alpha = 15.2$ m., an order of magnitude greater than the value calculated here. This was derived using a Grove and Beetem type of analysis to find the best fit to the data with porosity and dispersivity as the parameters, assuming an aquifer thickness of 4.3 m (14 ft). When the two solutions are plotted against the original breakthrough curve (see Figure 6-19), it can be seen that the solution based on Gelhar and Collins provides a better fit to the data; therefore, we have more confidence in this result.

Discussion and Recommendations

Based on the analyses presented in this section, we can make several observations on the usefulness of tracer tests in determining longitudinal dispersivity. In comparing doublet tests to radial tests, it appears that we obtain better fits of the experimental data to the type curves when the doublet test (with pulse input) is employed. The doublet with a pulse input is much more sensitive to dispersion and is therefore easier to interpret to obtain longitudinal dispersivity than is the doublet test with a step input.

Although the fits obtained with the doublet/pulse test seem to be better than those for radial flow tests, sometimes radial flow tests may be more convenient to run due to existing well configurations. It should be noted that the fits for the radial tests appear to be best for large distances between injection and observation wells -- i.e., after the longitudinal dispersivity has reached an asymptotic constant value and a Fickian type of solute transport equation is valid. In comparing radial flow test configurations, there are fewer complications in interpreting results from a divergent radial test with a pulse input than with the convergent pulse test, because the input mass of tracer is forced out of the injection well much more quickly. In the convergent test, elongated tails on breakthrough curves due to the "borehole flushing effect" make precise interpretation difficult.

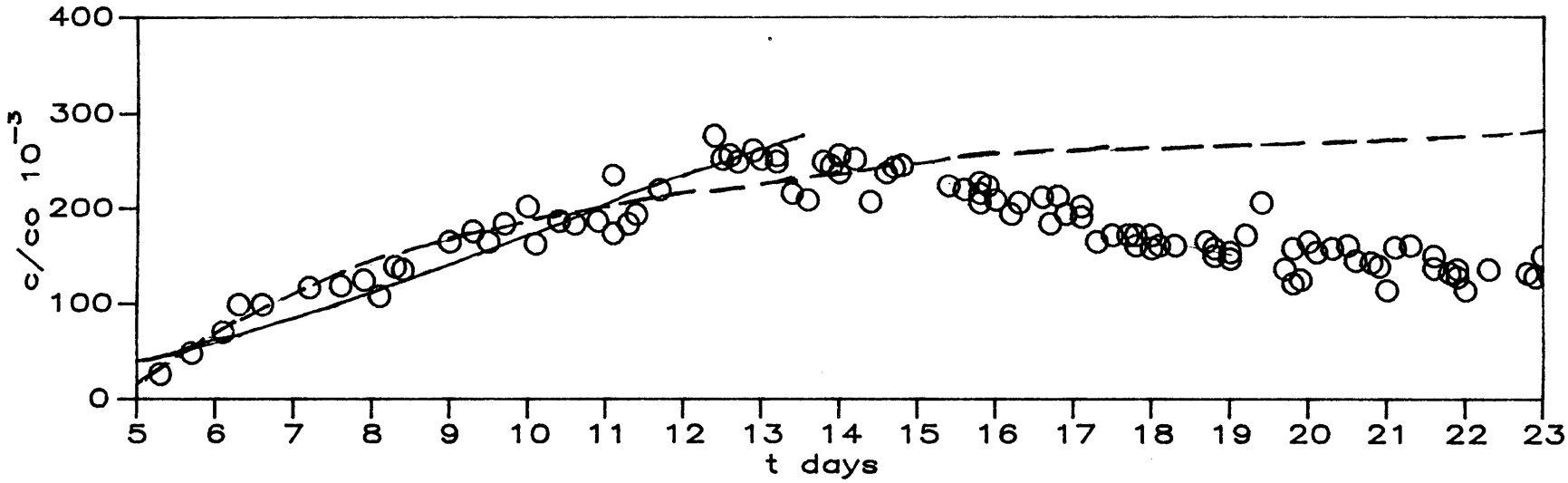

Figure 6-19. Breakthrough curve for continuous input in a doublet at Tucson, Arizona (from Wilson, 1971, Figure 18), and theoretical solutions determined by Robson (1974) (solid line) and by using the solution based on Gelhar and Collins (1971) (dashed line).

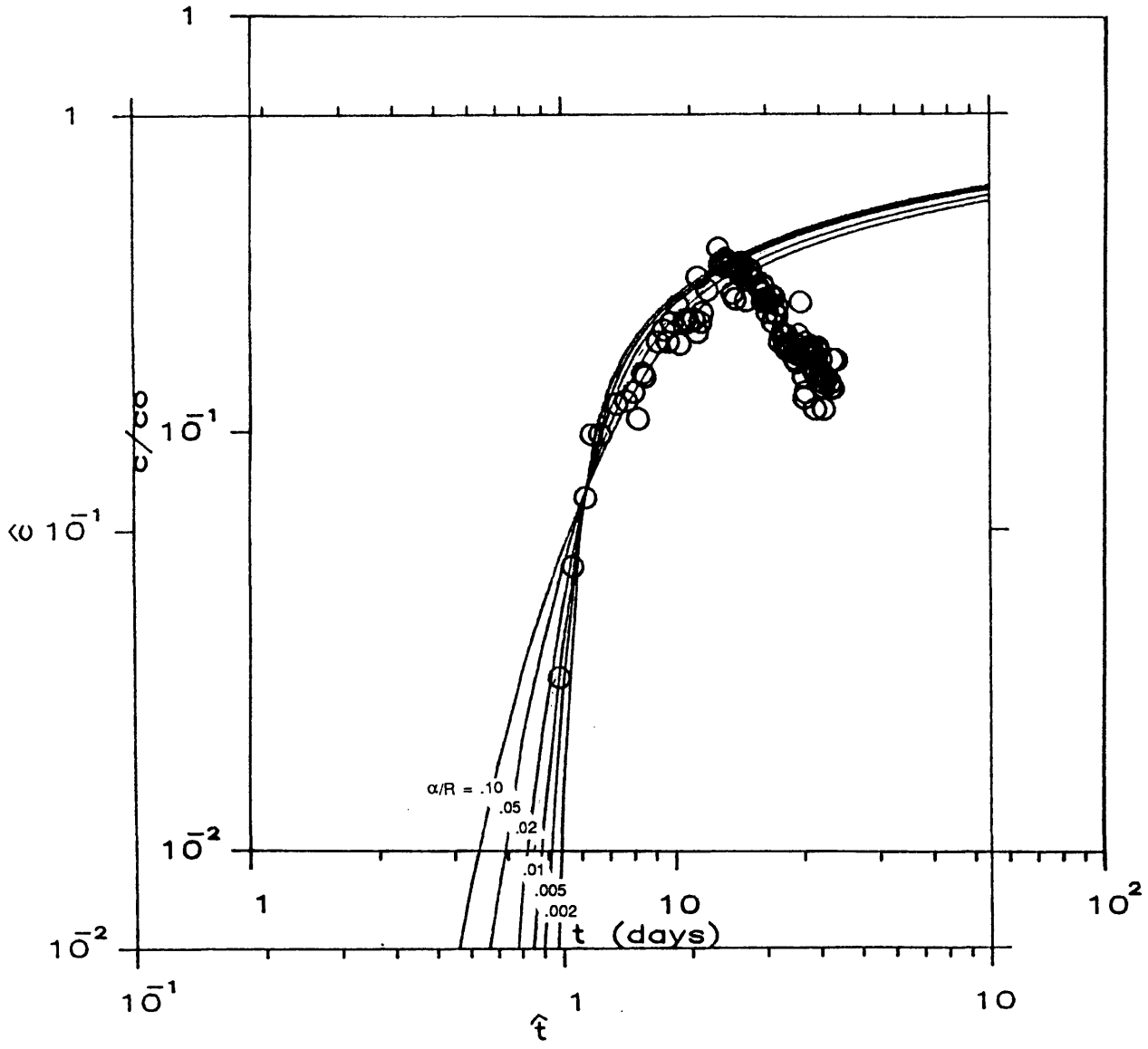

Figure 6-20. Type curve matching for breakthrough curve data from a two-well continuous input test at Tucson, Arizona.

In all cases our re-analysis of data yielded either lower dispersivities than were previously reported, or the same values with improved confidence in the results (see Figure 6-21). In cases where the values were the same, we were able to fit the data to breakthrough curves without having to make any assumptions about the nature of the geology or the flow regime. Our results point to improved analysis by using solutions to the advection-dispersion equation that account for non-uniform flow effects, non-constant dispersivities and borehole flushing. In no cases did we find any larger dispersivities as a result of our evalution. Although we could not re-evaluate any additional data on Figure 1-2 due to lack of detailed information, in the many cases where wrong solutions or assumptions have been used to evaluate data, this will tend to overestimate the dispersivities. Based on this observation, the "low quality data" indicating large dispersivities at large scales may be in error by as much as an order of magnitude, thereby erroneously indicating very large amounts of dilution or mixing when in fact this may not be the case for the scales in question.

In summary, we believe that tracer tests can be a useful tool in determining longitudinal dispersivity. Our analyses indicate that the doublet test with a pulse input and the radial divergent tests produce the most reliable results. The two-well test with a step input is not recommended for determining longitudinal dispersivity due to its insensitivity to dispersion.

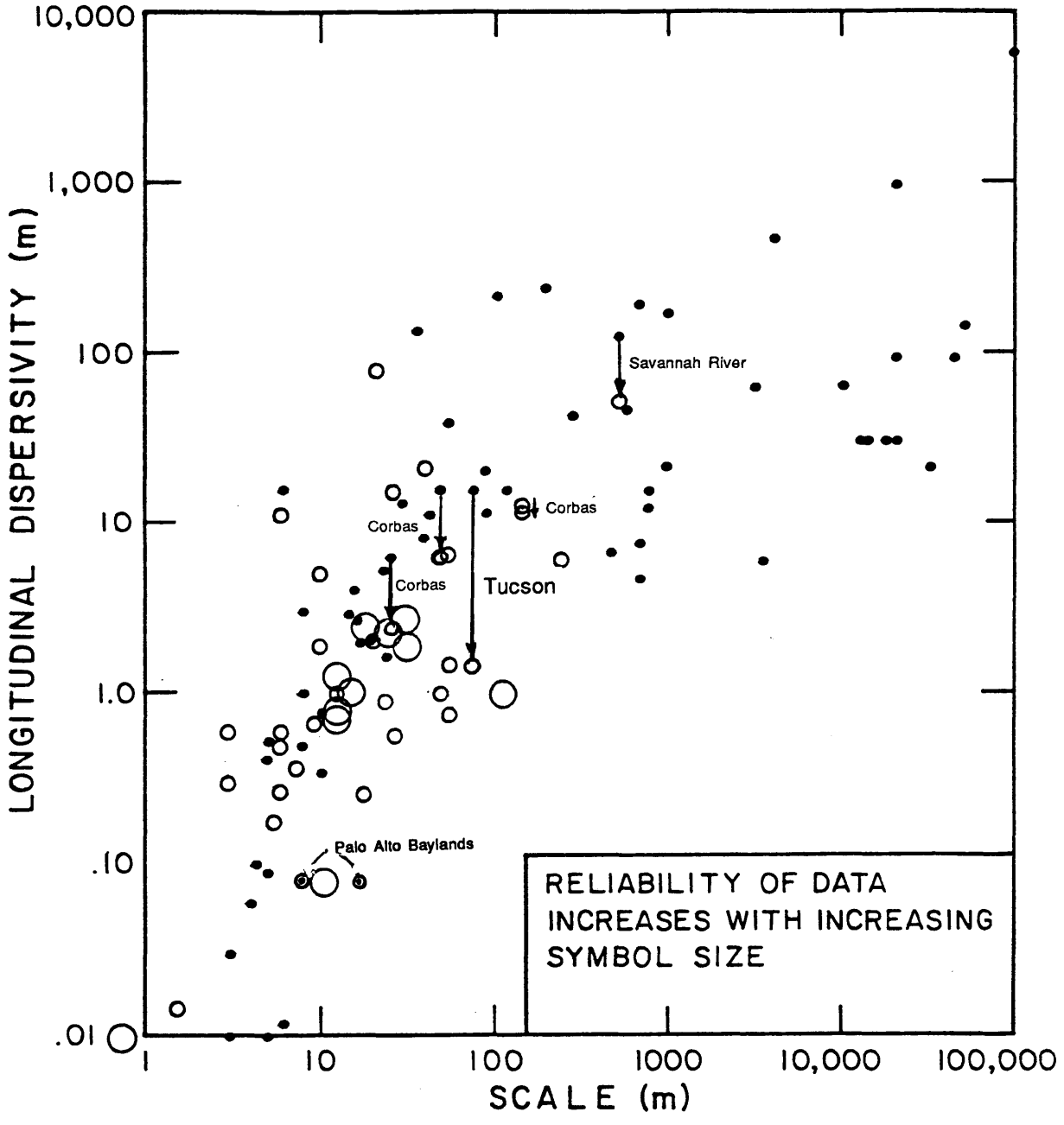

Figure 6-21. Re-evaluated dispersivity data plotted on Figure 1-2.

REFERENCES

Anderson, M. P. 1979. Using Models to Simulate the Movement of Contaminants through Groundwater Flow Systems. CRC Crit. Rev. Envir. Control, 9(11), 97-156.

Betson, R. P., J. M. Boggs, S. C. Young, and L. W. Gelhar, 1985. Appendix C in Macrodispersion Experiment (MADE): Design of a Field Experiment to Investigate Transport Processes in a Saturated Groundwater Zone. EPRI Report No. EPRI EA-4082, Palo Alto, CA.

Crank, J. 1956. Mathematics of Diffusion, Oxford University Press, New York and London, 347 pp.

Davis, S. N., G. M. Thompson, H. W. Bentley and G. Stiles. 1980. Groundwater Tracers--A Short Review. Ground Water, 18(1), 14-23.

Davis, S. N., D. J. Campbell, H. W. Bentley and T. J. Flynn. An Introduction to Groundwater Tracers. EPA Report No. EPA/600/2-85/022, NTIS publication No. PB86-100591, NTIS, Washington, D.C.

Gelhar, L. W. and M. A. Collins. 1971. General Analysis of Longitudinal Dispersion in Nonuniform Flow. Water Resources Research, 7(6), 1511-1521.

Gelhar, L. W., A. L. Gutjahr and R. L. Naff. 1979. Stochastic Analysis of Macrodispersion in a Stratified Aquifer. Water Resources Research, 15(6), 1387-1397.

Gelhar, L. W. 1982. Analysis of Two-Well Tracer Tests with a Pulse Input. Report No. RHO-BW-CR-131 P, Rockwell International, Richland, WA.

Gelhar, L. W. and C. L. Axness. 1983. Three-Dimensional Stochastic Analysis of Macrodispersion in Aquifers. Water Resources Research, 19(1), 161-180.

Gelhar, L. W., A. Mantoglou, C. Welty and K. R. Rehfeldt. 1985. A Review of Field Scale Physical Solute Transport Processes in Saturated and Unsaturated Porous Media. Electrical Power Research Institute, RP-2485-05.

Goblet, P. 1982. Interpretation d'Experiences de Tracage en Milieu Granitique (Site B). Report LHM/RD/82/11, Centre d'Information Geologique, Ecole Nationale Superieure des Mines de Paris, Fontainebleau, France.

Goblet, P. 1984. Interpretation des Tracages aux Lanthanides. Part II in Bigot, et al. 1984. Etudie Hydrodynamiques a L'Aide Traceurs D'un Doublet Hydrothermique En Roches Fissurees. Commission des communautes Europeennes, Institut National d'Astronomie et de Geophysique.

Grove, D. B. and W. A. Beetem. 1971. Porosity and Dispersion Constant Calculations for a Fractured Carbonate Aquifer Using the Two-Well Tracer Method. Water Resources Research, 17(1), 128-134.

Hoehn, E. and P. V. Roberts. 1982. Advection-Dispersion Interpretation of Tracer Observations in an Aquifer. Ground Water, 20(4), 457-465.

Hsieh, P. A., 1986. A New Formula for the Analytical Solution of the Radial Dispersion Problem. Water Resources Research, 22, 1597-1605.

Ivanovich, M. and D. B. Smith, 1978. Determination of Aquifer Parameters by a Two-Well Pulsed Method Using Radioactive Tracers. Journal of Hydrology, 36, 35-45.

Kreft, A. and A. Zuber, 1979. Determination of Aquifer Parameters by a Two-Well Pulsed Method Using Radioactive Tracers -- Comments. Journal of Hydrology, 41, 171-176.

Lallemand-Barres, A. and P. Peaudecerf. 1978. Recherche des Relations Entre la Valeur de la Dispersivite Macroscopique d'un Milieu Aquifere, ses Autres Caracteristiques et les Conditions de Mesure. Bulletin de Recherches Geologiques et Minieres, 2e Serie, Section III, No. 4, Orleans, France.

Lenda, A. and A. Zuber. 1970. Tracer Dispersion in Groundwater Experiments. In Isotope Hydrology. Proceedings of a Symposium on the Use of Isotopes in Hydrology. International Atomic Energy Agency. Paper No. IAEA-SM-129/37, 619-641, Vienna.

Ogata, A. and R. B. Banks. 1961. A Solution of the Differential Equation of Longitudinal Disperison in Porous Media. U.S. Geological Survey Professional Paper. 411-A, 7.

Robson, S. G. 1974. Feasibility of Digital Water Quality Modeling Illustrated by Application at Barstow, California. U.S.G.S. Water Resources Investigations 46-73. Report No. USGS/WRD-75/020. U. S. Geological Survey, Menlo Park, California.

Sauty, J. P. 1977. Contribution a l'Identification des Parameters de Dispersion dans les Aquiferes par Interpretation des Experiences de Tracage. Dissertation presented to l'Universite Scientifique et Medicale et Institut National Polytechnique de Grenoble. Grenoble, France.

Sauty, J. P. 1978. Identification des parametres du transport hydrodispersif dans les aquiferes par interpretation de tracages en ecoulement cylindrique convergent ou divergent. Journal of Hydrology, 39, 69-103.

Sauty, J. P. 1980. An analysis of hydrodispersive transfer in aquifers. Water Resources Research, 16(1), 145-158.

Webster, D.S., J. F. Proctor and J. W. Marine. 1970. Two-well Tracer Test in Fractured Crystalline Rock. U.S.G.S. Water Supply Paper No. 1544-I. U. S. Government Printing Office, Washington, DC.

Wilson, L. G. 1971. Investigations on the Subsurface Disposal of Waste Effluents at Inland Sites. Res. Develop. Prog. Report 650, U.S. Dept. of Interior, Washington, DC.

Zuber, A. 1974. Theoretical Possibilities of the Two-Well Pulse Method. In Isotope Techniques in Groundwater Hydrology, Vol. 2. Paper No. IAEA-SM-182/45, 277-294, Vienna.

Appendix A

Extension of Gelhar and Collins (1971) To Treat Spatially Variable α

If the dispersivity $\alpha(s)$ is spatially dependent then eq. (5) of Gelhar and Collins (1971) becomes

$$\frac{\partial C}{\partial t} + u\frac{\partial C}{\partial s} = \alpha u\frac{\partial^2 C}{\partial s^2} + u\frac{\partial a}{\partial s}\frac{\partial C}{\partial s} + D_m\left(\frac{\partial^2 C}{\partial s^2} - \frac{1}{u}\frac{\partial u}{\partial s}\frac{\partial C}{\partial s}\right) \qquad \text{(A1)}$$

The italicized term is the additional effect of variable α. The method of approximation is essentially the same but α is scaled as

$$\alpha(s) = \alpha_o f(s) = \varepsilon L_o f(s) \quad , \quad \varepsilon = \alpha_o/L_o$$

where α_o is some constant reference dispersivity (say the maximum value). Then following steps identical to Gelhar and Collins (1971), their eq. (15) becomes

$$\frac{\partial C}{\partial T} = \left(\frac{f}{U} + \frac{D}{U^2}\right)\frac{\partial^2 C}{\partial \zeta^2} - \varepsilon^{1/2}\left[\left(\frac{f}{U} + \frac{2D}{U^2}\right)\frac{\partial U}{\partial S} - \frac{\partial f}{\partial S}\right]\frac{\partial C}{\partial \zeta} \qquad \text{(A2)}$$

and for $\varepsilon^{1/2} << 1$ the second term on the right hand side is negligible. As a result eq. (22) is replaced by

$$\omega = \int_{s_o}^{s'} \frac{f(s')u(s') + D_m/\alpha_o}{u^3(s')}ds' \qquad \text{(A3)}$$

which for the radial flow case with $D_m = 0$ is equivalent to (5-19).

```
C                                                                  APPENDIX B
C-----------------------------------------------------------------------
C                              CONRAD3.FOR
C
C                                   by
C
C                              Claire Welty
C
C     This is a program to generate type curves for convergent radial
C     flow/pulse input tracer tests, accounting for the borehole
C     flushing effect. The analytical solution is derived using an
C     exponentially decreasing input rather than a pulse input,
C     and is based on the general solution of Gelhar and  Collins (1971),
C     assuming that longitudinal dispersivity is constant in space.
C     Because the resulting solution is a convolution integral,
C     numerical integration must be employed to generate the
C     type curves. Simpson's Rule is used to do the numerical integration
C     in this program.
C-----------------------------------------------------------------------
C
C                         DEFINITIONS OF VARIABLES
C
C     ALPHA = longitudinal dispersivity [L]
C
C     R = distance between injection borehole and pumping well [L]
C
C     C_HAT = breakthrough concentration at the pumping well
C             normalized by the input concentration
C
C          Input conc = M/[2*rho*pi*n*b*R*sqrt(4*pi*alpha*R/3)]
C
C     T_HAT = dimensionless time = Q*t/(pi*(r**2)*n*b)
C
C     TAUHAT = dummy time variable for numerical integration
C
C     PECINV = ALPHA/R = inverse peclet number (inverse dimensionless
C              distance)
C
C     THETA = R*n/(pi*d)
C
C             d = diameter of the borehole
C
C     NCURVS = number of type curves desired (one for every value of
C              ALPHA/R specified)
C
C     DTAUHAT = size of subinterval for numerical integration
C
C     M = number of subintervals for numerical integration
C
C-----------------------------------------------------------------------
      DOUBLE PRECISION C_HAT(102,10), PECINV(10), R, T_HAT(102),
     1     DT_HAT(10), OUTPUT(10,102), AA, BB, CC, DD, THETA(10),
     2     TAUHAT, DTAUHAT(10), C_HAT1, C_HAT2, C_HAT3, SUMEVN,
     3     SUMODD, MINT(10), MAXT(10)
      INTEGER I, J, K, KK, L, M, MM, NCURVS, NCOLS
      OPEN (UNIT=10, NAME = 'CONRAD3.IN', STATUS = 'OLD')
      OPEN (UNIT=11, NAME = 'CONRAD3.OUT', STATUS = 'NEW',
     1      CARRIAGECONTROL = 'LIST')
 5    READ (10,*)  NCURVS,(DT_HAT(I),PECINV(I),THETA(I),
     1             MINT(I), MAXT(I),DTAUHAT(I),I=1,NCURVS)
```

```
 7     WRITE (6,*)  NCURVS,(DT_HAT(I),PECINV(I),THETA(I),
     1              MINT(I), MAXT(I),DTAUHAT(I),I=1,NCURVS)
       IF (DT_HAT(1) .EQ. 0.0) GO TO 65
       CONST = 16./3.
       NCOLS = NCURVS + 1
C      -------------------------
C      Initialize output array.
C      -------------------------
       DO 10 J = 1,101
          DO 15 I = 1,10
          OUTPUT(I,J) = 0.0
 15       CONTINUE
 10       CONTINUE
C      ------------------------------------------------------
C      Loop on J for each pair of values of THETA and ALPHA/R.
C      ------------------------------------------------------
       DO 20 J = 1, NCURVS
          T_HAT(1) = MINT(J)
C         ---------------------------------
C         Loop on K for each value of T_HAT.
C         ---------------------------------
          KK = INT(MAXT(J)/DT_HAT(J))
          DO 30 K = 1, KK
C            ------------------------------
C            Calculate C_HAT at TAUHAT = 0.
C            ------------------------------
             TAUHAT = 0.00000001
             CALL C_HATCALC (TAUHAT,T_HAT(K),THETA(J),CONST,
     1                       PECINV(J), C_HAT1)
C            -------------------------------------
C            Calculate C_HAT at TAUHAT = T_HAT(K)
C            -------------------------------------
             TAUHAT = T_HAT(K)
             CALL C_HATCALC (TAUHAT,T_HAT(K),THETA(J),CONST,
     1                       PECINV(J), C_HAT2)
C            ------------------------------------------------
C            Calculate C_HAT for increments of TAUHAT.
C            ------------------------------------------------
             SUMEVN = 0.
             SUMODD = 0.
             MM = INT(T_HAT(K)/DTAUHAT(J)) - 1
             DO 25 I = 1,MM
                TAUHAT = FLOAT(I)*DTAUHAT(J)
                CALL C_HATCALC (TAUHAT,T_HAT(K),THETA(J),CONST,
     1                          PECINV(J),C_HAT3)
                IF (MOD(FLOAT(I), 2.) .EQ. 0. ) THEN
                   SUMEVN = SUMEVN + C_HAT3
                ELSE
                   SUMODD = SUMODD + C_HAT3
                END IF
 25             CONTINUE
             C_HAT(K,J) = DTAUHAT(J)*
     1                    (C_HAT1+C_HAT2+(2.*SUMEVN)+(4.*SUMODD))/3.
             WRITE (6,28) T_HAT(K), C_HAT(K,J)
 28          FORMAT(5X, 'T_HAT = ', D9.3, 2X, 'C_HAT = ', D9.3)
             IF (J .EQ. 1) THEN
                OUTPUT(1,K) = T_HAT(K)
                OUTPUT(2,K) = C_HAT(K,J)
             ELSE
                OUTPUT(J+1,K) = C_HAT(K,J)
```

```
            END IF
            T_HAT(K+1) = T_HAT(K) + DT_HAT(J)
 30         CONTINUE
 20       CONTINUE
      WRITE (11,40) NCOLS
 40   FORMAT ('CONVERGENT RADIAL FLOW WITH PULSE INPUT AND BOREHOLE'
     1         ' FLUSHING, ALPHA/R = CONST',/,I2,/,'T_HAT')
      WRITE (11,50) (DT_HAT(J),PECINV(J),THETA(J), DTAUHAT(J),
     1               J = 1,NCURVS)
 50   FORMAT ('DT_HAT = ', F6.3, 2X, 'ALPHA/R = ', F6.3, 2X,
     1         'THETA = ',F7.4,2X,'DTAUHAT = ',F7.4)
      WRITE (11,60) ((OUTPUT(N,M), N = 1,7), M = 1,KK)
 60   FORMAT(7(D9.3,X))
      GO TO 5
 65   CLOSE (UNIT = 10)
      CLOSE (UNIT = 11)
      STOP
      END
C*************************************************************************
      SUBROUTINE C_HATCALC(TAUHAT, T_HAT, THETA, CONST, PECINV, C_HAT)
      DOUBLE PRECISION AA, BB, CC, DD, THETA, CONST, T_HAT,
     1                 TAUHAT, C_HAT, PECINV
      AA = 1.- TAUHAT
      BB = DSQRT(DABS(AA))
      CC = 1./(1.-(AA*BB))
      DD = THETA*(T_HAT-TAUHAT)
      C_HAT = DSQRT(CC)*THETA*
     1               DEXP( -((AA**2)*CC/(CONST*PECINV)) - DD)
      RETURN
      END
```

CONVERGENT RADIAL FLOW WITH PULSE INPUT AND BOREHOLE FLUSHING
ALPHA/R = 0.050 DTAUHAT = 0.0001

T_HAT	THETA = 0.5	THETA = 1.0	THETA = 2.0	THETA = 100.0
0.100D+00	0.469D-11	0.937D-11	0.187D-10	0.691D-09
0.200D+00	0.293D-05	0.582D-05	0.115D-04	0.245D-03
0.300D+00	0.291D-03	0.575D-03	0.112D-02	0.144D-01
0.400D+00	0.303D-02	0.593D-02	0.114D-01	0.967D-01
0.500D+00	0.124D-01	0.240D-01	0.451D-01	0.271D+00
0.550D+00	0.207D-01	0.398D-01	0.739D-01	0.381D+00
0.600D+00	0.315D-01	0.603D-01	0.111D+00	0.488D+00
0.650D+00	0.449D-01	0.853D-01	0.155D+00	0.599D+00
0.700D+00	0.606D-01	0.114D+00	0.205D+00	0.701D+00
0.750D+00	0.782D-01	0.147D+00	0.259D+00	0.791D+00
0.800D+00	0.974D-01	0.181D+00	0.316D+00	0.864D+00
0.850D+00	0.118D+00	0.217D+00	0.373D+00	0.920D+00
0.900D+00	0.138D+00	0.253D+00	0.429D+00	0.959D+00
0.950D+00	0.159D+00	0.289D+00	0.482D+00	0.980D+00
0.100D+01	0.180D+00	0.324D+00	0.532D+00	0.100D+01
0.110D+01	0.219D+00	0.386D+00	0.613D+00	0.958D+00
0.120D+01	0.252D+00	0.435D+00	0.664D+00	0.848D+00
0.130D+01	0.277D+00	0.466D+00	0.682D+00	0.708D+00
0.140D+01	0.294D+00	0.481D+00	0.671D+00	0.567D+00
0.150D+01	0.304D+00	0.482D+00	0.638D+00	0.441D+00
0.160D+01	0.307D+00	0.472D+00	0.590D+00	0.338D+00
0.170D+01	0.306D+00	0.454D+00	0.535D+00	0.256D+00
0.180D+01	0.302D+00	0.432D+00	0.477D+00	0.194D+00
0.190D+01	0.295D+00	0.406D+00	0.420D+00	0.147D+00
0.200D+01	0.287D+00	0.379D+00	0.367D+00	0.111D+00
0.250D+01	0.236D+00	0.253D+00	0.169D+00	0.307D-01
0.300D+01	0.188D+00	0.160D+00	0.728D-01	0.102D-01
0.350D+01	0.148D+00	0.995D-01	0.306D-01	0.398D-02
0.400D+01	0.116D+00	0.614D-01	0.128D-01	0.174D-02
0.500D+01	0.705D-01	0.231D-01	0.236D-02	0.424D-03
0.600D+01	0.429D-01	0.864D-02	0.495D-03	0.130D-03
0.700D+01	0.260D-01	0.322D-02	0.126D-03	0.463D-04
0.800D+01	0.158D-01	0.120D-02	0.395D-04	0.184D-04
0.900D+01	0.959D-02	0.450D-03	0.147D-04	0.794D-05
0.100D+02	0.582D-02	0.169D-03	0.621D-05	0.370D-05